REPUBLIC OF TURKEY
ACIBADEM MEHMET ALİ AYDINLAR UNIVERSITY
INSTITUTE OF NATURAL AND APPLIED SCIENCES

MUTATED GENES IN LEPTOMENINGEAL CARCINOMA CAUSED BY NON-SMALL CELL LUNG CANCER AND THE EFFECTS OF INCREASED *SLPI* GENE IN THE A549 CELL LINE

İREM ÇONGUR

MASTER THESIS

DEPARTMENT of MOLECULAR and TRANSLASTIONAL BIOMEDICINE

SUPERVISOR
Asst. Prof. Dr. Zeynep Tokcaer Keskin

SECOND SUPERVISOR
Asst. Prof. Dr. Onur Emre Onat

Istanbul-2023

REPUBLIC OF TURKEY
ACIBADEM MEHMET ALİ AYDINLAR UNIVERSITY
INSTITUTE OF NATURAL AND APPLIED SCIENCES

MUTATED GENES IN LEPTOMENINGEAL CARCINOMA CAUSED BY NON-SMALL CELL LUNG CANCER AND THE EFFECTS OF INCREASED *SLPI* GENE IN THE A549 CELL LINE

İREM ÇONGUR

MASTER THESIS

DEPARTMENT of MOLECULAR and TRANSLASTIONAL BIOMEDICINE

SUPERVISOR
Asst. Prof. Dr. Zeynep Tokcaer Keskin

SECOND SUPERVISOR
Asst. Prof. Dr. Onur Emre Onat

Istanbul-2023

DECLARATION

I declare that this thesis study was conducted on the basis of information gathered by me in accordance with scientific regulations and ethical rules. All of the data, information, comments, and analysis have been obtained and processed using an academic and scientific style. In compliance with publication ethics, the literature used has been properly cited with the original sources.

22.05.2023
İREM ÇONGUR

ACKNOWLEDGEMENT

I would like to thank and express my gratitude to my advisor Asst. Prof. Dr. Zeynep TOKCAER KESKİN, who has been known me since my undergraduate studies and has always supported and encouraged me. She gave me continual guidance and advice during this period, and I am grateful to her for that. With all her helpfulness both academically and in everyday life, she became more than my adviser. I consider myself really privileged to work under her supervision and complete this project with her. I would like to thank to my second supervisor Asst. Prof. Dr. Onur Emre ONAT for his guidance while I was conducting the first part of this thesis study. I gained a lot from him as a foreigner working in the field of bioinformatics.

I would like to thank the Asst. Prof. Dr. Nazlı Keskin and Asst. Prof. Dr. Emre Deniz for getting me to where I am today since my undergraduate education and for their support whenever I needed it. Additionally, I want to express my gratitude to the jury members Cemaliye Akyerli Boylu and Esma Nur Okatan for their helpful feedback and guidance.

I would also like to express my gratitude to my colleague and dearest friend Ekin Köni, who was always there for me whenever I needed. We have experienced a lot together throughout this period, and I consider myself quite lucky to have spent this difficult but so enjoyable period with you. My interns Dafne Mutugu and Nurettin Cem Alişan have been incredibly supportive. They assisted me with this project, and I sincerely appreciate their friendship. I would also thank to my dearest friends Ezel Demir, Başak Kavaklıoğlu, and Emre Almaz for their love and support during this period.

Furthermore, my family, Yeşim and Hakkı Çongur, deserve special thanks for their endless love, support, and faith. I feel myself incredibly grateful to have loving and understanding parents. I would have been unable to accomplish anything without them.

Finally, I would like to thank TÜSEB for supporting some part of this thesis through TÜSEB project no 11899.

TABLE OF CONTENTS

LIST OF SYMBOLS AND ABBREVIATIONS

ALK	Anaplastic Lymphoma Kinase
ANOVA	Analysis of Variance
APC	Adenomatous Polyposis Coli
ATP	Adenosine Triphosphate
ATR	Ataxia Telangiectasia and Rad3-Related Protein
ATM	Ataxia Telangiectasia Mutated Gene
BBB	Blood-Brain Barrier
BER	Base Excision Repair
BLAST	Basic Local Alignment Search Tool
bp	Base Pair
BP	Biological Process
BRAF	v-Raf murine sarcoma viral oncogene homolog B
BRCA1	Breast-Cancer Susceptibility Gene 1
BRCA2	Breast-Cancer Susceptibility Gene 2
C3	Complement Component 3
CASP8	Caspase 8
CDH18	Cadherin 18
CCK8	Cell Counting Kit 8
CDK	Cyclin Dependent Kinases
cDNA	Complementary DNA
CDC25	Cell Division Cycle 25
CHEK1	Checkpoint Kinase 1
CHEK2	Checkpoint Kinase 2
CNS	Central Nervous System
CO_2	Carbon Dioxide
COSMIC	Catalogue of Somatic Mutations in Cancer
CSF	Cerebrospinal Fluid
CTC	Circulating Tumor Cell
CCND1	Cyclin D1
CCNE1	CyclinE1

CDKN2A	Cyclin Dependent Kinase Inhibitor 2A
dbSNP	Database of Single Nucleotide Polymorphisms
ddh_2O	Double Distilled Water
°C	Degree Celsius
Del19	Exon 19 Deletion
DDR	DNA damage repair
DGIdb	Drug-Gene Interaction Database
DMEM	Dulbecco's Modified Eagle Medium
DMSO	Dimethyl Sulfoxide
DNA	Deoxyribonucleic Acid
DSB	Double Strand Break
ECM	Extracellular Matrix
EcoRI	*Escherichia Coli*, RY13 Strain, One
E. coli	*Escherichia Coli*
EDTA	Ethylenediaminetetraacetic Acid
EGFR	Epidermal Growth Factor Receptor
ELISA	Enzyme-Linked ImmunoSorbent Assay
EML4	Echinoderm Microtubule-Associated Protein Like 4
EMT	Epithelial-Mesenchymal Transition
ER	Estrogen
ERK	Extracellular Signal-Regulated Kinase
FBS	Fetal Bovine Serum
FDA	Food and Drug Administration
FDR	False Discovery Rate
FGFR1	Fibroblast Growth Factor Receptor 1
G418	Geneticin
g	Gram
GAPDH	Glyceraldehyde-3-Phosphate Dehydrogenase
GC	Guanine Cytosine
gDNA	Genomic DNS
GFP	Green Fluorescence Protein
GO	Gene Ontology

h	Hour
HCL	Hydrochloric Acid
HER2	Human Epidermal Growth Factor Receptor 2
HGF	Hepatocyte Growth Factor
HGFR	Hepatocyte Growth Factor Receptor
HIF	Hypoxia-inducible Factor
HPR	Horseradish Peroxidase
HRR	Homologous Recombinational Repair
IR	Ionizing Radiation
ins	Insertion
KRAS	Kirsten Rat Sarcoma
KpnI	Klebsiella pneumoniae
L	Liter
LB	Lysogeny Broth
LMC	Leptomeningeal Carcinoma
LPS	Lipopolysaccharide
LUAD	Lung Adenocarcinoma
M	Molar
MAPK	Mitogen Activated Protein Kinase
MCODE	Molecular Complex Detection
MeOH	Methanol
MeSH	Medical Subject Headings
MMP	Matrix Metalloproteinase
µg	Microgram
µL	Microliter
min	Minute
mL	Milliliter
mM	Millimolar
mRNA	Messenger RNA
mTOR	Mammalian Target of Rapamycin
n	Number
NaCl	Sodium Chloride

NaOH	Sodium Hydroxide
NCI	National Cancer Institute
NEB	New England Biolabs
NF-κB	Nuclear Factor Kappa B
ng	Nanogram
NGS	Next-Generation Sequencing
NHEJ	Non-Homologous End Joining
NSB1	Nibrin
NIH	National Institutes of Health
nm	Nanomolar
no	Number
NSCLC	Non-small cell lung cancer
OD	Optical density
OPTIMEM	Optimized Minimum Essential Medium
p	Probability
PAGE	Polyacrylamide Gel Electrophoresis
PARP	Poly-(ADP-ribose) Polymerase
PBS	Phosphate Buffered Saline
PCR	Polymerase Chain Reaction
pg	Picogram
PIK3CA	Phosphatidylinositol-4,5-Bisphosphate 3-Kinase Catalytic Subunit Alpha
PI3K	Phosphatidylinositol 3-Kinase
PPI	Protein-protein Interactions
PRISMA	Preferred Reporting Items for Systematic Reviews and Meta-Analysis
PR	Progesterone
PTEN	Phosphatase and Tensin Homologue
PTK2	Protein Kinase 2
PVDF	Polyvinylidene Difluoride
qPCR	Quantitative Polymerase Chain Reaction
RAF	Rapidly Accelerated Fibrosarcoma

RAS	Rat Sarcoma
RB	Retinoblastoma
RE	Restriction Enzyme
RNA	Ribonucleic Acid
RTK	Receptor Tyrosine Kinase
RT-PCR	Reverse Transcriptase Polymerase Chain Reaction
ROS	Reactive Oxygen Species
rpm	Revolutions Per Minute
SCLC	Small Cell Lung Cancer
scRNA-seq	Single-cell RNA Sequencing
SDS	Sodium Dodecyl-Sulfate
sec	Second
STK11	Serine/threonine Kinase 11
SLPI	Secretory Leukocyte Protease Inhibitor
SNP	Single Nucleotide Polymorphism
SSB	Single Strand Break
TBS	Tris Buffered Saline
TERT	Telomerase Reverse Transcriptase
TEMED	Tetramethyl Ethylenediamine
TGF-β	Tumor Growth Factor Beta
TKI	Tyrosine Kinase Inhibitor
TLR	Toll-Like Receptor
Tm	Melting Temperature
TNBC	Triple Negative Breast Cancer
TP53	Tumor Protein P53
UALCAN	The University of Alabama at Birmingham Cancer Data Analysis Portal
UCSC	University of California Santa Cruz
UV	Ultraviolet
V	Volt
v	Volume
VEGF	Vascular Endothelial Growth Factor

WES	Whole Exome Sequencing

LIST OF FIGURES

LIST OF TABLES

SUMMARY

Leptomeningeal carcinoma (LMC) occurs mostly as a result of metastasis caused on by melanoma, breast cancer, and non-small cell lung cancer (NSCLC). Different sequencing techniques are used to analyze patients' mutations and gene expression changes. Molecular investigations are required to better understand LMC development. In the first part of this thesis genes mutated in NSCLC-LMC were analyzed to identify which pathways may be involved in the LMC development using an in-silico approach. Using data from 16 studies that applied various sequencing techniques to LMC patients caused by three primary cancers, a meta-analysis was performed. 87 genes were found to be mutated in NSCLC-LMC patients. Molecular pathways in which the altered genes function was identified through pathway enrichment analysis. 8 FDA approved drugs that treat NSCLC, cross blood-brain barrier (BBB), and target mutated genes in NSCLC-LMC were identified. In the second part of this thesis, single cell RNA sequencing (scRNA-seq) data of Ruan et al. 2020 study conducted on circulating tumor cells (CTC) of cerebrospinal fluid (CSF) samples of NSCLC-LMC patients were used. Serine leukocyte protease inhibitor (*SLPI*) gene, which encodes an inhibitor that shields epithelial tissues from serine proteases, has been selected to be investigaten in NSCLC, as it had high expression in NSCLC-LMC patients and low expression in lung adenocarcinoma (LUAD) according to UALCAN database. *SLPI* gene was overexpressed in the LUAD cell line, A549. It has been observed that overexpression of *SLPI* increased the migration and metastatic abilities of these cells, however, did not affect their proliferation rate.

Keywords: A549 cell line, leptomeningeal carcinoma, meta-analysis, non-small cell lung cancer, SLPI

ÖZET

Küçük Hücreli Dışı Akciğer Kanseri Nedenli Leptomeningeal Karsinomada Mutasyona Uğrayan Genler ve Artan *SLPI* Geninin A549 Hücre Hattında Etkileri

Leptomeningeal karsinom (LMC); çoğunlukla melanom, meme kanseri ve küçük hücreli dışı akciğer kanserinin (NSCLC) metastazı sonucu oluşur. Hastaların mutasyonlarını ve gen ifadelerindeki değişikliklerin analizi için farklı dizileme teknikleri kullanılmaktadır. Bu tezin ilk bölümünde, LMC'nin gelişimini aydınlatabilmek adına NSCLC-LMC hastalarında mutasyona uğramış genler analiz edilmiştir. Üç primer kanserin neden olduğu LMC hastalarına çeşitli dizileme teknikleri uygulayan 16 çalışmadan elde edilen veriler ile bir meta-analiz gerçekleştirilmiştir. NSCLC-LMC hastalarında 87 genin mutasyona uğradığı tespit edilmiş ve bu genlerin rol aldığı moleküler yolaklar belirlenmiştir. NSCLC hastalarında kullanılan, kan-beyin bariyerini geçen ve NSCLC-LMC'de mutasyona uğramış genleri hedef alan 8 ilaç belirlenmiştir. Bu tezin ikinci bölümünde Ruan ve ark. (2020) çalışmasında NSCLC-LMC hastalarının beyin omurilik sıvısında dolaşan tümör hücreleri üzerinde yaptığı tek hücreli RNA dizilemesinin verileri kullanılmıştır. Epitel dokularını serin proteazlardan koruyan bir inhibitörü kodlayan serin lökosit proteaz inhibitörü (*SLPI*) geni, NSCLC-LMC hastalarında yüksek, UALCAN veri tabanına göre akciğer adenokarsinomunda (LUAD) düşük ifade edildiği için NSCLC'da yüksek ifadesini araştırmak için seçilmiştir. *SLPI* gen ifadesi, LUAD hücre hattı A549'da arttırılmıştır. SLPI ifadesinin artması sonucunda bu hücrelerin göç ve metastaz kabiliyetleri artmış ancak çoğalma hızlarının etkilenmediği gözlenmiştir.

Anahtar Kelimeler: A549 hücre hattı, leptomeningeal karsinom, küçük hücreli dışı akciğer kanseri, meta-analizi, SLPI

1. AIM OF THE STUDY

LMC is mostly seen as a result of metastasis caused by melanoma, lung and breast cancer and formed by localization of tumor cells at the meninges in the brain. The average survival time for LMC patients is less than one year. Mutations and gene expression changes in patients are studied with next-generation sequencing (NGS) and scRNA-seq, but no study has yet been conducted to elucidate the molecular mechanism of the disease (1). Therefore, molecular studies investigating the development of LMC are needed. The main aim of this thesis is to gain insight into the molecular mechanisms that drive the development of LMC by investigating the mutational landscape and changes in gene expression.

The aim of the first part of this thesis is to analyze genes mutated in LMC caused by NSCLC to identify which pathways may be involved in the development of LMC using an in-silico approach. In order to achieve the goal, a meta-analysis was conducted utilizing information from 16 studies that performed different sequencing methods to individuals with LMC caused by NSCLC, breast cancer, and melanoma. Bioinformatic approaches were applied to analyze mutated genes in NSCLC-LMC patients. Molecular pathways in which the altered genes function was identified, as well as the potential drugs that interact with these genes.

In the second part, as preliminary research performed in order to fill in the information gap about the molecular mechanisms of LMC in the literature, scRNA-seq data of Ruan et al. 2020 study conducted on CTC of CSF samples of NSCLC-LMC patients were used (2). The genes with high expression were listed and then the publicly available UALCAN cancer database (https://ualcan.path.uab.edu/analysis.html) (3) was used to investigate the expression levels of the same genes in LUAD. Genes that have high expression in NSCLC-LMC

patients and low expression in LUAD were identified and the list was shortened by choosing those that had not previously been studied. The cellular components in which genes function were identified using gene ontology (GO) analysis (http://geneontology.org/) (4). Following this research, the highest association was discovered between the formation of vesicles and the extracellular environment of exosomes. The expression of the *SLPI* gene was discovered to be increased in LMC and decreased relative to normal lung in LUAD.

SLPI gene, encodes an inhibitor that shields epithelial tissues from serine proteases, has increased in a variety of cancers. The gene's precise function in cancer is not well understood, and its exact function in lung cancer is yet unknown. There hasn't been research done on how the *SLPI* gene affects LMC (5). Therefore, the aim of the second part of this thesis is to investigate the effect of expression change of SLPI on cancer metastasis, proliferation and migration using the A549 lung cancer cell line in *vitro*. For this purpose, *SLPI* gene was overexpressed in the A549 cell line and proliferative, metastatic and migration properties of the cells were investigated.

2. INTRODUCTION

2.1 Cancer

Cancer is the second most common cause of mortality in the United States and a major global public health issue. From 2015 to 2019, women's lung cancer incidence declined at a rate that was half that of men, whereas melanoma, and breast cancer rates all rose. In spite of the pandemic and in contrast to other primary causes of mortality, the death rate of cancer decreased by 1.5% between 2019 and 2020. This development mainly reflects treatment advancements, which are most striking in the rapid decrease in mortality for, melanoma, kidney cancer, and leukemia. There were 233,834 instances of cancer diagnosed in Turkey in 2020, while 126,335 cancer-related fatalities were recorded (6). In the United States, it is anticipated that there will be 1,958,310 new cancer cases and 609,820 cancer caused deaths in 2023 (7).

Carcinogenesis, also referred as oncogenesis or tumorigenesis, is the process by which cancer develops as a result of complex, multifaceted molecular processes involving interactions between an organism's genes and environment. Cause of cancer can be heterogeneous ranging from genetic alterations (somatic/inherited changes, or errors in DNA replication), to epigenetic alterations (hypo/hyper methylations of oncogenes/tumor suppressors), to viral infections. Lifestyle and/or exogenous risk factors can also be the cause of certain cancer types. All of these kinds of alterations gradually change the metabolism and behavior of cells. They can become immortal, proliferate indefinitely, invade adjacent tissues, and evade from immune cells. Moreover, their communication with their surrounding is also affected, which leads to disruption of the cellular homeostasis (8).

In 2000, Weinberg and Hanahan proposed a group of functional abilities that healthy cells acquire as they become capable to produce malignant tumors. They called these “hallmarks of cancer” as they believed that they represented shared cellular phenotypic characteristics that unite all different types of cancer cells. There were initially 6 hallmarks, but in 2011 that number was raised to 8 hallmarks and two acquired capabilities and in 2022, they added four new hallmarks and characteristics as shown in **Figure 2.1** (9).

To understand the pathogenesis that causes malignancy, it is very important to identify the altered genes and their products, which will provide the necessary information that can be used in the diagnosis and treatment of cancer (10).

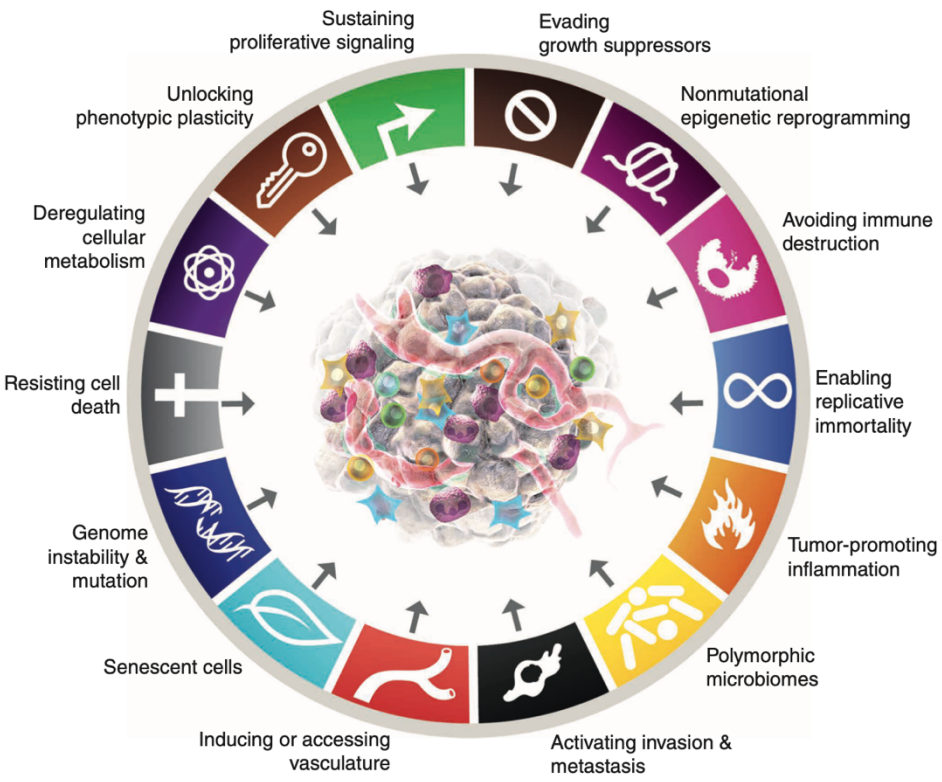

Figure 2.1 Hallmarks of cancer (9)

2.1.1 Breast Cancer

The most frequent malignancy in the world is breast cancer, which develops when breast cells proliferate abnormally due to genetic alterations, obesity, family history and aging. With 685,000 deaths from cancer-related deaths in 2020, breast cancer continues to be the second leading cause among females (11). In 2023, an estimated 297,790 new cases of invasive breast cancer will be diagnosed in women in the US (7).

According to histological and molecular evidence, breast cancer can be divided into three subtypes: breast cancer that express hormone receptor (progesterone (PR+) or estrogen (ER^+), breast cancer that express human epidermal growth factor receptor 2 (HER2+), and triple negative breast cancer (TNBC) (PR-, ER-, HER2-) (12). Each subgroup clearly differs from the others in terms of overall survival rate, incidence, and responsiveness to treatment, enabling clinicians to analyze clinical findings in breast cancer patients and provide them with the best treatments (11). HER2 is a member of the epidermal growth factor receptor (EGFR) family of receptor tyrosine kinases (RTKs), which also includes EGFR (HER1), HER3, and HER4. Cell differentiation and proliferation are two biological processes that are regulated by EGFR family receptors, which are expressed in a variety of organs (13). Activation of HER receptors results in the activation of the mitogen activated protein kinases/extracellular signal-regulated kinase (MAPK/ERK) and phosphatidylinositol 3-kinase (PI3K/AKT) signaling pathways (14). The MAPK/ERK pathway is a crucial signaling pathway that regulates molecular processes such as cell proliferation, survival, and differentiation, as well as tumor invasion (15). The PI3K/AKT signaling pathway is involved in various essential molecular mechanisms such as angiogenesis, cell survival, proliferation, growth, metabolism, and migration (16).

Genetic susceptibility accounts for 5–10% of all breast cancer cases, making it a significant risk factor for the development of the cancer. The most frequent genetic cause of hereditary breast cancer is the breast-cancer susceptibility genes 1 and 2 (*BRCA1&BRCA2*). *BRCA1* and *BRCA2* function as tumor suppressor genes by promoting the repair of double-strand breaks and assisting in the maintenance of genomic integrity. Breast cancer susceptibility has been also linked to a variety of DNA repair genes, including Ataxia Telangiectasia Mutated (*ATM)* and checkpoint kinase 2 (*CHEK2)*, as well as an apoptosis gene, caspase 8 (*CASP8)*. Studies demonstrated that high-penetrance genes such as phosphatase and tensin homologue (*PTEN*), negative regulator of PI3K pathway and the primary tumor suppressor *TP53*, have been linked to an increased risk of breast cancer. According to recent reports, women who carry the *PTEN* mutation are 85% more likely than non-carriers to get breast cancer throughout their lifetime, with 50% penetrance by the age of 50. 2-7% of early-onset breast cancers include *TP53* mutations, which are associated with a risk of the disease that is at least ten times higher (13).

The most frequent type of breast cancer is the breast cancer expressing hormone receptor, which accounts approximately for 65% of incidences of breast cancer, particularly in women who are in the pre-menopausal period. Hormonotherapy is thus the most widely applied therapeutic strategy. When compared to hormone receptor+ subgroups, HER2+ cancers, which are characterized by HER2 protein overexpression and/or gene amplification, have a less favorable clinical prognosis, and occurs in 25–30% of breast cancer patients (12, 13). Combination of chemotherapy, surgery, radiation, and HER2-targeted therapy such as HER2 monoclonal antibodies may be beneficial for HER2+ breast cancer patients. Treatment of TNBC is much more challenging than the other breast cancer groups. Chemotherapy is the main treatment approach for this group (12). For instance, upon binding to HER2, trastuzumab inhibits the proliferation of the breast cancer cells by inhibiting homo- and heterodimerization of HER2 as well as its downstream signaling pathways. The first DNA damage repair (DDR) inhibitor to be applied in clinical practice is the poly-(ADP-ribose) polymerase (PARP) inhibitor. PARP inhibitors have been tested in patients with *BRCA1/2* germline

mutations. It has been shown that vascular endothelial growth factor (VEGF) secretion is increased by AKT-induced hypoxia-inducible factor (HIF), which in turn promotes angiogenesis (13). The alternate therapy could involve combining chemotherapy with a humanized recombinant monoclonal antibody against factor VEGF (12).

2.1.2 Melanoma

The most fatal and aggressive type of skin cancer is melanoma. Incidence has progressively increased over the past few decades, particularly among Caucasians. Presently, fair-skinned individuals, particularly those with red hair or blonde and those have eyes with light colors, are more likely to develop this malignancy than others. In contrast to other tumor types, young people and middle-aged adults are primarily affected by melanoma. Through the years, melanoma-related fatality has risen in tandem with the rise in incidence rate, reaching a one-in-four fatality rate (17). In 2023, an estimated 58,120 and 39,490 new cases of melanoma will be diagnosed in men and women in the US, respectively (7).

Cutaneous melanocytes, which is found in epidermis's basal layer can cause melanoma formation. Due to its detrimental effects on the skin and DNA damage, UV radiation plays a significant role in cutaneous melanomagenesis and accelerates carcinogenesis. Melanoma risk has also been associated to intermittent and intense sun exposure. Related risk factors that contribute to the melanoma development include nevi number, family history, and genetic susceptibility (17).

Currently, it is established that important signaling pathways such as MAPK, NFκB, and PI3K are dysregulated and associated with melanoma. Effective therapeutic approaches for unresectable stage III and IV melanoma have been developed as a result of the advancement the understanding of this disease's molecular mechanisms. With *BRAF* accounting for 40–60% of cases, it is both the most significant therapeutic target and the most common genetic mutation in cutaneous melanoma. Between 10 to 25% of melanomas patients have *NRAS* mutations. However, *NRAS* is not a target for the treatment, in contrast to *BRAF*. Although *NRAS* and BRAF mutations often mutually exclusive, their co-existence has been recorded. According to several research, melanoma patients with NRAS mutations had a markedly worse prognosis. Since the development of inhibitors of BRAF/MEK tyrosine kinase and immune checkpoint, patients with melanoma now have a far better prognosis and survival rate (17).

2.1.3 Lung Cancer

Lung cancer remains one of the most frequently diagnosed malignancies and the leading cause of cancer-related fatalities globally, having an anticipated 2 million new cases and 1.79 million mortalities per year (18). In 2023, an estimated 117,550 and 120,790 new cases of lung cancer will be diagnosed in men and women in the US, respectively (7). Lung cancer ranks as the second most frequent malignancy in women and men in the United States, following breast cancer and prostate cancer, respectively. The historical trends in smoking tobacco are mostly responsible for the regional differences by nation/region and among men and women (19).

The clinicopathological characteristics of lung cancer are highly variable. Non-small cell lung cancer (NSCLC) and small cell lung cancer (SCLC), which make up 85% and 15% of cases, respectively, are the two primary forms of lung cancer (18).

SCLC is distinguished by a great early response to radiation and chemotherapy, as well as high rates of proliferation and metastasis. By using light microscopic criteria, the morphological variations among SCLC and NSCLC could be determined. In general, SCLC has a larger nuclear/cytoplasmic ratio, nucleoli are missing, nuclear chromatin is finely granular, and the tumor is frequently fusiform in shape. Due to the small amount of patient samples that are accessible for research, extensive whole genome studies on the oncogenic driver mutations for SCLC are currently proceeding slower than studies on other types of cancer. The loss of *RB1* and *TP53* genes, as well as amplification of *MYC* are the two most significant gene changes in SCLC patients (20).

The most widely used forms of lung cancer therapy at the present include chemotherapy, immunotherapy, surgery, radiation therapy, and targeted therapy (20). New treatment approaches for immunotherapy and targeted therapy have been made possible by the discovery of potential biomarkers (18). These treatments might be essential for enhancing lung cancer patient outcomes (19).

2.1.3.1 Non-small Cell Lung Cancer (NSCLC)

Any epithelial lung cancer form besides SCLC is referred to as NSCLC. NSCLC arises from the lung's epithelial cells of the central bronchi to terminal alveoli. NSCLC develops from lung epithelial cells within terminal alveoli of the central bronchi (21). Lung adenocarcinomas (LUAD) account for 40% of NSCLC cases, followed by approximately 25% of squamous cell carcinoma (SCC), and around 12% of large cell carcinomas (19). The NSCLC's histological type and its origin site are correlated. Usually, adenocarcinomas start in the peripheral lung tissue, and squamous cell carcinoma originates closes to a central bronchus. Moreover, adenocarcinoma can also be seen in individuals who have never smoked, despite the fact that NSCLCs are associated with tobacco smoking (21).

2.1.3.2 NSCLC Biomarkers

With to developments in genomic profiling, it has become possible to classify and characterize NSCLC according to tumor biomarkers and genetic changes such as gene mutations, expression, rearrangements, and amplifications as shown in **Table 2.1.** They can be taken advantage of with particular targeted drugs or immune-checkpoint blockades and are essential for the growth of tumor and overall survival (19).

Table 2. 1 Frequency of Somatic Mutations and Alterations in NSCLC (19)

Gene	Alteration type	Frequency in NSCLC
EGFR	Mutation	10–35%
KRAS	Mutation	15–25%
FGFR1	Amplification	20%
PTEN	Mutation	4–8%
ALK	Rearrangement	3–7%
HER2	Mutation	2–4%
MET	Amplification	2–4%
BRAF	Mutation	1–3%
PIK3CA	Mutation	1–3%
AKT1	Mutation	1%
RET	Rearrangement	1%
ROS1	Rearrangement	1%

EGFR is a member of the RTK family, which also includes HER2, HER3, and HER4. It activates PI3K/AKT and MAPK signaling pathways (13). EGFR is essential for cellular growth, apoptotic inhibition, angiogenesis, metastatic progression, along with chemoresistance. The first four exons (exons 18–21) of the tyrosine kinase domain of EGFR are the only ones that are affected by *EGFR* mutations in NSCLC. These mutations, which include deletions, insertions, and missense point mutations, all assemble around the ATP binding pocket of the EGFR's tyrosine kinase domain. Mutations such as this cause the receptor's autoinhibited conformation to become

unstable, which causes the protein to become constitutionally activated and have pro-oncogenic effects. As opposed to that, these mutations are known as "sensitizing" *EGFR* mutations since they increase sensitivity to tyrosine kinase inhibitors (TKIs). The most active member of this family of receptors, HER2, has no known ligands but has the ability to directly influence EGFR signaling. Gene amplifications and mutations are two types of *HER2* changes found in NSCLC. Regarding the type of mutation and particular clinico-pathological characteristics, *HER2* driver mutations and *EGFR* changes are strikingly similar (22).

Kirsten Rat Sarcoma (*KRAS)*, a proto-oncogene, regulates the proliferation, maturation, and differentiation of cells by acting as a molecular on/off switch. *KRAS* is the most prevalent oncogene in cancer, and mutations in it have been identified in a wide range of cancers, including gynecological, gastric, biliary, skin, and lung cancers. Most activating *KRAS* mutations in NSCLC are located in codons 12 and 13, which alter the amino acid glycine in the KRAS protein. It is unclear how *KRAS* mutations in NSCLC affect prognosis. Tumors with somatic *KRAS* mutations had a worse prognosis and exhibit a diminished or nonexistent response to EGFR TKIs, according to several investigations and a meta-analysis of 28 studies (22).

Fibroblast growth factor receptor 1 (FGFR1), a RTK, promotes cell differentiation, survival, and growth by downstream activation of RAS-MAPK, STAT, and PI3K signaling pathways. By activating these pathways, FGFR1 promotes tissue remodeling and the epithelial-mesenchymal transition (EMT) and upregulating its expression results in cell transformation and cancer (23). Gene amplification, translocation, or activating mutations are the main three mechanisms by which constitutive activation of *FGFR1* occurs. It has been found that *FGFR1* amplification occurs more frequently in lung SCC than LUAD. Amplification of *FGFR1* in lung cancer cells results in a phenotype that is highly tumorigenic, and *FGFR1* controls the stem cell-like phenotype of SCC in the lung (24).

Lipid phosphatase PTEN removes phosphate groups from phosphoinositide signaling molecules. By controlling the PI3K signaling pathway's activity, this activity often governs growth and survival signals. PTEN functions as a tumor suppressor by preventing the activation of the PI3K pathway. Particularly in tumor cells, the lack of *PTEN* function results in constitutive activation of this pathway, which increases cell proliferation. Loss of *PTEN* in NSCLC has been linked to both a poor clinical outcome and drug resistance to a variety of chemotherapeutic substances. The most frequent genetic change in the PI3K pathway found in NSCLC is *PTEN* loss. Nevertheless, it seems to be just one of several genetic changes that cancers make to continuously activate the PI3K pathway. *AKT1* and phosphatidylinositol-4,5-bisphosphate 3-kinase catalytic subunit alpha (*PIK3CA*), the alpha isoform of PI3K's catalytic subunit, have both been linked to genetic changes in the PI3K/AKT pathway. A member of the serine-threonine protein kinase family, AKT promotes cell cycle progression and inhibits apoptotic signals (25).

Anaplastic lymphoma kinase (ALK) is an RTK that is a member of the insulin receptor superfamily and is crucial for brain development. However, it is also expressed in sporadic adult cells including neurons, glial cells, testicles, pituitary gland, hypothalamus, and endothelial cells. The majority of changes are chromosomal rearrangements that cause minor inversions on chromosome 2 to result in fusion genes. The exons 19–20 or exons 20–21 are often where the *ALK* genes' break sites for translocations are found. The first to be discovered were fusion genes involving the echinoderm microtubule-associated protein like 4 (*EML4*) and the *ALK* genes, which are also the most common in NSCLC and account for around 80% of all fusion occurrences. Because of the enhanced tyrosine kinase activity mediated by the fusion partner, the resultant chimera proteins typically contain the whole kinase domain and are highly oncogenic. Evidence suggests that, when compared to patients with wild-type *ALK*, those with ALK-positive NSCLC exhibit a very aggressive clinical behavior and have a tendency to be diagnosed at an earlier clinical stage (22).

Hepatocyte growth factor receptor (*HGFR*), another name for the proto-oncogene *MET*, encodes an RTK for hepatocyte growth factor (HGF). The protein's intracellular juxta membrane domain, which is encoded by exon 14, contains essential regulatory components, such as the direct binding site for the ubiquitin ligase that facilitates the degradation of the MET protein. Exon 14 can be skipped by mutations in the *MET* gene, and the resulting mutant receptor exhibits enhanced signaling and carcinogenic potential. Protein overexpression as well as gene amplification and mutation are the three basic causes of *MET* dysregulation in NSCLC. In EGFR-mutated NCSLC cancers, *MET* amplification promotes in *vitro* cell proliferation and migration, accelerating disease progression and metastasis development (22).

v-Raf murine sarcoma viral oncogene homolog B (BRAF) is one of three serine-threonine kinases that make up the RAF kinase family, which also includes ARAF and CRAF. Once activated, the BRAF protein interacts with other RAF kinases and homodimers of itself to regulate the MAPK/ERK signaling cascade. Studies demonstrated that *BRAF* mutations cause the MAPK/ERK signaling pathway to be constitutively activated, which promotes uncontrolled cell proliferation and survival. *BRAF* mutations have been found in many tumor types, including NSCLC and they are commonly found in exons 11 and 15 (22).

The ROS1 protein functions as an orphan RTK receptor with an unidentified ligand and shares several structural and functional characteristics with the ALK protein. Wild-type *ROS1* activation has been linked to cellular differentiation throughout the development of lung, lung, small intestine, and kidney cancers as well as the EMT. By acquiring certain gene fusions, ROS1 kinase activity is dysregulated, which activates the downstream cascades of a number of pathways, including PI3K and RAS-MAPK/ERK. Various fusion patterns have so far been identified, CD74-ROS1, SLC34A2-ROS, and tropomyosin 3, syndecan 4 (SDC4-ROS1). Advanced NSCLC clinical stages had a significantly higher incidence of ROS1 rearrangements (22).

2.1.3.2.1 Secretory Leukocyte Protease Inhibitor (SLPI)

Variety of human epithelia, including those lining the gastrointestinal, genitourinary, and respiratory tracts as well as skin's epidermis and salivary glands express *SLPI*. It is also expressed in macrophages, mast cells, fibroblasts, and neutrophils. SLPI belongs to the family of four disulphide core-containing whey-acidic proteins. Mucus and saliva secrete high levels of SLPI (5).

SLPI has multiple functions ranging from preventing the destruction of tissues to inflammation regulation and antimicrobial activity. Serine proteases are strongly inhibited by SLPI. In order to migrate more easily through the tissues' extracellular matrix (ECM) and to eliminate microorganisms that were phagocyted, leukocytes secrete proteases. The C-terminal domain of SLPI contains the area in charge of the protein's protease inhibitory action. The single elastase inhibitor identified in saliva, SLPI, also functions as the primary inhibitor of neutrophil elastase in the cytoplasm of neutrophils. In addition to preventing the development of neutrophil extracellular traps, SLPI reduces the generation of matrix metalloproteinases (MMPs) by monocytes. By suppressing the action of these proteases, SLPI helps to maintain tissue homeostasis and reduces tissue damage by innate immune cells. Pro-inflammatory cytokines' production and the consequent activation of immune cells may also be prevented by SLPI. Due to its ability to prevent lipopolysaccharide (LPS) uptake, SLPI inhibits toll-like receptor (TLR) activation. Nuclear Factor kappa B (NF-κB) signaling is also inhibited by SLPI and the cellular cytokine production balance is shifted by preventing activated macrophages, dendritic cells, and monocytes from producing proinflammatory cytokines. In general, SLPI preserves balanced immune responses at mucosal barrier tissues by inhibiting the production of a variety of pro-inflammatory cytokines and indirectly attenuating adaptive inflammatory immune responses. Moreover, SLPI also has antibacterial, antiviral, and antifungal activities. While the C-terminus of SLPI has only a slight antibacterial action, the N-terminal domain has both antibacterial and antifungal properties. As a result, it is likely that SLPI's

antiprotease activity is unrelated to its antibacterial activity. However, it is unclear exactly how SLPI eliminates microorganisms. *Escherichia Coli (E. coli)* mRNA and DNA can bind to SLPI, which prevents translation and halts bacterial development. Binding of SLPI to *E. coli* bacterial mRNA and DNA results in the inhibition of translation and an arrest in growth of bacteria. The cationic characteristics of SLPI may also enable the protein to bind to and disrupt the anionic bacterial cell membrane (5).

2.1.3.2.2 SLPI in NSCLC

SLPI is upregulated in a variety of carcinomas, such as breast ovarian, gastric, and pancreatic cancer, however its role in cancer is still not entirely understood. Several mechanisms have been proposed for the involvement of SLPI in cancer. Since the ECM must be degraded for tumor growth and invasion, protease inhibitors were initially expected to prevent cancer. Recent research revealed that SLPI promotes tumor growth and metastasis, despite the fact that, some of SLPI's functions may actually prevent cancer (5).

Previous studies have shown that, NSCLC expressed SLPI at a higher level in comparison to SCLC. When compared to healthy controls, patients with NSCLC had greater levels of serum SLPI. This suggested a connection between serum SLPI and tumor growth or size. However, whether SLPI is secreted from tumor cells or increased in tumor cells has not been investigated in these publications (5). On the other hand, it was found that the *SLPI* gene expression decreased relative to normal in patients with LUAD in the publicly available database UALCAN and GEPIA (3, 26). According to a study performed on Lewis Lung Carcinoma 3LL-S cell line, increasing *SLPI* expression enhanced 3LL-S cell tumor progression and lung colonization capacity

(27). In another study, it was observed that SLPI stimulated the proliferation of human LUAD cell lines in *vitro*. However, no similar study has been found in A549 cells and how SLPI specifically contributes to lung cancer is unknown (5).

2.1.3.3 NSCLC Treatment Strategies

The response rate to chemotherapy and radiation therapy is frequently lower for NSCLC compared to SCLC. Surgery or chemotherapy combined with surgery may be used for the treatment of patients with resectable cancer (21). TKIs were developed as a result of the identification of mutations of the *EGFR* in NSCLC patients. When compared to traditional chemotherapy, these drugs more than doubled the lifespan of individuals with *EGFR* mutations, revolutionizing the treatment strategies of these patients. The rising incidence of TKI resistance led the gradual development of novel drugs that target various molecular changes and pathways. For instance, crizotinib is currently suggested for patients with *ROS1* rearrangements, alectinib or brigatinib for those with *ALK* rearrangements, and osimertinib, a third-generation anti-EGFR, for those with *EGFR*-mutated NSCLC. Dabrafenib and trametinib can also be used in combination to treat patients with malignancies that have the *BRAF* V600E mutation (22).

2.2 Tumor Metastasis

When cells from a primary tumor separate and move through the bloodstream or lymphatic system to colonize a specific microenvironment and initiate a malignant development, this is referred to as metastasis. As the primary factor affecting a patient's cancer's aggressiveness, prognosis, and course of treatment, metastasis is theoretically the optimal and favored target of therapeutics for cancer management and treatment. Based on the primary tumor, metastasizing cells may travel all through the body, however they frequently target particular organs. For instance, lung cancer generally metastasizes to the bones, adrenal glands, liver, and brain; breast cancer can metastasize to the lungs, brain, and liver (8).

Although metastasis is the main reason why cancer treatments fail and patients die, it is still not fully understood. Cancer cells must leave their primary site, travel through the circulation, tolerate blood vessel pressure, adapt to new biological conditions in a secondary site, and avoid lethal battles with immune cells in order to develop metastases. One of the key characteristics of cancer malignancy continues to be the invasion of local tissue and seeding at distant places that generate metastases. The early stages of the invasion-metastasis cascade are preceded by the cancer cell dissemination. The cascade results from chromosomal instability, which is brought on by persistent errors in the separation of chromosomes in mitosis. Micronuclei rupture and genomic DNA secretion into the cytosol results due to errors in chromosome separation, which then stimulates cytosolic DNA-sensing pathways and downstream NFκB signaling (28).

The transdifferentiation process known as EMT gives altered epithelial cells the capacity to disseminate, invade, and resist stress (28). Initially identified as an essential feature of morphogenesis during embryonic development, the EMT was later discovered to play a role in various kinds of pathogenic processes, such as wound healing, metastasis, and fibrosis. Loss of adhesion junctions and apical-basal polarity, development of the mesenchymal phenotype, and gains in motility and invasion are the distinguishing features of the EMT. Epithelial cells are distinguished by intact cell-cell connections that are facilitated by adhesion molecules such as cytokeratin and E-cadherin (29). EMT mediates the reversible biochemical changes that enable a particular epithelial cell to develop a mesenchymal phenotype and grants epithelial cells epithelial-mesenchymal plasticity, which is essential for the development and metastasis of cancer (28). EMT has been linked to a few developmental signaling pathways, including WNT, RTKs, NOTCH, and tumor growth factor beta (TGF-β), under specific physiological circumstances. EMT is thought to be primarily induced by the cytokine TGF, which is released in the tumor microenvironment by stromal fibroblasts and tumor cells. Epithelial junction protein-coding genes are downregulated as a result of epithelial-mesenchymal transition transcription factor activity. Changes in epithelial junctions have an impact on a variety of downstream pathways that may further encourage EMT and invasion since these junctions not only sustain epithelial structure but also modulate a variety of signaling pathways through their associated proteins. The concept that EMT is a crucial process for efficient metastatic dissemination is solidly established by several research using cancer cell lines, mice tumor models, and human tumor samples (29).

2.2.1 Brain Metastasis

Brain metastases dramatically raise the morbidity and mortality of cancer. Adult intracranial neoplasms are most usually caused by brain metastases, which occurs 10 times more commonly than de novo brain malignancies. A metastatic brain tumor is predicted to appear in approximately 17% of cancer patients at a certain time

throughout treatment. A rise in the prevalence of brain metastasis may derive from improved treatment strategies, greater surveillance techniques, and population-wide cancer burden brought on by an older population (30).

As with any organ, metastasis to the brain necessitates intricate networks that facilitate communication among the invading cell and the local cell population. Tumor cells have the ability to alter the microenvironment before reaching the site of metastasis to make it more favorable for their outgrowth and survival. The development of the pre-metastatic niche is the theory behind this finding. Extracellular vesicles produced by cancer cells have been identified as one of the major contributors to the development of the pre-metastatic niche. Exosomal integrins were profiled in one study, and it was discovered that their distinct expression patterns were associated with organ-specific colonization of the malignant cells in which they were derived. They also discovered that exosomes released by tumors were sufficient to control metastasis to particular organs. The BBB, a continuous endothelium that tightly controls accessibility to the brain, is perhaps the most distinctive barrier preventing metastasis of the brain. This barrier must be penetrated for cells to metastasis to the brain, which can happen if the BBB's structural integrity is compromised. It has been discovered that brain metastatic cells secrete cathepsin S, a protease that breaks down the junctional adhesion molecules and permits the transit of tumor cells (30).

Regardless of the primary tumor type, individuals with brain metastases have a low overall survival of only 6 months. The BBB generally prevents systemic medicines from reaching at the region of a brain metastasis, therefore it is not unexpected that chemotherapy has had unsatisfying efficacy. New small molecule treatments and recent advancements in targeted treatments have shown encouraging outcomes for individuals with brain metastases, particularly when combined to traditional forms of therapy (30).

2.2.2 Leptomeningeal Carcinoma (LMC)

LMC is characterized as a primary solid tumor infiltrating the leptomeninges, which includes the subarachnoid space, arachnoid, and pia mater. Following brain metastases, LMC is the second most common central nervous system (CNS) metastases (31). LMC develops approximately 12% of cancer patients, and individuals with this condition have a short lifespan of only about 6 months following diagnosis. LMC is most frequently caused by lung cancer (9%–25%), melanoma (6%–18%), and breast cancer (5%–8%) (1). The development of better diagnostic and monitoring tools has led to an increase in the prevalence of LMC (31).

2.2.2.1 Pathogenesis of LMC

Following surgery, malignant cells may migrate from the choroid plexus, brain parenchyma, CSF, or blood to settle in the leptomeninges **(Figure 2.2)**. Tumor growth following LMC development may result in hydrocephalus, inflammation, and dysfunction of the cranial nerves (1). New studies are being conducted to understand the molecular mechanisms of the LMC development. It was found that complement component 3 (C3) that is produced by tumor cells found in the CSF, was overexpressed in LMC models of breast cancer and NSCLC. C3 interacts with its receptor on the choroid plexus epithelial cells, disrupting function of the barrier and allowing the passage of mitogen factors, which promote leptomeningeal tumor growth (31).

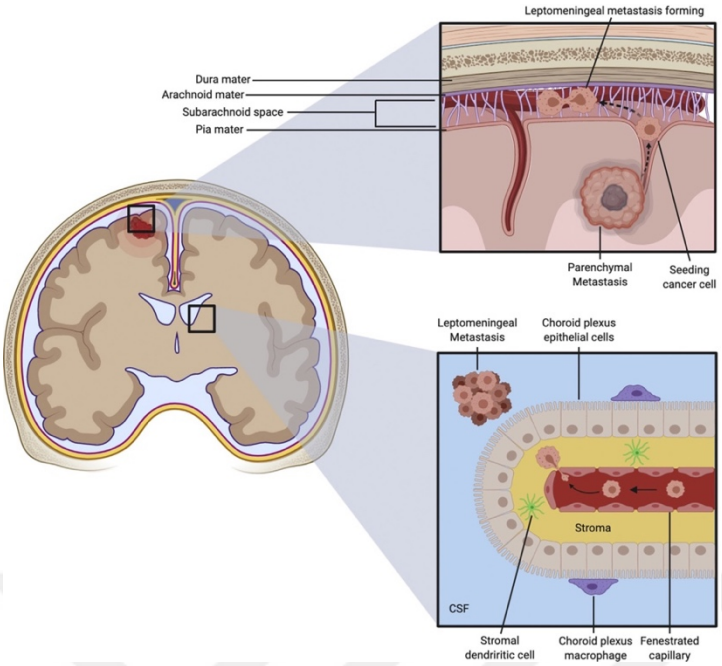

Figure 2.2 Possible routes for leptomeningeal spread. Following surgical resection, tumor cells might spread from the CSF, blood, choroid plexus, or brain parenchyma to seed the leptomeninges (1).

2.2.2.2 Diagnosis of LMC

A combination of neurological testing, a spinal axis and brain MRI, or the detection of tumor cells within the CSF is used to make the diagnosis of LMC (31). The understanding of pathology and biology at the single-cell level has advanced exponentially in recent years, and technical advancements suggest that cell-free nucleic acid assays might replace with solid tissue biopsy. Emerging tools, such as scRNA-seq, are ideally suited to explore the molecular landscapes of widely heterogeneous and inaccessible human malignancies. Recent research has enabled the investigation of circulating tumor cells in CSF, cell-free RNA, and circulating tumor DNA (ctDNA) using a liquid biopsy technique and NGS technology. CSF analysis has great promise not only for diagnosing LMC, but also its epigenetic and genetic characterization, and discovering mechanisms cause resistance in treatment (1).

2.2.2.3 Treatment of LMC

Due to the low rate of incidence, rapid progression of the disease, the diversity of populations of LMC and a lack of sufficient data from randomized trials, the standard of treatment for LMC has not been determined. The goals of LMC treatment are to ameliorate neurologic symptoms and prolong life-expectancy. Intrathecal and systemic chemotherapy, and radiation therapy are available treatments for LMC. Due to the blood-CSF barrier and BBB, it is difficult to administer chemotherapeutic drugs at appropriate dose levels in the CSF area. Individuals who have brain metastases have higher BBB permeability due to tumor disturbance and the impact of antigen-rich regions inside the brain metastases. As systemic chemotherapeutic treatments, high-dose cytosine arabinoside and methotrexate have been utilized for the treatment of LMC, but their efficacy in cases of lung and breast cancer is quite low. In order to overcome challenges with the BBB and blood-CSF barrier, intrathecal chemotherapy was developed. A lumbar puncture or an intraventricular catheter can be used to administer therapeutic agents directly into the CSF area. The most widely utilized intrathecal chemotherapeutic drugs since the invention of the technique include thiotepa, arabinoside and methotrexate. These agents have demonstrated efficacy whether used alone or in combination. The current findings show that the treatment of LMC with molecular targeted drugs with the correct dosage and administration is effective in specific patient groups. For instance, using EGFR TKI in NSCLC-LMC patients with EGFR mutation, and intrathecal administration of trastuzumab in HER2+ breast cancer-LMC patients (32).

2.3 Meta-Analysis

Clinicians must frequently evaluate a considerable amount of new data due to the number of rapid rises in the number of scientific publications. However, since the results of individual studies are not always easily replicated, they are frequently insufficient to provide specific solutions. A meta-analysis is a statistical method for combining the results of multiple studies on a single topic, and it may be useful in resolving discrepancies between studies. By integrating the results of prior research, meta-analysis is a quantitative and objective synthesis of scientific data that overcomes the problem of inadequate sample size and statistical power. It can investigate the causes of heterogeneity and find subgroups connected to the factor of interest, thus offering new perspectives for further research (33).

The Preferred Reporting Items for Systematic Reviews and Meta-Analysis (PRISMA) statement was created in to aid systematic reviewers in transparently describing the review's purpose, the authors' methodology, and the results they found. It was updated in 2020 reporting guidelines that take into consideration advancements in methods for discovering, selecting, analyzing, and summarizing studies. There are 27 items on the checklist, an extended checklist with reporting guidelines for each item, a checklist for abstract, and revised flow diagrams for the original and modified reviews (34).

2.4 Databases and Tools

2.4.1 STRING

Protein regulatory and functional interactions account for a large portion of cellular complexity. Although the fundamentals of these interactions are becoming more understood, new interactions are still being discovered. Protein-protein interactions (PPI), including both physical and functional interactions, are systematically gathered and integrated in the STRING database. The data comes from various sources, such as computerized text mining of published studies, computational interaction estimations from co-expression and interaction experiments databases. Utilizing hierarchical orthology data, each of these interactions is evaluated critically, scored, and then automatically translated to less well-investigate organisms (35)

2.4.2 g:Profiler

Gene lists derived from numerous studies are frequently dealt with in processing biological data. The g:Profiler toolset is frequently used to find biological groups that are enriched in lists of genes, to convert among gene identifiers, and to map to their orthologs. The objective of g:Profiler is to provide a reliable service that makes use of up-to-date, high-quality data in a useful manner across a variety of evidence formats and organisms. The primary data source for g:Profiler is Ensembl. A web design that is both configurable and interactive is used to offer the results. Findings are available for download as delimited text files or visualizations that are publication-ready (36).

2.4.3 Cytoscape

An open-source software, Cytoscape combines data of high-throughput expression with networks of biomolecular interactions into a single framework. Network layout, visual integration of the network with phenotypes, expression profiles, and connection to functional annotations databases are all features that are provided with the Core software of Cytoscape. A simple plug-in architecture makes the core flexible, enabling the quick creation of new computational studies and functionalities (37).

The plug-in “Enrichment Map” is network-based method for visualizing the results of gene-set enrichment analysis. Gene-sets are arranged in a network, with each set acting as a node, and the edges connecting sets signifying gene overlap (38) “MCODE” plug-in stands for "Molecular Complex Detection" and it finds densely connected regions in huge PPI networks. By removing the dense areas surrounding a protein of interest, MCODE also enables managing the visualization of huge networks possible (39).

2.4.4 Drug Gene Interaction Database (DGIdb)

DGIdb, which was created in 2013, presents information about drug-gene interactions and genes that can be druggable. It makes use of resources such as database, articles, and other online sources to produce theories regarding the potential therapeutic targeting or drug development priorities for altered genes. New data sources are added with the new updates, several enhancements are made to search results, and drug normalization was enhanced (40).

2.4.5 National Cancer Institute (NCI)

One of the National Institutes of Health's (NIH) institutes and centers is the NCI, and it is the main federal organization in responsible of both conducting and funding research on cancer. NCI improves the quality of care for every cancer patient and decreases the burden caused by cancer (41). Its website contains all kinds of information regarding to cancer, such as its diagnosis and treatment, including the list of drugs approved by the US Food and Drug Administration (FDA) for particular cancer types. FDA is essential to both the economy and patient treatment. For patients and clinicians to be able to trust that approved pharmaceuticals will work as intended and be relatively safe, the FDA enforces standards set forth by Congress for the efficacy and safety of prescribed drugs (42).

2.4.6 ClinVar

ClinVar is an open-access, publicly available archive of human genetic variants and analyses of their relevance to disease, and it is preserved at the NIH. ClinVar receives claims of the clinical relevance of a variant/set of variants from clinical test centers, research laboratories, panels, databases, and other organizations. On its website, a set of variant call format files containing the data gathered by the variant are available. ClinVar has lately begun accepting submissions, which are mainly concerned with offering phenotypic details to those who have undergone genetic testing, and it keeps enhancing its retrieval and search capabilities (43).

2.4.7 dbSNP: Single Nucleotide Polymorphism (SNP) Database

The relationship between sequence variation and heritable traits is a crucial area of genetics research. SNPs are one of the most frequent genetic variations. Along with the National Human Genome Research Institute, the SNP Database was created by the National Center for Biotechnology Information. Data from Human Genome Project, PubMed, GenBank, and LocusLink are integrated with entries to dbSNP. Other laboratories may utilize the sequencing details regarding the polymorphism and the particular experimental settings for further studies after such variations are detected and cataloged in the database (44).

2.4.8 COSMIC

The most thorough and in-depth tool for examining somatic mutations' effects on human cancer is COSMIC, the Catalogue of Somatic Mutations in Cancer. Qualified manual curators examine and analyze academic journals to extract the specific mutation information and any other relevant data, such as environmental parameters or predisposition of patients that may be available. These data are then used to create COSMIC's main data set. A second curation method operates concurrently with this extensive procedure and contributes a substantial amount of information to COSMIC through main cancer data portals, as well as from supplemental tables and downloads of publications that have been carefully selected. A combination of these data makes COSMIC the main resource to investigate the etiology and mutational landscape of human cancer (45).

3. MATERIALS AND METHODS

3.1.1 Part I: Mutated Genes in Leptomeningeal Carcinoma Caused by Non-Small Cell Lung Cancer

3.1.1 Meta Analysis

The meta-analysis was carried out and reported in accordance with the PRISMA declaration guidelines (34).

3.1.2 Literature search

The Medical Subject Headings (MeSH) indexing terms and keywords linked with leptomeningeal carcinoma were used in a literature search on the PubMed database.

Search query on PubMed: (Leptomeningeal carcinomatosis OR leptomeningeal carcinoma OR leptomeningeal disease OR leptomeningeal metastases OR leptomeningeal metastasis) AND (liquid biopsy OR cerebrospinal fluid OR cerebral spinal fluid OR circulating tumor cells) AND (Next-generation sequencing OR RNA sequencing OR whole exome sequencing OR mutation OR non-small cell lung cancer OR NSCLC OR breast cancer OR melanoma) NOT (review OR drug trial OR clinical trial).

The search was conducted in English without the application of any further publication restraints. The studies that presented mutant genes among LMC patients and were published between February 16, 2012, and February 16, 2022, were included in this analysis. This time period was chosen to incorporate more recent investigations, highlighting the importance of sequencing technologies. Although an investigation of the grey literature was not done, citations from articles that were included were also examined in the review procedure.

3.1.3 Criteria for Inclusion and Exctraction

Clinical studies that applied NGS to breast cancer, melanoma, or NSCLC-related LMC patients were included.

Studies that failed to apply NGS to CSF samples, failed to offer correct information on mutant genes, were conference abstracts, editorials, or reviews, or whose main goal was the detection of malignancies were all disqualified. Studies that did not involve the use of human subjects were likewise disqualified. **(Figure 3.1)**. As stated in the following steps and depicted in **Figure 3.2**, a workflow was followed.

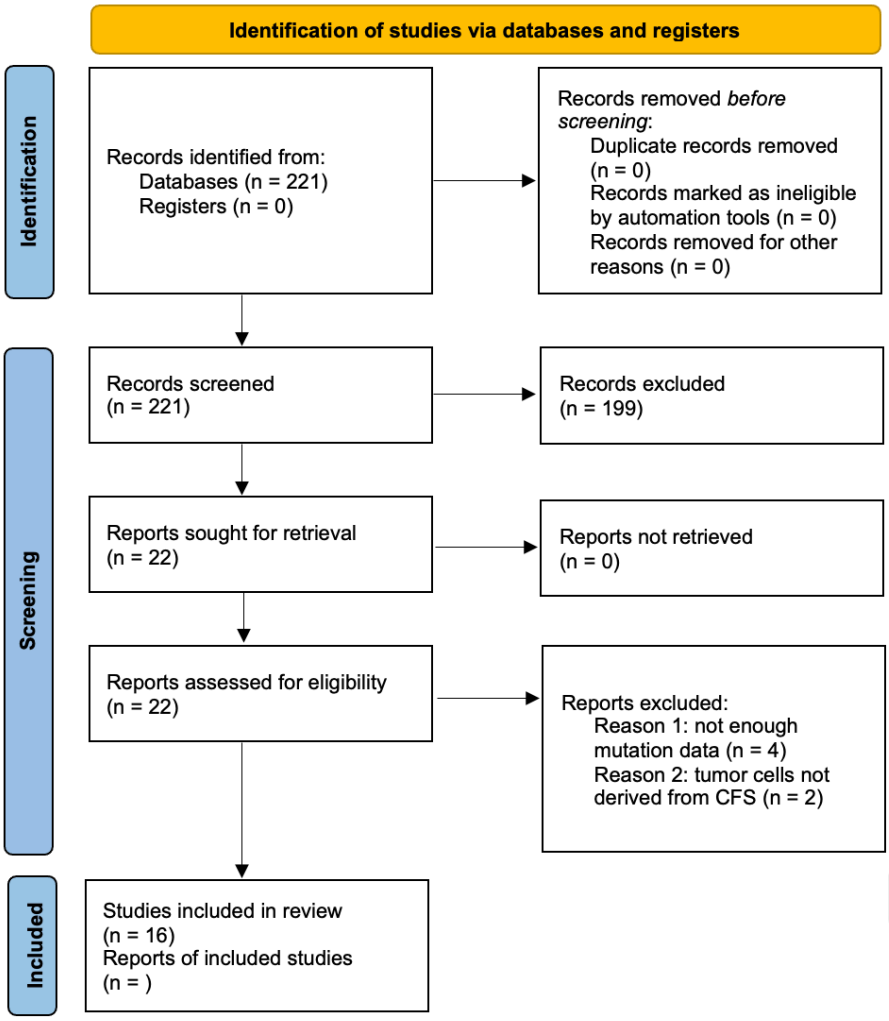

Figure 3.1 Flow diagram of the study selection

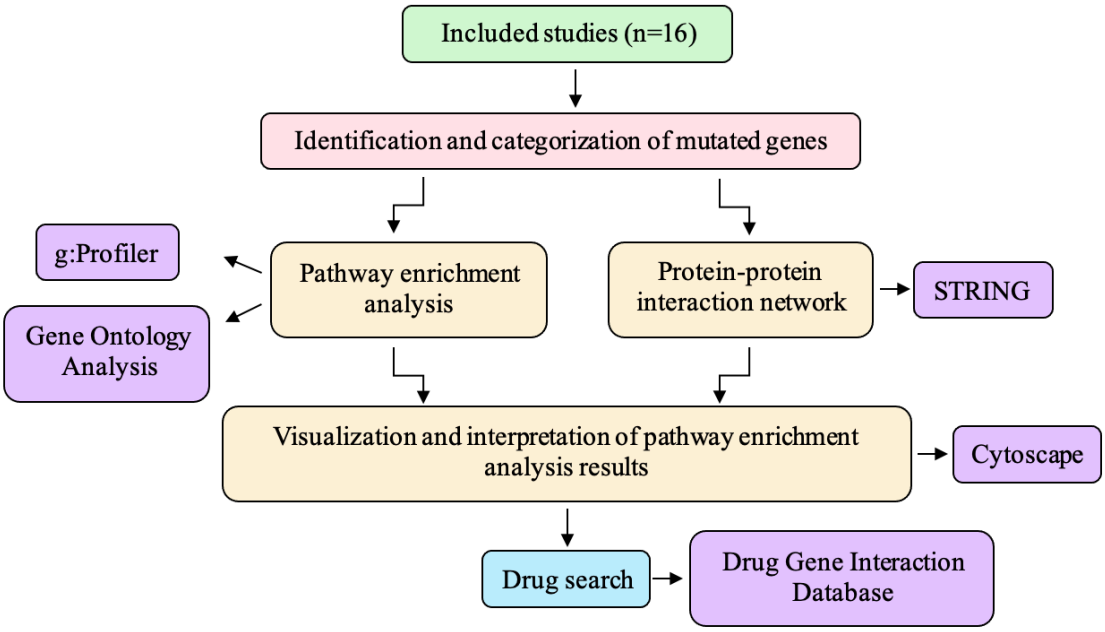

Figure 3.2 Systematic workflow of the methodology.

3.1.4 Mutated gene identification and classification

On the basis of the primary tumor site, 16 papers were divided into three categories: 11 NSCLC-LMC, 3 breast-LMC, and 2 melanoma-LMC **(Table 3.1)**. Three primary cancers had different formation cause and prevalence.

As a result, the selected studies omitted to include the detailed patient characteristics (age, gender, initial tumor mutation, treatment prior to LMC diagnosis, and NGS), but they contained the mutant genes identified by NGS applied to CSF samples of LMC patients. This data was gathered from “results” or “supplementary information” of each study. Mutated genes found in only one patient were excluded. Further investigations were done with the mutated genes found in two and more patients (n≥2, n=patient number).

Table 3.1. Articles included in the current study.

Study	Author	Primary Tumor Location
Recurrently Mutated Genes Differ between Leptomeningeal and Solid Lung Cancer Brain Metastases (46)	Li Y et al. 2018	NSCLC
Detection of Driver and Resistance Mutations in Leptomeningeal Metastases of NSCLC by Next-Generation Sequencing of Cerebrospinal Fluid Circulating Tumor Cells (47)	Jiang et al. 2017	NSCLC
Unique genetic profiles from cerebrospinal fluid cell-free DNA in leptomeningeal metastases of EGFR-mutant non-small-cell lung cancer: a new medium of liquid biopsy (48)	Li YS et al. 2018	NSCLC
Unique genomic profiles obtained from cerebrospinal fluid cell-free DNA of non-small cell lung cancer patients with leptomeningeal metastases (49)	Shenpeng et al. 2019	NSCLC
Unique Genomic Alterations of Cerebrospinal Fluid Cell-Free DNA Are Critical for Targeted Therapy of Non-Small Cell Lung Cancer with Leptomeningeal Metastasis (50)	Wang et al. 2021	NSCLC
Circulating tumor cell characterization of lung cancer brain metastases in the cerebrospinal fluid through single-cell transcriptome analysis (2)	Ruan et al. 2020	NSCLC
Different next-generation sequencing pipelines based detection of tumor DNA in cerebrospinal fluid of lung adenocarcinoma cancer patients with leptomeningeal metastases (51)	Ge et al. 2019	NSCLC
Detection of circulating tumor DNA from non-small cell lung cancer brain metastasis in cerebrospinal fluid samples (52)	Ma et al. 2020	NSCLC
Clinical Utility of Cerebrospinal Fluid Cell-Free DNA as Liquid Biopsy for Leptomeningeal Metastases in ALK-Rearranged NSCLC (53)	Zheng et al. 2019	NSCLC
Brain tumor mutations detected in cerebral spinal fluid (54)	Pan et al. 2015	NSCLC
Cell-Cycle and DNA-Damage Response Pathway Is Involved in Leptomeningeal Metastasis of Non–Small Cell Lung Cancer (55)	Fan et al. 2018	NSCLC
Genotyping tumour DNA in cerebrospinal fluid and plasma of a HER2-positive breast cancer patient with brain metastases (56)	Siravegna et al. 2017	Breast cancer
Clinical significance of detecting CSF-derived tumor cells in breast cancer patients with leptomeningeal metastasis (57)	Li X et al. 2017	Breast cancer
Cerebrospinal fluid-derived circulating tumour DNA better represents the genomic alterations of brain tumours than plasma (58)	De Mattos-Arruda et al. 2015	Breast cancer
Tumor DNA in cerebral spinal fluid reflects clinical course in a patient with melanoma leptomeningeal brain metastases (59)	Li Y et al. 2016	Melanoma
Evaluating Circulating Tumor DNA From the Cerebrospinal Fluid of Patients with Melanoma and Leptomeningeal Disease (60)	Ballester et al. 2018	Melanoma

NSCLC, non-small cell lung cancer

3.1.5 Protein-protein interaction (PPI) network construction

This thesis study was continued with 11 NSCLC-LMC articles. For each mutated genes in NSCLC-LMC, The STRING database, version 11.5, (http://string-db.org/) (61) was used to create the PPI network. Full STRING network and confidence boxes were marked in the default configuration.

3.1.6 Pathway enrichment analysis

The pathway enrichment analysis was conducted using g:Profiler (https://biit.cs.ut.ee/gprofiler/gost) (36) version e105_eg52_p16_e84549f (database updated on 03/01/2022). The ordered query box was selected in the options section following choosing *Homo sapiens* as the specific organism (62). After that, for GO analysis, section biological process (GO: BP) and for biological pathways part Reactome database were selected. For advanced options, “only annotated genes” for statistical domain scope, “g:SCS threshold” for significance threshold and “0.05” for user threshold were chosen.

3.1.7 Visualization and interpretation of pathway enrichment analysis results

In order to be edited, the string output was uploaded to Cytoscape (https://cytoscape.org) version 3.9.1 (37). The results of g:Profiler was then visualized and interpreted using a pathway network that was built in Cytoscape using the result files. The software's EnrichmentMap and MCODE plug-ins were employed. FDR Q value cutoff had been adjusted to 0.01 in the input panel of EnrichmentMap number of nodes section (62). Predetermined parameters were utilized to determine the number

of edges. Default parameters were applied in the input panel of MCODE: degree cutoff = 2, node score cutoff = 0.2, k-score = 2, and max. Depth = 100.

3.1.8 Investigation of *EGFR* mutations

From the 11 publications that made up this meta-analysis, *EGFR* mutation information was obtained. The mutations were searched using the databases ClinVar (https://www.ncbi.nlm.nih.gov/clinvar)(43),dbSNP(https://www.ncbi.nlm.nih.gov/snp/) (44), and COSMIC (https://cancer.sanger.ac.uk/cosmic) (45).

3.1.9 Drug Search

The National Cancer Institute (https://www.nih.gov/) (63) was utilized to identify NSCLC treatment options that have received FDA approval. Drugs unable to traverse the BBB were removed. The interaction between the altered genes in NSCLC-LMC and drugs that may pass through the BBB has been identified using DGIdb (https://www.dgidb.org/) version v4.2.0 - sha1 (accessed on 28.03.2023) (40).

3.2. Part II: The Effects of Overexpressed *SLPI* cDNA in the A549 Cell Line

3.2.1 Mammalian Cell Culture and Maintenance

3.2.1.1 Cell Lines and Media

Non-small cell lung cancer cell line A549 was cultured in high glucose DMEM (Gibco™, catalog no. 11965092) containing 10% Fetal Bovine Serum (FBS) (Gibco™, catalog no. 10270106) and 1% pen-strep (Gibco™, catalog no. 15140122).

3.2.1.2 General Cell Culture Procedures

3.2.1.2.1 Freezing A549 Cells

Freezing Medium: All the cells were frozen in medium containing DMSO at a final concentration of 10% (v/v) at -80°C in Mr. Frosty for 3 days then stored in liquid nitrogen.

3.2.1.2.2 Thawing Frozen A549 Cell Line

The cell suspension, which was preserved in the liquid nitrogen tank, was thawed in a 37°C water bath until a small portion remains frozen. Then cells were

dropwise diluted into a 5mL high glucose DMEM containing falcon tube and centrifuged at 1500 rpm for 5 min. The supernatant was discarded, pellet was resuspended with 10mL high glucose DMEM, and transferred to 10cm cell culture plate. The cells were incubated at 37°C, 5% CO_2.

3.2.1.2.3 Passaging of Cell Line

The medium was aspirated from the plate. The plate was washed with 10mL 1xPhosphate-buffered saline (PBS, Gibco™, catalog no. 10010023). Cells were treated with 2mL trypsin-EDTA (Gibco™, catalog no. 25200056) for 2 minutes at 37°C, 5% CO_2 for the detachment of cells from the plate surface. Growth medium was added to the plate to inactivate trypsin-EDTA. The cell suspension was centrifuged at 1500 rpm for 5 min. The pellet was resuspended with 10 mL high glucose DMEM and transferred to a 10mL cell culture plate. The cells were incubated at 37°C, 5% CO_2.

3.2.1.2.4 Cell Counting

Cells were mixed with trypan blue at a ratio of 1: 1 (v/v). The cell suspension was loaded on a hemocytometer. Cells were counted in 4 quadrants at 10X and then the cell viability was calculated by taking the average of 4 quadrants and multiplying by 10^4 and dilution factor.

$$\frac{(\text{\# of cells in 4 quadrants})}{4} \times 10^4 \times \text{dilution factor} \times (\text{Volume of DMEM that was used to suspend the cells.})$$

3.2.2 Protein Isolation

The medium was aspirated from the plate. The plate was washed with 5mL cold 1X PBS. Another 5 mL cold PBS was added, and cells were scraped with a cell scraper and collected in a falcon, and then centrifuged at 1500 rpm for 5 min. The supernatant was discarded, and the pellet was stored at -20°C until it was used.

200µL RIPA buffer (A.B.T., catalog no. B08-01-01) containing 1X protease inhibitor cocktail (BOSTER, catalog no. AR1182) was added to the pellets and incubated on ice for 30 minutes and vortexed with five minutes intervals. After the 20 minutes of centrifugation at 13000 rpm and 4°C, the supernatant was transferred to a new eppendorf while being careful to not lose the pellet.

3.2.2.1 BCA Protein Assay

BCA protein assay kit (Thermo scientific, catalog no. 23225) was used to measure absorbance values of isolated proteins. 2 mg/mL albumin standard was taken, and three sets of protein standards were prepared: 20µg/µL, 15µg/µL, 10µg/µL, 7.5µg/µL, 5µg/µL, 2.5µg/µL, 1.25µg/µL, and 0.25µg/µL as well as a blank tube containing RIPA buffer only. 10µL of standards and protein samples were loaded into 96-well plate in three replicas. 200µL of working reagent (prepared with mixing 50 parts of BCA reagent A with 1 part of BCA reagent B) was added in each well and incubated at 37°C for 30 minutes, and then plate was placed into Varioskan (microplate reader) absorbance was measured at 562nm. An absorbance vs concentration curve was plotted in excel, trendline, R square, and equation was added. Concentration of the protein samples were calculated from the equation.

3.2.3 RNA Isolation

Harvesting Cells for RNA Isolation: The medium was aspirated from the plate. The plate was washed with 10mL PBS. Cells were treated with trypsin-EDTA for 3 minutes at 37°C, 5% CO_2. 5mL of high glucose DMEM was added, and cells were centrifuged at 1500 rpm 5 min. The supernatant was discarded, and the pellet was stored at -80°C until it was used.

Before isolation all the equipment was cleaned with RNAse ZAP. iNtRON Biotechnology RNA-spinTM Total RNA Extraction Kit (for Cell/Tissue) was used to isolate total RNA from A549 cell line. Pellet was loosened thoroughly by repetitive tapping the tube before use. It was ensured that ß-mercaptoethanol was added to the R-buffer. 350µL of freshly prepared R-buffer was added with a syringe and homogenized by pipetting 10 times. 1 volume of R-buffer of 70% EtOH was added to the lysate and mixed thoroughly by pipetting. Cell lysates were loaded into the column and then centrifuged at 13,000rpm for 30 sec. The supernatant was discarded. 700µL of washing buffer A was added to the column and then centrifuged at 13,000rpm for 30 sec. The supernatant was discarded and 700µL of washing buffer B was added to the column and centrifuged at 13,000rpm for 30 sec. The flow-through was discarded and then the sample was centrifuged for 2 min at 13,000rpm in order to dry the RNA-spinTM membrane. The column was placed in a new 1.5mL tube. 50µL of RNAse free ddH_2O was added onto the membrane and incubated at room temperature for 1 min, and then it was centrifuged for 1 min at 13,000rpm to elute. RNA concentration was measured and stored at -80°C until it was used.

3.2.4 Primer Design

SLPI cDNA sequences were obtained from the ENSEMBL database (https://www.ensembl.org/index.html) (64) and restriction enzymes (RE) with "0 cutter" were searched in the NEBcutter software (http://nc2.neb.com/NEBcutter2/) (65), inorder to choose a RE that does not digest the cDNA sequence. The restriction enzymes *Eco*RI and *Kpn*I, which can be cloned with N-Terminal p3XFLAG-CMV plasmid, have also been chosen as suitable enzymes for *SLPI* gene. Primers were purchased from Thorvacs Biotechnology LLC.

*Eco*RI restriction site is 5'...GAATTC...3'.

*Kpn*I restriction site is 5'...GGTACC...3'.

UCSC in-silico PCR (http://genome.cse.ucsc.edu/cgi-bin/hgPcr) (66) and NCBI Primer-BLAST (https://www.ncbi.nlm.nih.gov/tools/primer-blast/) (67) were used to find GC content and melting temperatures of the primers that were designed **(Table 3.2)**.

Table 3.2 Sequences of designed primers

SLPI Forward: *Eco*RI GC: 57.14% Tm: 69.75°C	5’ GCGAATTCAAAGTCCAGCGGCCTCTTCC 3’
SLPI Reverse: *Kpn*I GC: 56.67% Tm:70.71°C	5’GCGGTACCTCAAGCTTTCACAGGGGAAACG3’
FLAG TAG Forward: GC: 47,6% TM: 56.6 ºC	5’ GACTACAAAGACCATGACGGT 3’

3.2.2.5 cDNA Synthesis

Vazyme HiScript III RT SuperMix for qPCR (+gDNA wiper) kit was used to convert A549 RNA to cDNA. Before usage, each component was completely thawed and mixed and the reaction was set on ice.

An RNase-free centrifuge tube was used for mixing the subsequent components are listed in **Table 3.3.**

Table 3.3 Components for the removal of genomic DNA

RNase-free ddH_2O	up to 16μL
4 × gDNA wiper Mix	4μL
Template RNA	1000ng

Components were pipetted up and down several times to mix thoroughly, then incubated at 42°C for 2 min. 4µL of 5 × HiScript III qRT SuperMix was added to the mixture of previous step to prepare reverse transcription reaction mixture. Thermocycling conditions for cDNA synthesis are listed in **Table 3.4**. QI amplifier 96 PCR equipment was used.

Table 3.4 Thermocycling conditions for cDNA synthesis

Temperature	Duration
50°C	15 min
85°C	5 sec

3.2.6 Polymerase Chain Reaction (PCR)

New England BioLabs Taq DNA Polymerase with Standard Taq (Mg-free) Buffer kit (M0320S) was used to amplify the *SLPI* gene from cDNA. *Cyclophilin A* forward and reverse primers were used as positive control. Before usage, each component was completely thawed and vortexed briefly and the PCR reaction was set on ice. All components listed in **Table 3.5** were mixed in a PCR tube and spun down briefly. The reaction was run at the thermal cycler conditions listed in **Table 3.6.** Thermocycling conditions for PCR are listed in **Table 3.7.** QI amplifier 96 PCR equipment was used.

Table 3.5 Primer Sequences of *Cyclophilin A*

CYCLOPHILIN A Forward: GC: 55% TM: 61.18	5'AATGGCACTGGTGGCAAGTC 3'
CYCLOPHILIN A Reverse: GC: 55% TM: 59.82	5' GCTCCATGGCCTCCACAATA 3'

Table 3.6 PCR kit components

Component	Volume	**Final concentration**
10X Standard Taq Reaction Buffer	2.5µL	1X
25mM MgCl2	1.5µL	1.5mM
10mM dNTPs	0.5µL	200µM
10µM Reverse Primer	0.5µL	0.2µM
10µM Forward Primer	0.5µL	0.2µM
Template DNA	1µL	<1.000ng
Taq DNA Polymerase	0.125µL	1.25 units/ 50µL PCR
Nuclease-Free Water	Up to 25µL	

Table 3.7 Thermocycling conditions for PCR

Step	Temperature	Duration	Cycle
Initial Denaturation	95°C	30 seconds	1
Amplification	95°C	30 seconds	30
	65°C	30 seconds	
	68°C	30 seconds	
Final Extension	68°C	5 minutes	1

3.2.7 Agarose Gel Electrophoresis

1.5% agarose gel was prepared: 0,9g of agarose and 60mL of 1X TAE were put in a beaker, it was microwaved until agarose dissolved completely and it was checked occasionally to avoid boiling. When the mixture was cooled down, 1µL DNA stain (purchased from SERVA, catalog number: 39803) was added. The comb was placed in the electrophoresis tank, and then the agarose gel was poured. After the gel was solidified the comb was gently removed.

1µL of agarose gel loading dye was mixed with 5µL PCR product on a parafilm. Sample mixture was loaded into respective well of agarose gel. A cover is placed on the electrode box and gel was electrophoresed at 84V for 35 minutes. DNA fragments were visualized in the Bio-Rad ChemiDoc MP Imaging System.

3.2.8 Gel Extraction

GeneAll® Expin™ Gel SV kit was used to perform gel extraction to reverse transcriptase (RT)-PCR product. Before using it for the first time, absolute ethanol was added into buffer NW as demonstrated. Using a transilluminator and a razor blade that had been cleaned with ethanol, the DNA band of SLPI was excised. Gel slice was weighed in a 15mL falcon tube. 3 volumes (µL) of Buffer GB were added to 1 volume (mg) of gel. The sample was incubated at 50°C until the agarose gel was melted completely (5 to 10 min). Throughout the incubation, the tube was vortexed every 2 to 3 minutes. The color of the solution was examined for yellowness after the gel had completely dissolved. Isopropanol was added to the sample in a volume equal to one gel volume and vortexed to mix. The solution was transferred to a Column Type D (mini) and centrifuged for 1 min at 12,000 rpm. The supernatant was discarded. 500µL

of Buffer GB was added into the column and centrifuged for 30 sec at >12,000 rpm. The supernatant was discarded. 700µL of Buffer NW was added into column and centrifuged for 30 sec at at >12,000 rpm. The supernatant was discarded. To eliminate any remaining wash buffer, the sample was centrifuged for an additional minute at maximum speed. The mini column was transferred to a new 1.5mL tube. 50µL sterile ddH_2O was added into the center of the membrane in the column, incubated for 1 min and then centrifuged for 1 min at >12,000 rpm. The concentration of the extracted product was measured and stored at -20°C until it was used.

3.2.9 PCR Purification

GeneAll - Expin PCR SV kit was used for purification of digested N-Terminal p3xFLAG-CMV vector and gel extraction product when required. 5 volumes of Buffer PB were added to 1 volume of the sample and mixed. The solution was transferred to an SV column and then centrifuged for 30 sec. The supernatant was discarded. 700uL of Buffer NW was added and then centrifuged for 30 sec. The supernatant was discarded. To remove any remaining wash buffer, the mixture underwent an additional minute of centrifugation. The SV column was transferred to a new 1.5mL tube. 50uL ddH_2O was added to the center of the membrane in the SV column, incubated for 1 min, and then centrifuged for 1 min.

3.2.10 Restriction Enzyme Digestion

*Eco*RI and *Kpn*I restriction enzymes from New England Biolabs were used for digestion of N-Terminal p3xFLAG-CMV vector and SLPI RT-PCR product. The following reaction was set on ice. All components listed in **Table 3.8** were mixed in a PCR tube and spun down briefly. The mixture was incubated at 37°C for 1 hour.

Table 3.8 Enzyme digestion kit components

Components	50µL Reaction	Final Concentration or amount
DNA		1ug
10X NEBuffer (rCutSmart)	5µL	1X
Restriction Enzyme (*Eco*RI and *Kpn*I)	1uL	10 units
Nuclease-free water	up to 50µL	

3.2.11 Ligation

T4 DNA Ligase from New England Biolabs was used for ligation of purified *SLPI* cDNA sequence (insert DNA) with N-Terminal p3xFLAG-CMV vector. All components listed in **Table 3.9** were mixed in a PCR tube and spun down briefly. The mixture was incubated at 25°C for 1 hour.

Table 3.9 Components of ligation with molar ratio of 1:3 and 1:6 vector to insert

Components	20µL Reaction
T4 DNA Ligase Buffer (10X)*	2µL
Vector DNA	50ng
Insert DNA**	9.281ng / 18.562ng
T4 DNA Ligase	1µL
Nuclease free water	up to 20µL

* At room temperature, the T4 DNA Ligase Buffer was thawed and resuspended.
** 9.281ng DNA was used for 1:3 ratio, 18.562ng DNA was used for 1:6 ratio

3.2.12 Cloning of *SLPI* cDNA Into N-Terminal p3xFLAG-CMV Vector

E. coli DH5α strain was stored at -80°C. Bacterial culture medium was prepared with 25g/L LB (Caisson, catalog no. LBP01) and 15g/L agar (Caisson, catalog no. LBP04) and then autoclaved at 121°C for 20 min. 100µL/mL ampicillin was used as antibiotics. Culture was stored at 4°C.

3.2.12.1 Transformation

N-Terminal p3xFLAG-CMV vector represented in **Figure 3.3** and competent cells were gifts from Asst. Prof. Dr. Nazlı Keskin Toklu. Transformation of N-Terminal p3xFLAG-CMV vector and ligation product into *E. coli* were performed separately. 50µL component cells, 1ng/µL N-Terminal p3xFLAG-CMV vector, and 5µL of ligation product were used.

Plasmid and competent cells were thawed on ice. Competent cells were mixed with plasmid DNA by fingertipping and then the mixture was incubated on ice for 30 min. Cell suspension was subjected to a heat shock procedure that involved incubating them at 42°C for 30 seconds and then incubating for two minutes. Up to 1mL of LB was added and then incubated at 250 rpm and 37°C rpm for 1 hour in the shaker. Cells were centrifuged at 5000 rpm for 5 min. 900µL of supernatant was discarded. 100µL cell suspension was spread on ampicillin containing LB agar plates with a spreader. Plates were incubated at 37°C overnight. After overnight incubation replica plate was prepared with respective colonies.

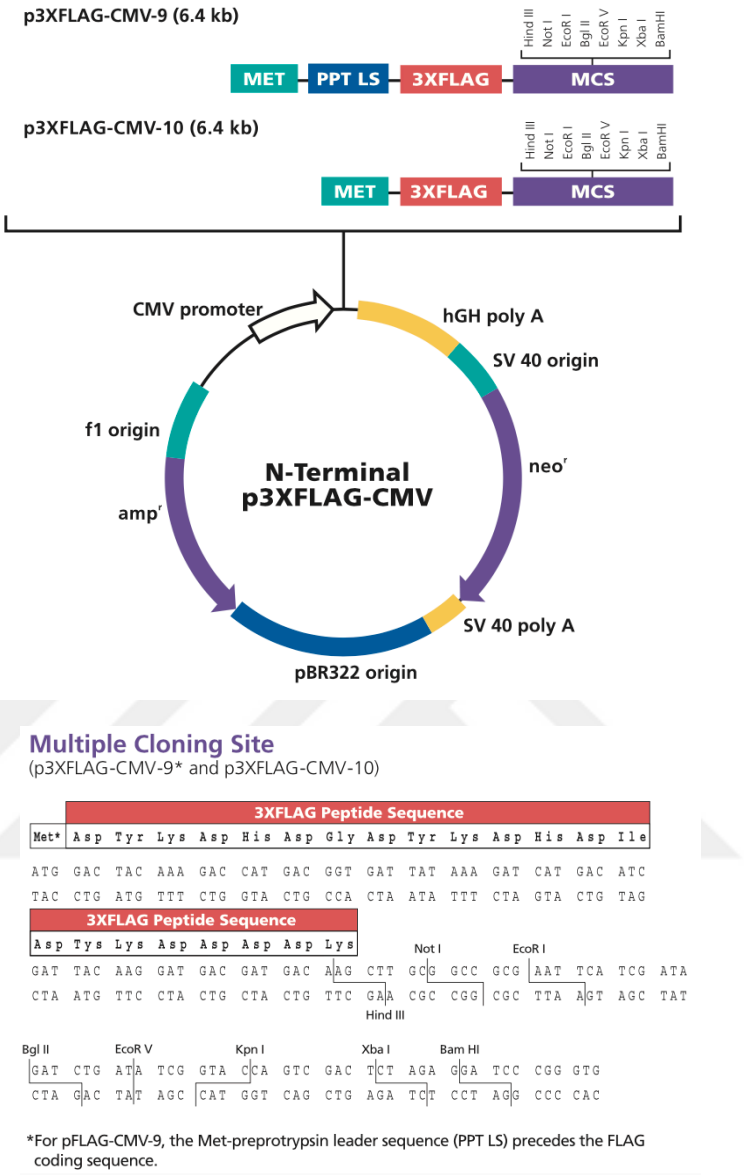

Figure 3.3 N-Terminal p3XFLAG-CMV vector (Sigma-Aldrich, catalog no. E9783) used in this thesis.

3.2.12.2 Transformation Efficiency

The colony numbers of overnight cultures were used to determine the transformation efficiency; the following formula was used:

$$\frac{\text{n (transformants)}}{\mu\text{g of DNA}} \times \frac{\text{final volume at recovery (mL)}}{\text{volume plated (mL)}}$$

The colonies formed after the transformation were transferred to a replica plate with ampicillin and the presence of inserts in them was confirmed with colony PCR.

3.2.12.3 Colony PCR

In order to confirm the existence of *SLPI* gene, colony PCR was carried out from the replica plate. During the transfer of the colonies to a replica a small smear from the colonies were dipped into the PCR mix and the DNA were amplified at the below listed conditions **(Table 3.10** and **Table 3.11).**

Table 3.10 Colony PCR kit components

Component	Volume	**Final concentration**
10X Standard Taq Reaction Buffer	2.5µL	1X
25mM MgCl2	1.5µL	1.5 mM
10mM dNTPs	0.5µL	200µM
10µM Reverse Primer	0.5µL	0.2µM
10µM Forward Primer	0.5µL	0.2µM
Template DNA	1µL	<1.000 ng
Taq DNA Polymerase	0.125µL	1.25 units/ 50µL PCR
Nuclease -Free Water	Up to 25µL	

Table 3.11 Thermocycling conditions for colony PCR

Step	Temperature	Duration	Cycle
Initial Denaturation	95°C	30 seconds	1
Amplification	95°C	30 seconds	30
	65°C	30 seconds	
	68°C	30 seconds	
Final Extension	68°C	5 minutes	1

3.2.12.4 Miniprep Plasmid DNA Isolation

GeneAll® Exprep™ Plasmid SV mini (101-150, 101-102) was used to perform plasmid miniprep to N-Terminal p3xFLAG-CMV and *SLPI* ligated vector containing bacterial cultures.

Transformed *E. coli* were cultured in 5 mL LB with %1 ampicillin at 250 rpm and 37°C overnight. Before using it for the first time, absolute ethanol was added into buffer AW and PW as described. RNase A was added into buffer S1 before first use and buffer S1 was stored at 4°C after addition of RNase A.

Preparation of Cleared Lysate: The bacterial culture was centrifuged for 5 min at 10,000 x g. Supernatant was discarded. Pelleted bacterial cells were resuspended thoroughly in 250µL of buffer S1. Suspension was transferred to a new 1.5mL tube. 250µL of buffer S2 was added and then mixed by inverting the tube four times. 350µL of buffer S3 was added and immediately mixed by inverting the tube 4 to 6 times. The mixture was centrifuged for 10 min at full speed.

Isolation and Purification of Plasmid DNA: Centrifugation Protocol: The supernatant was transferred carefully to an SV column by pipetting. The mixture was centrifuged for 30 sec at full speed. The supernatant was discarded. 700uL of buffer PW was added and then centrifuged for 30 sec at full speed. The supernatant was discarded. To remove any remaining wash buffer, the mixture underwent an additional minute of centrifugation. The SV column was transferred to a new 1.5mL tube. 30µL ddH_2O was added, incubated for 1 min, and then centrifuged for 1 min. The concentration of the isolated product was measured.

PCR was performed as described in section 3.2.6 with the purified plasmids to verify the presence of the insert and sent to Macrogen for sequencing.

3.2.12.5 Glycerol Stock Preparation and Inoculation

Glycerol stocks of *E. coli* transformed with N-Terminal p3xFLAG-CMV vector and *E. coli* transformed with *SLPI* overexpression vector, were prepared. Transformed *E. coli* was mixed with 50% sterile glycerol at a ratio of 1: 1 (v/v) and stored at -80°C. Also, the colony that had the correct *SLPI* cDNA sequence in it (SLPI culture) was cultured in 25mL LB at 250 rpm and 37°C overnight. *SLPI* culture was mixed with 50% sterile glycerol at a ratio of 1: 1 (v/v) and stored at -80ºC.

In order to recover the transformed bacteria from glycerol stock, some of the frozen bacteria were scraped slightly from the surface of the stock using a pipette tip, inoculated to a 5mL LB tube with %1 ampicillin and the tube was incubated at 250 rpm and 37°C for 2 hours. 1mL from the culture was added to 24mL LB with 24uL ampicillin for overnight incubation at 250 rpm, 37°C.

3.2.12.6 Midiprep Plasmid DNA Isolation

PureLinkTM HiPure Plasmid DNA Purification Kit was used to perform plasmid midiprep to glycerol stock of *E. coli* transformed with N-Terminal p3xFLAG-CMV vector and *E. coli* transformed with *SLPI* overexpression vector, which had the correct sequence of the desired gene.

Before usage RNase A was added to resuspension buffer as described. 10mL equilibration buffer was added to the HiPure Midi Column. Solution was drained by gravity flow. Cells were centrifuged at 4,000 × g for 10 min. Supernatant was discarded. 4mL resuspension buffer containing RNase A was added to the cell pellet and the pellet was resuspended until it was homogeneous. 4mL lysis buffer was added and mixed by inverting until the mixture was homogeneous and then incubated at room temperature for 5 minutes. 4 mL precipitation buffer was added and mixed by inverting the tube until the mixture was homogeneous. The lysate was centrifuged at >12,000 × g for 10 min at room temperature. Supernatant was loaded onto the equilibrated column. Solution was drained by gravity flow. 10mL wash buffer was added to the column. The supernatant was discarded. This step was repeated twice. A sterile 15mL centrifuge tube was placed under the column and 5mL elution buffer was added. Solution was drained by gravity flow. The elution tube contained the purified DNA. 3.5mL isopropanol was added to the eluate and mixed thoroughly. The mixture was centrifuged at >12,000 × g for 30 minutes at 4°C. The supernatant was discarded. The pellet was washed in 3mL 70% ethanol and then centrifuged the tube at >12,000 × g for 5 minutes at 4°C. The supernatant was discarded. The pellet was air-dried for 10 min, then purified plasmid DNA was resuspended in 100µL sterile ddH_2O. Plasmid DNA concentration was measured and was stored at −20°C until it was used.

3.2.13 G418 Kill Curve Assay

Cell density of 2 x 10^5 adherent A549 cells were plated in an antibiotic-free growth medium in a 24-well cell culture plate and then incubated at 37°C for 24 hours. Medium was removed and then medium with varying concentrations of G418 (0, 100, 400, 700, and 1,000µg/mL) was added and incubated at 37°C. The medium was replaced every 5 days using fresh medium with the appropriate G418 concentration and the percentage of surviving cells were observed in that period. The lowest antibiotic concentration that kills the majority of cells in 13 days was identified. The transfected cell line was selected using this concentration to obtain the vector transfected A549 cells.

3.2.14 Transfection

jetOPTIMUS® transfection reagent was used to transfect pcDNA-GFP mammalian expression vector, N-Terminal p3xFLAG-CMV vector containing the desired gene sequence and N-Terminal p3xFLAG-CMV vector into A549 cells. Transfection conditions are demonstrated in **Table 3.12.**

Table 3.12 Transfection conditions of used vectors

Vector	Culture vessel	Number of wells	Volume of medium during transfection	Volume of buffer	Amount of DNA	Volume of reagent
pcDNA-GFP	24-well plate	40000-100000	0.5mL	50µL	250ng, 500ng, 750ng	0,25µL, 0,5µL, 0,75µL
p3xFLAG-CMV	10mL cell culture plate	1x106 - 4x106	8mL	1mL	10µg	10µL

Transfection was performed when cells reached to 60-80% confluency. Respective amount of DNA demonstrated in **Table 3.13** was diluted into jetOPTIMUS® buffer, vortexed for 1 sec and then spun down briefly. jetOPTIMUS® reagent was vortexed for 5 sec and spun down before use. Respective amount of jetOPTIMUS® reagent was added into respective DNA solutions, vortexed for 1 second and spun down briefly. The mixtures were incubated for 10 min at room temperature. Transfection mixtures were added dropwise onto respective cells and distributed evenly. Plates were rocked back and forth gently and from side to side and then incubated at 37 °C. The medium was replaced with high glucose DMEM containing 10% FBS after 4 hours to increase transfection efficiency. In order to find optimum transfection conditions, pcDNA-GFP mammalian expression vector was transfected into A549 cells with three different amounts (250ng, 500ng, and 750ng) before the transfection of N-Terminal p3xFLAG-CMV vector. Transfection was performed in two different medium (OPTIMEM and high glucose DMEM containing 10% FBS) and medium replacement was performed at different hours post transfection. Transgene expression was analyzed after 24-48-72 hours under fluorescence microscope.

Table 3.13 Transfection optimization table according to their DNA amount, and medium conditions

Amount of DNA	Medium during transfection	Medium change (in hours)	Replacement medium
250ng, 500ng, 750ng	high glucose DMEM containing 10% FBS	4	high glucose DMEM containing 10% FBS
250ng, 500ng, 750ng	OPTIMEM	4	high glucose DMEM containing 10% FBS
500ng	high glucose DMEM containing 10% FBS	6	high glucose DMEM containing 10% FBS
500ng	OPTIMEM	6	high glucose DMEM containing 10% FBS
500ng	high glucose DMEM containing 10% FBS	8	high glucose DMEM containing 10% FBS
500ng	OPTIMEM	8	high glucose DMEM containing 10% FBS

3.2.2.14.1 Selection of Stable Transfected Cell Line

The optimum antibiotic concentration that kills the majority of cells within 13 days was identified using the kill curve assay. This concentration was used for selection of a stable transfected cell line. Fresh medium containing an appropriate concentration of G418 was used to replace the used medium every four days.

3.2.15 Verification of Overexpression

3.2.15.1 Verification of mRNA Expression via RT-PCR

cDNA conversion was done regarding **Table 3.3.** mRNA levels were detected after PCR with ELK Biotechnology's Taq DNA Polymerase kit (EQ005). *CYCLOPHILIN A* forward and reverse primers were used as positive control. All components listed in **Table 3.14** were mixed in a PCR tube and spun down briefly. Thermocycling conditions for ELK Biotechnology's Taq DNA Polymerase kit are listed in **Table 3.15.**

Table 3.14 ELK Biotechnology's Taq DNA Polymerase kit conditions

Component	Volume
ddH_2O	41.5-nμL
10×PCR Buffer	5μL
Forward Primer (10μM)	1μL
Reverse Primer2 (10μM)	1μL
dNTPs (10mM each)	1μL
Taq DNA Polymerase	0.5μL
Template DNA	nμL
Total	50μL

Table 3.15 Thermocycling conditions for ELK Biotechnology's Taq DNA Polymerase kit

Step	Temperature	Duration	Cycle
Pre-Denaturation	94°C	5 minutes	1
Denaturation	94°C	30 seconds	23
Annealing	56°C	30 seconds	
Extended	72°C	30 seconds	
Final extended	72°C	5 minutes	1

3.2.15.2 Verification of Secreted Protein Levels via Enzyme-Linked ImmunoSorbent Assay (ELISA)

ELISA Kit of ELK Biotechnologies was used for overexpression confirmation. The experiment was carried out based on the instructions in the kit's manual. Standards have diluted in accordance with the kits instructions and loaded into wells as two replicas to produce a more precise absorbance curve.

Cell culture medium was collected at different time intervals (24-, 48-, and 96-hours) after seeding the 350.000 cells. Then samples were centrifuged at 1500rpm for 5 minutes and then the supernatant was collected. Cell lysate was collected, and protein was isolated as described before. All the kit components were left to come to room temperature before usage. Wash buffer (25X) was diluted to 1X with ddH_2O. Standard working solution was prepared via serial dilution of the serial diluent and the lyophilized standard. Standard diluents were prepared with final concentration of 4000pg/mL, 2000pg/mL, 1000pg/mL, 500pg/mL, 250pg/mL, 125pg/mL, 62.5pg/ml and 0pg/mL respectively. After that Biotinylated Antibody and Steptavidin-HPR were prepared via dilution from 100X to 1X.

Wells for diluted standard, blank, and sample were determined. 100µL of each standard or sample is added to the appropriate wells. 2 replicas for standards and 3 replicas for samples were made. Then the wells were sealed with cover and then incubated for 80 minutes for 37°C. This step was also performed as incubating at +4°C, overnight. After incubation, liquids were removed and washed with 200µL 1X wash buffer 3 times. Each wash step should be incubated 1-2 minutes before removing the media. After each wash step well should be blotted on a filter paper several times to remove bubbles and get rid of the buffer. After the washing steps 100µL biotinylated antibody was added to each well and the wells were covered with plate sealer and then

incubated for 50 minutes for 37°C. Aspiration and wash steps were repeated for three times. Then 100µL Steptavidin-HPR was added to each well, wells were covered with plate sealer and incubated for 50 minutes for 37°C. Aspiration and wash steps were repeated 5 times, then 90µL TMB substrate was added to each well. Wells were covered with plate sealer and incubated for 20 minutes for 37°C. After incubation, 50µL stop reagent was added to each well. After adding the stop reagent plate was placed into Varioskan (microplate reader) immediately and absorbance was measured at 450nm. An absorbance vs concentration curve was plotted in excel, trendline, R square, and equation was added. Concentration of the protein samples were calculated from the equation. Statistical analysis (2way ANOVA) was performed with Graphpad Prism 9 program by taking the average of measurements from each replica.

3.2.15.3 Verification of Protein Levels via Western Blot

Proteins were isolated and quantified as described before. Sodium dodecyl sulphate (SDS)-polyacrylamide gel electrophoresis (PAGE) was performed to separate proteins of untransfected, vector only, and *SLPI* transfected cells. The denaturing gel was prepared with 17% separating gel for proteins smaller than 15kDa and 4% stacking gel for proteins bigger than that size. The 30-50µg of protein samples were mixed with cracking buffer (2X protein/sample loading buffer) and then heated at 95°C for 5 min in heat block. Samples were put on ice and centrifuged at full speed for 1 minute. Then, gel was soaked into the 1X running buffer and proteins were loaded into respective wells as well as BLUeye prestained protein ladder (GeneDirex, catalog no. PM007-500). Then, they were run at 55V with 15V increments after every 30 minutes.

Proteins were transferred to 0,2µm pore sized PVDF membrane in the Bio-Rad Trans-Blot Turbo Transfer System, and run at 0,6A, 25V for 30 minutes. Before performing the transfer, the gel was incubated in transfer buffer for 5-10 minutes, and

the PVDF membrane was washed in methanol for 30 seconds and also soaked into transfer buffer for 10 min. After the transfer, the gel was stained in Coomassie blue staining solution for 1 h to control if the transfer was successful. It was then incubated in destaining solution on an orbital shaker overnight at room temperature for the removal of the dye.

The membrane was blocked with blocking solution (Bio-Rad EveryBlot Blocking Buffer, catalog no. 12010020) for 15 minutes on an orbital shaker. Then the membrane was split into three with a sterile blade according to the prestained marker positions to detect the housekeeping protein (GAPDH), the vector, and SLPI protein. Membranes were incubated with primary antibodies at concentrations of 1:5000 for FLAG tag (Elabscience, catalog no. E-AB-2006), 1:500 for SLPI Rabbit pAb (ELK Biotechnology, catalog no. ES11078), and 1:100 for GAPDH, and incubated at +4°C overnight on an orbital shaker. The following day, the membrane was washed with 1X TBS-T containing 0.1% Tween-20 three times for 10 minutes on an orbital shaker. Then, membranes were incubated with respective secondary antibodies for 60 minutes on an orbital shaker at room temperature: HRP conjugated AffiniPure Goat Anti-Rabbit IgG (BOSTER, catalog no. BA1054-05) 1:1000 and Goat Anti-Mouse IgG HRP conjugated (Merck, catalog no. AP130P) 1:1000. Afterward, membranes were washed as described before. Finally, chemiluminescent reagent ECL (GeneDireX Simply, catalog no. SM801-0500) was applied on the membrane and incubated in the dark for 2-3 minutes. Bio-Rad ChemiDoc MP Imaging System was used to visualize the membrane and ImageJ was used to analyze the results.

3.2.16 Wound Healing Assay

On a 6-well plate, cells were seeded with DMEM containing different concentrations of FBS (%10 and %2) and different cell numbers (200.000, 350.000, and 500.000) in order to find the ideal number of cells to begin the wound healing experiment. A 200µL pipette tip was used to make scratches in the wells 24 hours after seeding. The optimal seeding cell number was determined 24 hours after this procedure by comparing the scratch gap filling levels of the cells using an EVOS microscope and ImageJ wound healing size tool.

The optimal number of cells were seeded in 6-well plates as a total of 5 replicas at two different time points. Using a 200µL pipette tip, just as in the optimization step, a wound was made in the center of the wells after 24 hours had passed. After 24 and 48 hours had passed, 10 photographs were taken with EVOS microscope on 10X for each well. The wound healing distance was calculated over 0-, 24-, and 48-hours using ImageJ wound healing size tool. Two-way ANOVA was performed with Graphpad Prism 9 program by taking the average of 10 different measurements from each replica.

3.2.17 Cell Counting Kit - 8 (CCK8) Assay

CCK8 assay (Sigma-Aldrich, catalog no. 96992) was performed to quantitate the number of viable cells in proliferation. Different number of cells (1000, 2500, 5000, 7500, 10000) were seeded on the 96-well plate to determine the ideal number of cells to use in the experiment.10µL of CCK8 were added to each well after 24 hours. Optical densities (OD) were measured at 450 nm following a 4-hour incubation period at 37^{o}C on Varioskan. The optimal number of cells for the experiment in this study was determined to be the number of cells with an OD below 1.

Optimal number of cells were seeded to two new 96-well plates in 3 replicates of each type of cells. These plates were set up in which one would be incubated for 24 hours and the other for 48 hours. 10µL of CCK8 was added to each well 24 hours after seeding, and the cells were then incubated at 37°C for 4 hours. After the incubation, optical densities were measured at 450nm on Varioskan. The same procedure was performed on the 48-hour incubation plate. Two-way ANOVA was performed with Graphpad Prism 9 program.

3.2.18 Matrigel Invasion Assay

The Matrigel (Corning® Matrigel® Basement Membrane Matrix, LDEV-free, 10 mL, catalog no. 354234) was diluted 1:50 on ice with high glucose DMEM. 50µL was added to the two 24-well cell culture plates in a suitable transwell insert and incubated for 1 hour at 37°C to gel. Then, the non-gelled solution was carefully aspirated from the surface and 10000 cells were seeded on transwell inserts in high glucose DMEM containing 1% FBS in 3 replicates for each group. These plates were set up in which one would be incubated for 24 hours and the other for 48 hours. High glucose DMEM containing 10% FBS medium was added to the bottom chamber of the transwell plate. Cells were incubated for 24- and 48-hours. After 24 hours, transwell insert was removed and put in TrypLE Express (Catalog number: 12605010) and incubated at 37°C for 2 minutes. Activity of TrypLE Express was inhibited with addition of high glucose DMEM. Number of cells that were not migrated to bottom chamber, but invaded to the bottom of the transwell insert was calculated with trypan blue as described before.

Medium at the bottom chamber was aspirated and washed with 1X PBS. Then, cells were fixed with ice cold 100% methanol for 10 minutes, methanol was aspirated, and washed with PBS at RT, then stained with Giemsa stain (Merck, catalog no.

1.09204.0500) for 5 minutes. The excess stain was washed with ddH_20, and the remaining solution was aspirated. Photographs of migrated cells were taken with EVOS microscope on 10X and analyzed with ImageJ. The same procedure was performed on the 48-hour incubation plate. Two-way ANOVA was performed with Graphpad Prism 9 program.

3.3 Buffers and Solutions

Separating Gel (%17)

- 4,25mL %40 Acrylamide/ %0.8 Bis acrylamide
- 2,6mL 1.5 M Tris pH:8.8
- 100µL %10 SDS (BioFroxx, catalog no. 1177GR100)
- 10mg %10 Ammonium persulfate (BioShop, catalog no. AMP001.100)
- 10µL TEMED (BioShop, catalog no TEM001)
- up to 10mL ddH_2O

Stacking Gel (4%)

- 0,5mL %40 Acrylamide/ %0.8 Bis acrylamide
- 2,6mL 0.5M Tris pH:6.8
- 50µL %10 SDS
- 5mg %10 Ammonium persulfate (Bioshop, catalog no. AMP001.100)
- 5µL TEMED
- up to 5mL ddH_2O

Cracking Buffer (2X Protein/sample Loading Buffer)

- 5mL 0,5M Tris HCl pH: 6,8 (50mM final concentration)
- 0,2mL 0,5M EDTA pH: 6,8 (2mM final concentration
- 5mL 10% SDS (1% final concentration)
- 10mL Glycerol (ISOLAB, catalog no. 927.043) (20% final concentration)
- 10mg Bromophenol blue (Labochem, catalog no. LC-6554.1)
- Add 1% ß-mercaptoethanol (Bioshop, catalog no. MER002.100) prior to use

All the components were mixed, and the pH was adjusted to 6.8 with HCl. This buffer can be stored at room temperature for up to 6 months.

5X Running Buffer

- 15g Tris base
- 72g Glycine (Bioshop, catalog no. GLN002.1)
- 5g SDS
- 1L ddH_2O

1X working solution was prepared by diluting the 5X SDS-PAGE running buffer 5 times, stored at 4°C. All the components were mixed, and the pH was adjusted to 8.3 with HCl. This buffer can be stored at room temperature for up to 6 months.

Transfer buffer

- 3g Tris
- 14,25g Glycine
- 200mL MeOH (ISOLAB, catalog no. 947046)
- Complete to 1L

All the components were mixed, and the pH was adjusted to 8.3 with HCl. This buffer can be stored at room temperature for up to 6 months.

Destaining Solution

- 100mL MeOH
- 35mL Acetic Acid
- 365mL ddH_2O

0.5M EDTA

- 93.05g EDTA
- 300mL ddH_2O

All the components were mixed, and the pH was adjusted to 8.0 with NaOH (ISOLAB, catalog no. 969112), total volume brought to 500mL by adding ddH_2O.

10X TBS

- 12.19g Tris
- 87,76g NaCl

All the components were mixed, and the pH was adjusted to 8, total volume brought to 1L by adding ddH_2O.

1X TBS-T 0.1%

- 50mL 10X TBS
- 450mL ddH_2O
- 500mL Tween-20 (Sigma-Aldrich, catalog no. P1379)

All the components were mixed, and the pH was adjusted to 7.5, total volume brought to 500mL by adding ddH_2O.

Coomassie Blue Staining Solution

- 0,25g Coomassie brilliant blue
- 45mL MeOH
- 45mL ddH_2O
- 10mL glacial acetic acid

Agarose Gel Loading Dye

- 0,009g Bromophenol blue
- 2,8mL ddH_2O
- 1,2mL 0,5M EDTA
- 11mL Glycerol

4. RESULTS

4.1 Part I: Mutated Genes in Leptomeningeal Carcinoma Caused by Non-Small Cell Lung Cancer

4.1.1 Identification of Mutated Genes in LMC Patients Based on Their Primary Tumor Sites

A total of 221 studies were chosen after extensive search. The search was conducted using PubMed, thus there were no duplicate results. Only 23 of the 221 articles were eligible for a full-text examination after their titles and abstracts were evaluated. As stated in **Table 3.1**, a total of 16 studies were included and evaluated in this investigation.

To observe altered genes according to the primary tumor areas, a Venn diagram was made **(Figure 4.1)**. Due to the small number of studies, specific patient characteristics such as age, gender, initial tumor mutation, treatment previous to LMC diagnosis and treatment prior to sequencing were disregarded. In total, 96 genes -97 NSCLC, 24 breast and 13 melanoma- were discovered to have mutations in all cancer types. NSCLC and breast cancer shared 16 of them, melanoma and NSCLC shared 11 of them, and breast cancer and melanoma shared 6 of them.

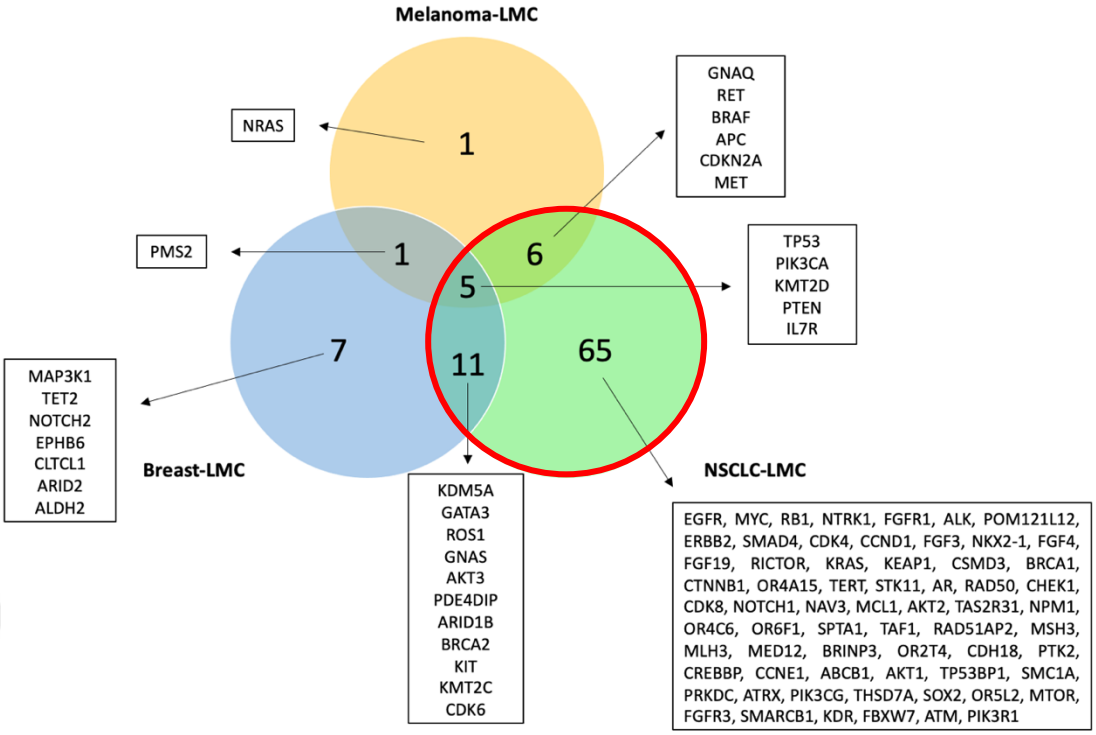

Figure 4.1 Venn diagram showing mutated genes in NSCLC, breast, and melanoma LMC patient from selected studies.

4.1.2 PPI Network Construction of Mutated Genes

Figure 4.2A shows the genes in NSCLC-LMC that mutated in more than two cases. A PPI network was built using the STRING database to examine the potential connections of genes altered in NSCLC-LMC patients. The PPI network contained 87 nodes and 1181 edges. 12 proteins did not interact with any other proteins as shown in **Figure 4.2B**.

A.

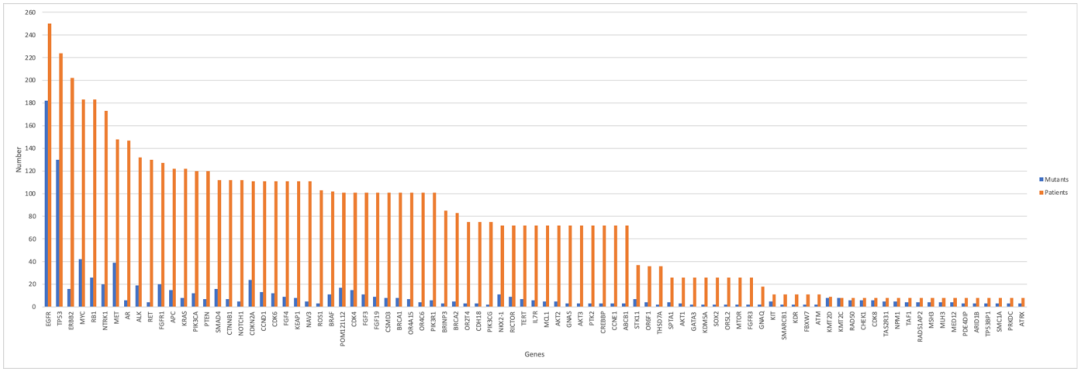

B.

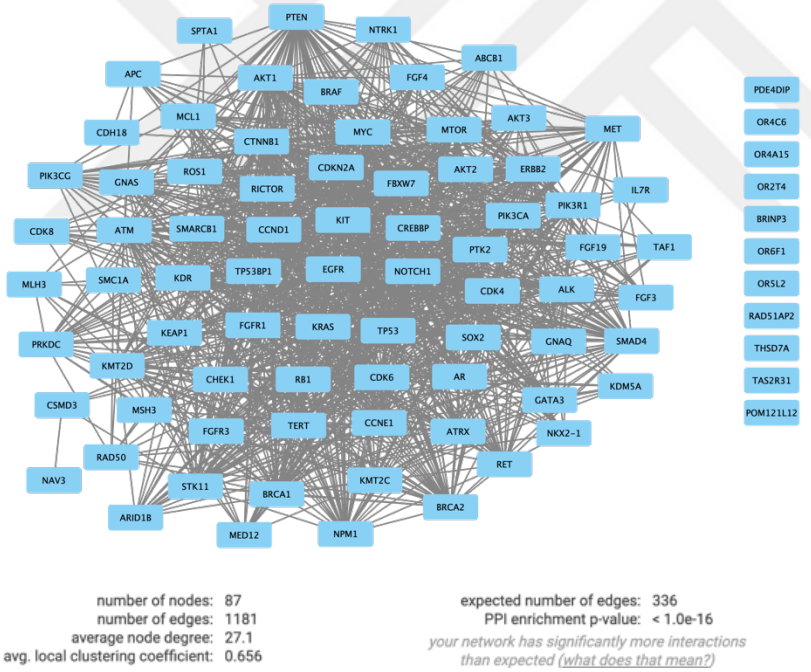

Figure 4.2 Mutated genes and their interactions with each other in NSCLC-LMC. A. Bar graph showing mutated genes in NSCLC-LMC (n≥2). B. PPI network of mutated genes in NSCLC-LMC using STRING database. PPI, protein-protein interaction; n=patient number.

4.1.3 Pathway Enrichment Analysis

Pathway enrichment analysis was performed to mutated genes in NSCLC-LMC using g:Profiler. The pathway enrichment analysis was visualized with Cytoscape. The network contained 856 nodes and 31411 edges. MCODE plug-in found in the Cytoscape was used to interpret the results due to high number of nodes and edges. The clusters created with MCODE are represented in **Table 4.1**. A total of 25 clusters were created. Each cluster consisted of multiple pathways, each node represented the different pathways, and each edge represented the interactions with each other.

Table 4.1. Clusters created with MCODE plug-in of Cytoscape

Cluster	Nodes	Edges	Pathways
1	146	4788	Regulation of biosynthetic and metabolic process
2	200	3746	Regulation of cellular differentiation and cell death
3	101	816	Cell morphogenesis and localization
4	146	1118	Cell communication and cell cycle
5	12	54	Reproductive system development
6	7	21	Skin development
7	7	21	Reproductive process
8	7	19	Response to radiation and environmental stimulus
9	15	40	Regulation of cytoskeleton and autophagy
10	8	18	Central nervous system development
11	5	10	Carbohydrate transport
12	49	112	Cellular response to stress and cell growth
13	7	13	Regulation of cell cycle
14	4	6	Mitotic G1 phase and G1/S transition
15	4	6	Aging
16	9	16	DNA repair and regulation of TP53 activity
17	4	6	Regulation of protein localization
18	4	6	Nuclear division
19	8	13	Cell cycle, DNA pairing and transcriptional regulation
20	3	3	Catabolic process
21	3	3	Cell adhesion
22	3	3	ERBB2 signaling
23	3	3	Response to alcohol
24	3	3	Myelination
25	3	3	G beta:gamma signaling

This thesis focused on six clusters as they may be more important to understand the mechanism under this metastasis and to find potential drug targets: “response to radiation and environmental stimulus”, “DNA repair and regulation of TP53 activity”, “regulation of cell cycle”, “DNA pairing and transcriptional regulation”, “regulation of protein localization”, and “cell adhesion”. Genes that play role in the respective pathways were listed next to each pathway **(Figure 4.3)**.

A.

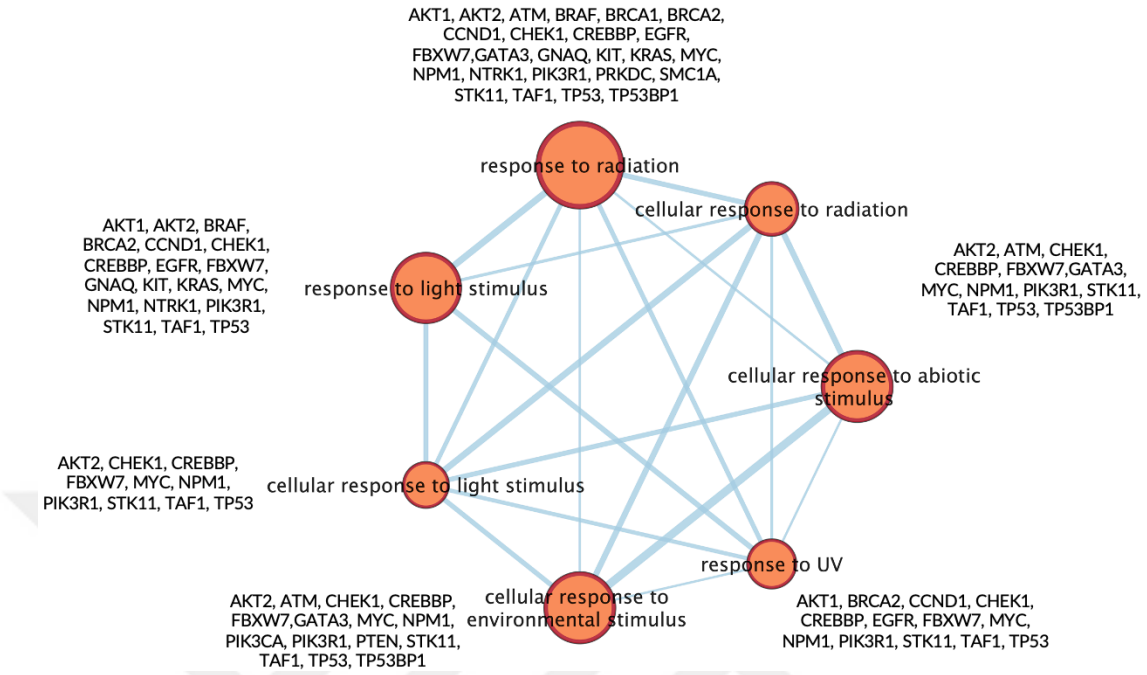
AKT1, AKT2, ATM, BRAF, BRCA1, BRCA2, CCND1, CHEK1, CREBBP, EGFR, FBXW7,GATA3, GNAQ, KIT, KRAS, MYC, NPM1, NTRK1, PIK3R1, PRKDC, SMC1A, STK11, TAF1, TP53, TP53BP1
response to radiation
cellular response to radiation
AKT1, AKT2, BRAF, BRCA2, CCND1, CHEK1, CREBBP, EGFR, FBXW7, GNAQ, KIT, KRAS, MYC, NPM1, NTRK1, PIK3R1, STK11, TAF1, TP53
response to light stimulus
AKT2, ATM, CHEK1, CREBBP, FBXW7,GATA3, MYC, NPM1, PIK3R1, STK11, TAF1, TP53, TP53BP1
cellular response to abiotic stimulus
AKT2, CHEK1, CREBBP, FBXW7, MYC, NPM1, PIK3R1, STK11, TAF1, TP53
cellular response to light stimulus
response to UV
AKT2, ATM, CHEK1, CREBBP, FBXW7,GATA3, MYC, NPM1, PIK3CA, PIK3R1, PTEN, STK11, TAF1, TP53, TP53BP1
cellular response to environmental stimulus
AKT1, BRCA2, CCND1, CHEK1, CREBBP, EGFR, FBXW7, MYC, NPM1, PIK3R1, STK11, TAF1, TP53

B.

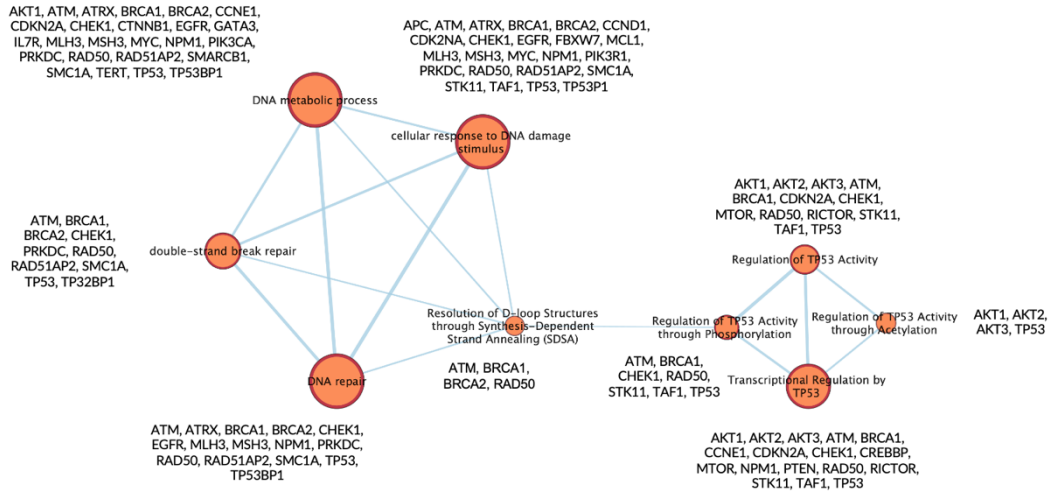
AKT1, ATM, ATRX, BRCA1, BRCA2, CCNE1, CDKN2A, CHEK1, CTNNB1, EGFR, GATA3, IL7R, MLH3, MSH3, MYC, NPM1, PIK3CA, PRKDC, RAD50, RAD51AP2, SMARCB1, SMC1A, TERT, TP53, TP53BP1
APC, ATM, ATRX, BRCA1, BRCA2, CCND1, CDK2NA, CHEK1, EGFR, FBXW7, MCL1, MLH3, MSH3, MYC, NPM1, PIK3R1, PRKDC, RAD50, RAD51AP2, SMC1A, STK11, TAF1, TP53, TP53P1
DNA metabolic process
cellular response to DNA damage stimulus
ATM, BRCA1, BRCA2, CHEK1, PRKDC, RAD50, RAD51AP2, SMC1A, TP53, TP32BP1
double-strand break repair
Resolution of D-loop Structures through Synthesis-Dependent Strand Annealing (SDSA)
DNA repair
ATM, BRCA1, BRCA2, RAD50
ATM, ATRX, BRCA1, BRCA2, CHEK1, EGFR, MLH3, MSH3, NPM1, PRKDC, RAD50, RAD51AP2, SMC1A, TP53, TP53BP1
AKT1, AKT2, AKT3, ATM, BRCA1, CDKN2A, CHEK1, MTOR, RAD50, RICTOR, STK11, TAF1, TP53
Regulation of TP53 Activity
Regulation of TP53 Activity through Phosphorylation
Regulation of TP53 Activity through Acetylation
AKT1, AKT2, AKT3, TP53
ATM, BRCA1, CHEK1, RAD50, STK11, TAF1, TP53
Transcriptional Regulation by TP53
AKT1, AKT2, AKT3, ATM, BRCA1, CCNE1, CDKN2A, CHEK1, CREBBP, MTOR, NPM1, PTEN, RAD50, RICTOR, STK11, TAF1, TP53

C.

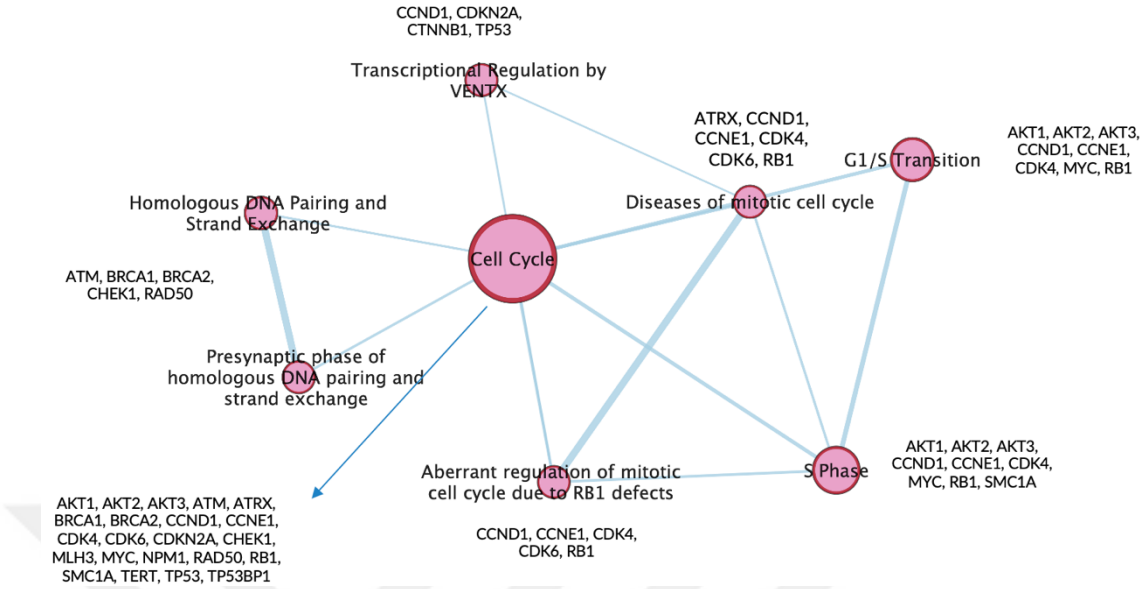
CCND1, CDKN2A, CTNNB1, TP53
Transcriptional Regulation by VENTX
ATRX, CCND1, CCNE1, CDK4, CDK6, RB1
G1/S Transition
AKT1, AKT2, AKT3, CCND1, CCNE1, CDK4, MYC, RB1
Homologous DNA Pairing and Strand Exchange
Diseases of mitotic cell cycle
Cell Cycle
ATM, BRCA1, BRCA2, CHEK1, RAD50
Presynaptic phase of homologous DNA pairing and strand exchange
Aberrant regulation of mitotic cell cycle due to RB1 defects
S Phase
AKT1, AKT2, AKT3, CCND1, CCNE1, CDK4, MYC, RB1, SMC1A
AKT1, AKT2, AKT3, ATM, ATRX, BRCA1, BRCA2, CCND1, CCNE1, CDK4, CDK6, CDKN2A, CHEK1, MLH3, MYC, NPM1, RAD50, RB1, SMC1A, TERT, TP53, TP53BP1
CCND1, CCNE1, CDK4, CDK6, RB1

D.

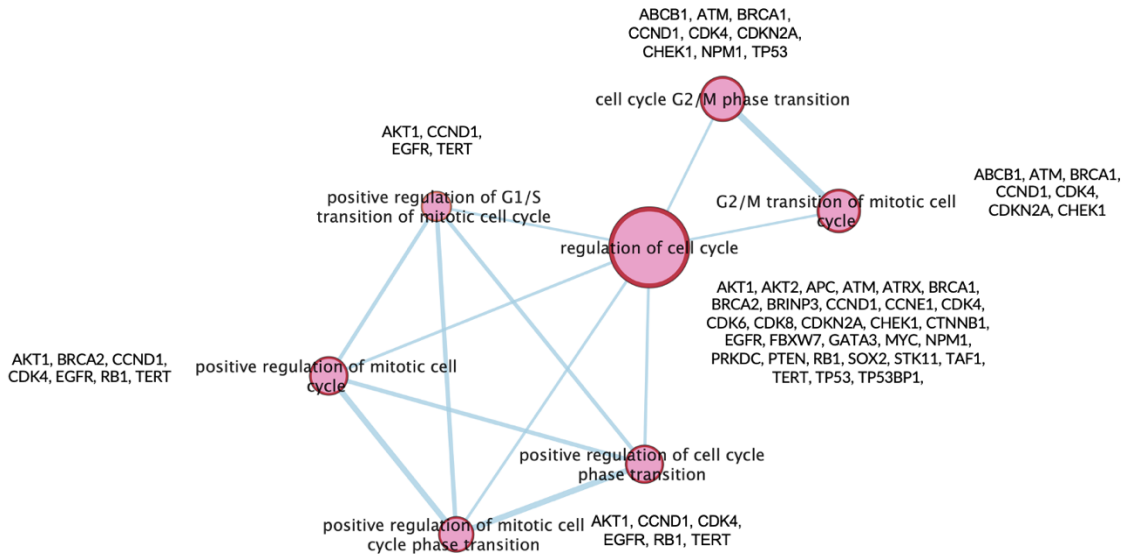
ABCB1, ATM, BRCA1, CCND1, CDK4, CDKN2A, CHEK1, NPM1, TP53
cell cycle G2/M phase transition
AKT1, CCND1, EGFR, TERT
positive regulation of G1/S transition of mitotic cell cycle
G2/M transition of mitotic cell cycle
ABCB1, ATM, BRCA1, CCND1, CDK4, CDKN2A, CHEK1
regulation of cell cycle
AKT1, AKT2, APC, ATM, ATRX, BRCA1, BRCA2, BRINP3, CCND1, CCNE1, CDK4, CDK6, CDK8, CDKN2A, CHEK1, CTNNB1, EGFR, FBXW7, GATA3, MYC, NPM1, PRKDC, PTEN, RB1, SOX2, STK11, TAF1, TERT, TP53, TP53BP1,
AKT1, BRCA2, CCND1, CDK4, EGFR, RB1, TERT
positive regulation of mitotic cell cycle
positive regulation of cell cycle phase transition
positive regulation of mitotic cell cycle phase transition
AKT1, CCND1, CDK4, EGFR, RB1, TERT

E.

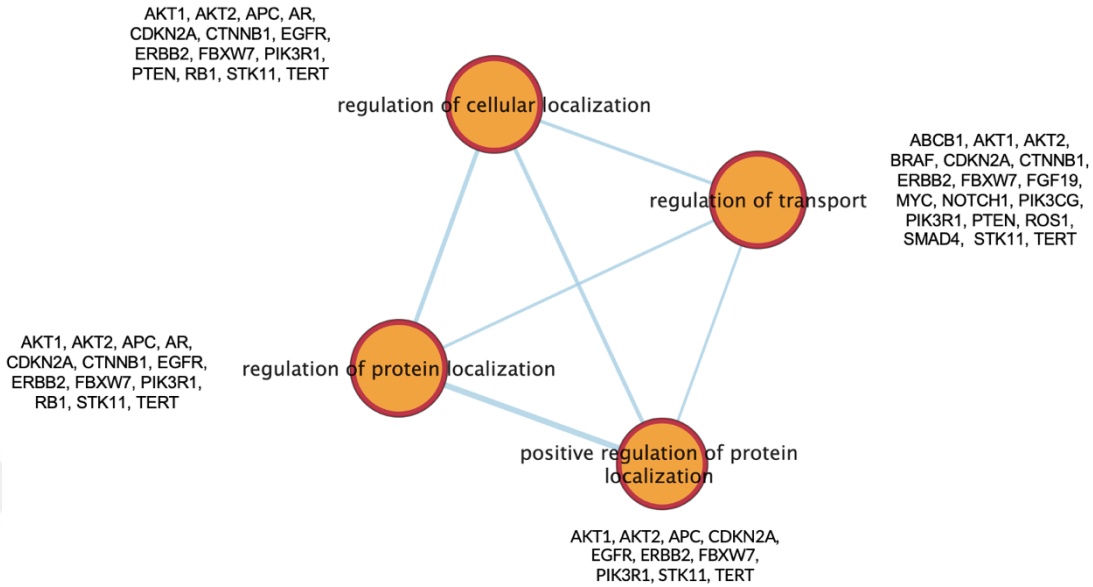

F.

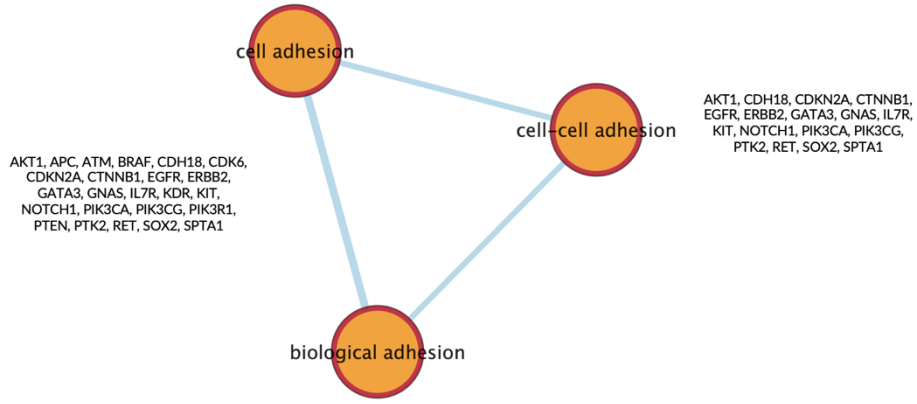

Figure 4.3 Visualization of pathway enrichment analysis of mutated genes in NSCLC-LMC using Cytoscape. Genes that have a role in the pathways of A. response to radiation and environmental stimuli, B. DNA repair and TP53 activity, C. regulation of cell cycle, D. cell cycle, DNA pairing and transcriptional regulation, E. regulation of protein localization, F. cell adhesion.

4.1.4 Investigation of *EGFR* Mutations

The mutation data of *EGFR* was extracted from studies included in this meta-analysis. 12 *EGFR* mutations were found **(Figure 4.4)**. 40% and 39% of NSCLC-LMC patients harbored two hot spot mutations: exon 19 deletion (del19) (E746_A750del), and L858R, respectively. T790M mutation and insertion in exon 20 (20 ins) were seen in 8% and 5% of the patients respectively. The remaining mutations were only seen in 1% of NSCLC-LMC patients. The mutations were searched in dbSNP, ClinVar, and COSMIC database **(Table 4.2).**

EGFR mutations are found in or connected to the kinase's ATP-binding site. L861Q and L858R are localized in the kinase's activation loop. Residues between the loop and C-helix are removed by del19, whereas ins20 adds residues at the C-helix's opposite end or within the N-terminal. As a result of L858R mutation, the tyrosine kinase domain' equilibrium between inactive and active states of is shifted in favor to the active state. Efficiency of EGFR inhibitors are thought to decrease with the increased EGFR's affinity for ATP due to T790M mutation (68). The covalent bond formation with irreversible EGFR inhibitors is prohibited due to C797S mutation (69).

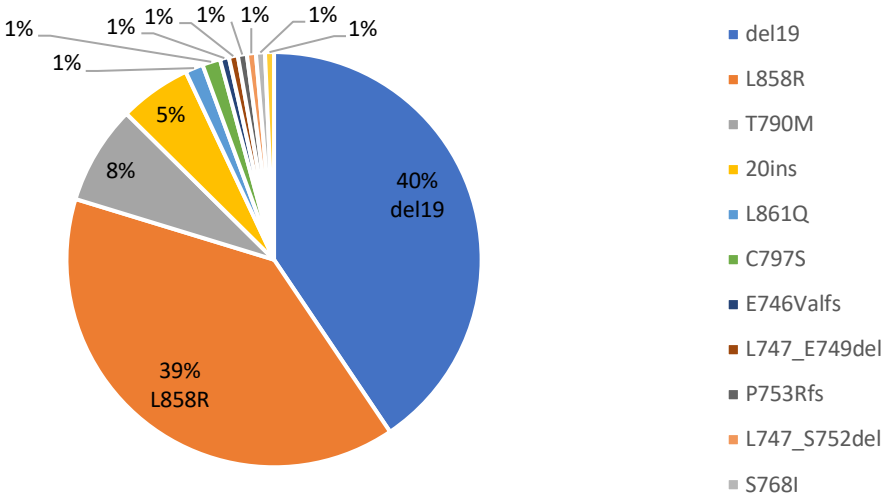

Figure 4.4 Pie chart showing the frequencies of *EGFR* mutations in NSCLC-LMC patients.

Table 4.2 *EGFR* mutations in NSCLC-LMC patients

Mutation	RS ID	ClinVar	COSMIC
L858R	1057519848	376282	COSV51765161
Del19	121913421	163343	COSV51765119
T790M	121434569	16613	COSV51765492
L861Q	121913444	163380	COSV51766344
C797S	1057519861	376342	COSV51766493

4.1.5 Drug Search

Drugs that specifically target the mutant genes in NSCLC-LMC have been investigated. Drugs for NSCLC that have received FDA approval were examined. Of these, drugs that can cross the BBB to reach the tumor location were chosen, and the DGIdb database was examined for interactions with the altered genes **(Table 4.3)** 8 of the drugs were capable of crossing BBB. Two of them, bevacizumab and everolimus, were also used to treat brain tumors. In addition, the interaction between the mutated genes and drugs used for LMC treatment were investigated. It was found that methotrexate and cytarabine drugs used in the treatment of LMC interacted with at least 4 mutated genes in NSCLC-LMC patients.

Table 4.3 Candidate drugs for NSCLC-LMC treatment

Drugs	Genes
Afatinib	*EGFR, ERBB2, KRAS, BRAF, MET*
Bevacizumab	*ERBB2, KRAS, MET, PIK3CA, TP53, BRAF, KIT, EGFR*
Capmatinib	*MET, BRAF, EGFR, TP53*
Cytarabine*	*ABCB1, GATA3, KIT, TP53*
Erlotinib	*ALK, ABCB1, APC, BRAF, EGFR, ERBB2, KRAS, MET, PIK3CA, PTEN, RET, TP53*
Everolimus	*ABCB1, AKT1, AKT2, AKT3, ATM, BRAF, BRCA1, BRCA2, EGFR, ERBB2, GNAQ, KRAS, MTOR, NOTCH1, PIK3CA, PIK3R1, PTEN, RB1, RET*
Gefitinib	*ABCB1, EGFR, ERBB2, FGFR1, BRAF, KRAS, MET, PIK3CA, PTEN*
Lorlatinib	*ALK, NPM1, RB1, ROS1, TP53*
Methotrexate*	*GATA3, NOTCH1, NTRK1, RB1, TP53*
Osimertinib	*EGFR, ERBB2, KRAS, MET*

*Used for the LMC treatment

4.2 Part II: The Effects of Increased *SLPI* Expression in the A549 Cell Line

4.2.1 Cloning of *SLPI* cDNA into N-Terminal p3XFLAG-CMV vector

In order to clone *SLPI* cDNA into N-Terminal p3XFLAG-CMV vector, cell pellet of A549 cells was collected. RNA was isolated from those cells, converted into cDNA, and then amplified by PCR with primers containing flanking enzyme digest sites. The expected PCR product size for the amplified *SLPI* gene is 396bp and *Cyclophilin A* is 220bp **(Figure 4.5)**.

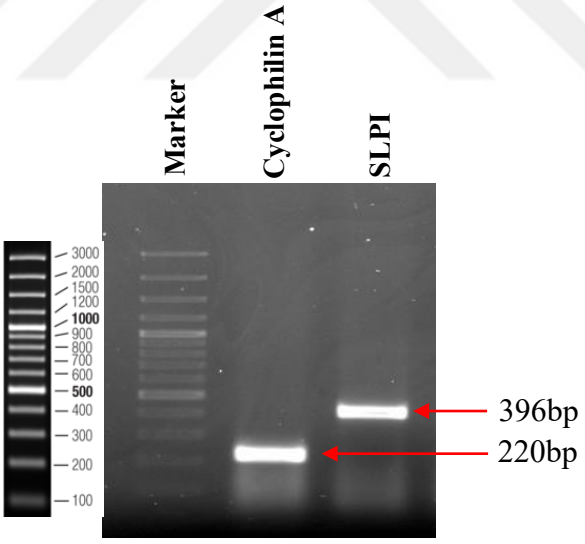

Figure 4.5 Agarose gel image showing the PCR products. 1st lane marker, Cyclophilin A (positive control). 2nd lane, *SLPI*. Lane marker: 100bp DNA Ladder (Invitrogen Gene ruler 15628050)

Gel extraction was performed to obtain the desired gene product and eliminate the primer dimers; purified *SLPI* RT-PCR product and the vector were digested with restriction enzymes and then ligated. The vector to insert ratios were 1:3 and 1:6. Then vector containing the desired gene product was transformed into *E. coli*. Transformation efficiency was calculated. Only four colonies were formed. This indicated that there were 80 transformants in 1µg plasmid. A replica plate was created by streaking four colonies to an ampicillin agar plate. Then sequentially, colony PCR was performed to determine the colonies that had the insert **(Figure 4.6)**. Two of the plasmids that contained the insert were isolated from the colonies (colony 2 and 3) by miniprep and then sent to sequencing for the verification of the *SLPI* cDNA sequence.

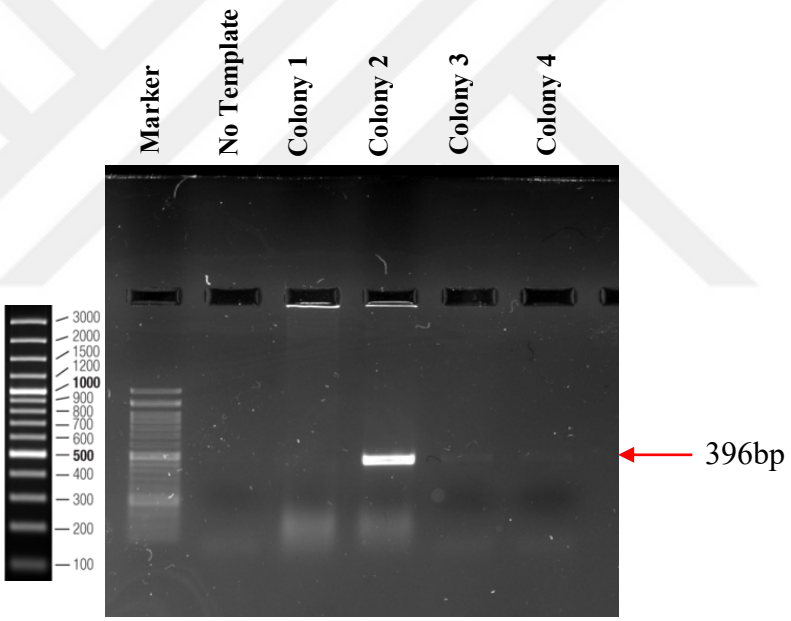

Figure 4.6 Agarose gel image showing the colony PCR products. 1st lane marker, 2nd lane negative control (no template), the remaining lanes are the respective colonies. Lane marker: 100 bp DNA Ladder (Invitrogen Gene ruler 15628050)

CLC Workbench was used for the analysis of sequencing results **(Figure 4.7)**. Only one plasmid (colony 2) was aligned 99%, with a base substitution (on position 36, showed in red box. However, it was on the wobble position causing a synonymous mutation. Hence, the protein structure was not changed. SLPI CCDS represents the consensus coding sequence (CCDS) of *SLPI*. S1_p3XFLAG-CMV represents the

plasmid that was sequenced. The dashed lines are the part where vector is inserted. Colored box shows the bases, adenine (A), thymidine (T), cytosine (C), and guanine (G). The letters under the codons represent the respective amino acids.

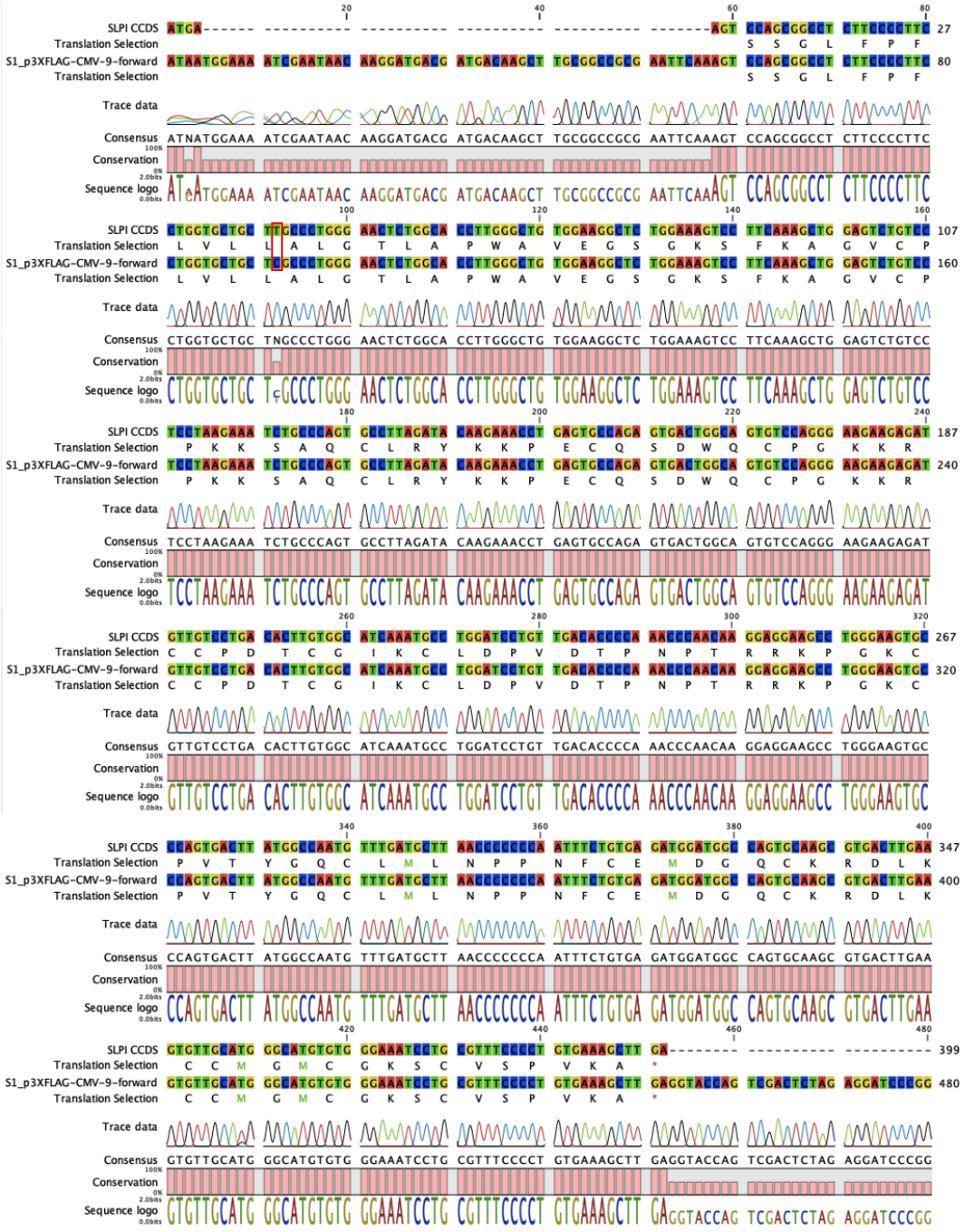

Figure 4.7 Sequencing results of plasmid isolated from colony 2 containing the *SLPI* cDNA sequence generated in CLC Workbench. Red box is showing the base substitution, T to C conversion.

4.2.2 Transfection of N-Terminal p3XFLAG-CMV Vector Containing *SLPI* cDNA Into A549 Cells

4.2.2.1 Optimization of Transfection with pcDNA-GFP Vector

A549 cells were transfected with the pcDNA-GFP vector at three different concentrations (250, 500, and 750 ng), in two different media (OPTIMUM and high glucose DMEM with 10% FBS), and the medium was changed at different intervals after transfection. Number of GFP+ cells were very low (less then 250 at the end of 72h) when seeded in OPTIMEM in general, regardless of the concentration of the vector (**Figure 4.8A and 4.8.C**).

It was found that the most optimal condition to perform transfection was using 500ng DNA:500µL transfection reagent in DMEM and changing the medium 4 hours after transfection **(Figure 4.8 and 4.8.D)**.

A.

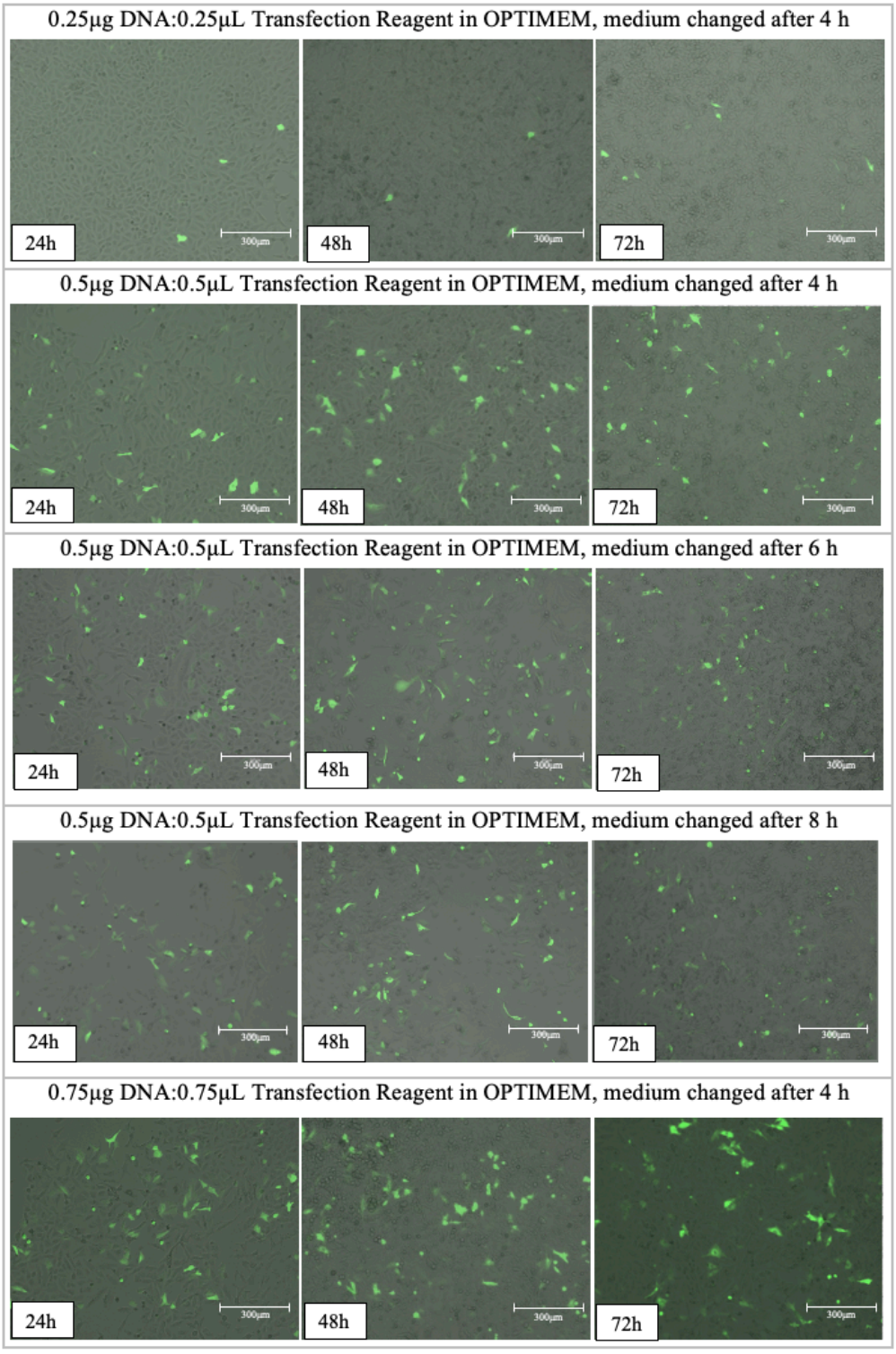
0.25µg DNA:0.25µL Transfection Reagent in OPTIMEM, medium changed after 4 h
24h
48h
72h
0.5µg DNA:0.5µL Transfection Reagent in OPTIMEM, medium changed after 4 h
24h
48h
72h
0.5µg DNA:0.5µL Transfection Reagent in OPTIMEM, medium changed after 6 h
24h
48h
72h
0.5µg DNA:0.5µL Transfection Reagent in OPTIMEM, medium changed after 8 h
24h
48h
72h
0.75µg DNA:0.75µL Transfection Reagent in OPTIMEM, medium changed after 4 h
24h
48h
72h

B.

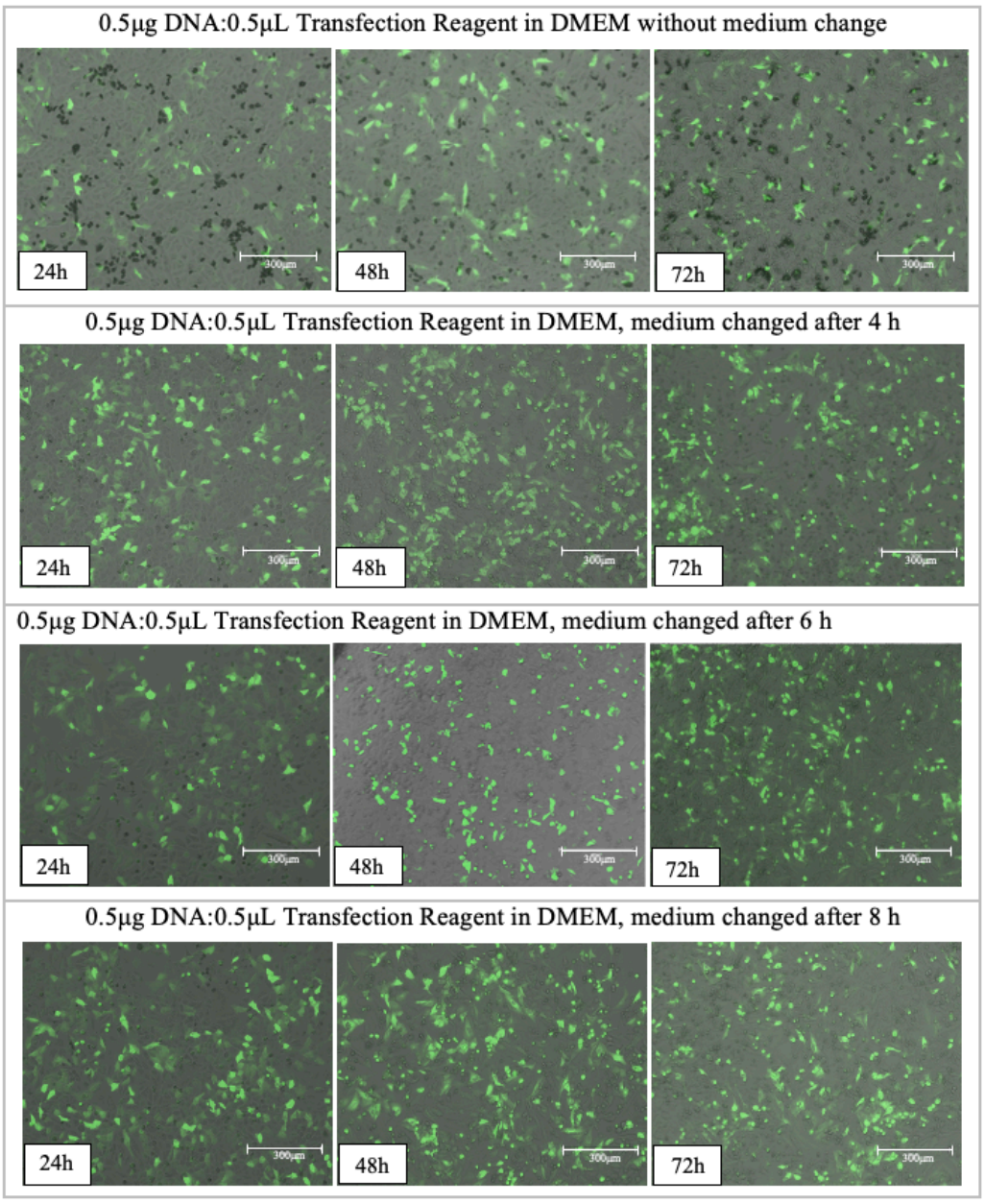
0.5µg DNA:0.5µL Transfection Reagent in DMEM without medium change
24h
48h
72h
0.5µg DNA:0.5µL Transfection Reagent in DMEM, medium changed after 4 h
24h
48h
72h
0.5µg DNA:0.5µL Transfection Reagent in DMEM, medium changed after 6 h
24h
48h
72h
0.5µg DNA:0.5µL Transfection Reagent in DMEM, medium changed after 8 h
24h
48h
72h

C.

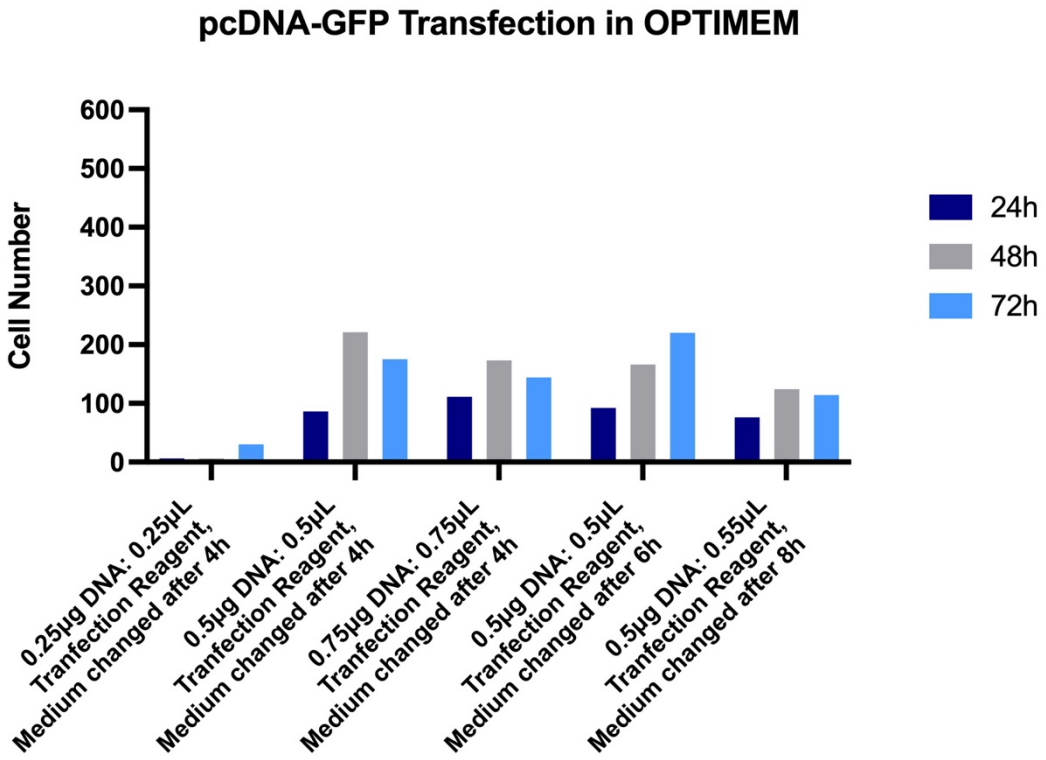
pcDNA-GFP Transfection in OPTIMEM
Cell Number
600
500
400
300
200
100
0
24h
48h
72h
0.25µg DNA: 0.25µL Tranfection Reagent, Medium changed after 4h
0.5µg DNA: 0.5µL Tranfection Reagent, Medium changed after 4h
0.75µg DNA: 0.75µL Tranfection Reagent, Medium changed after 4h
0.5µg DNA: 0.5µL Tranfection Reagent, Medium changed after 6h
0.5µg DNA: 0.55µL Tranfection Reagent, Medium changed after 8h

D.

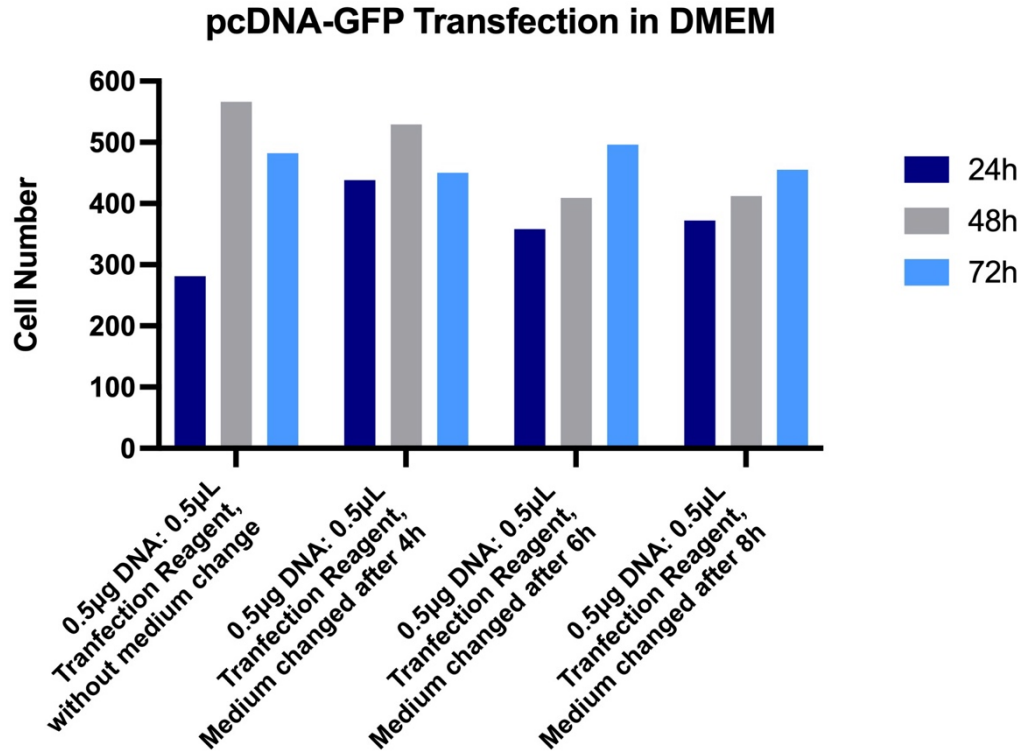
pcDNA-GFP Transfection in DMEM
Cell Number
600
500
400
300
200
100
0
24h
48h
72h
0.5µg DNA: 0.5µL Tranfection Reagent, without medium change
0.5µg DNA: 0.5µL Tranfection Reagent, Medium changed after 4h
0.5µg DNA: 0.5µL Tranfection Reagent, Medium changed after 6h
0.5µg DNA: 0.5µL Tranfection Reagent, Medium changed after 8h

Figure 4.8 Optimization of transfection conditions via pcDNA-GFP with different medium, time, and concentrations. 10X Fluorescent images showing the best representative of A549 cells transfected in A. OPTIMEM B. DMEM. Scale bar 300µm. Graphs showing the GFP+ cell number of transfected cells in C. OPTIMEM D. DMEM.

4.2.2.2 Kill Curve Assay

Kill curve assay was performed in order to determine the minimum amount of antibiotics that should be given to A549 cells for the selection of stable transfected cell line. A549 cells were treated with G418 with different concentrations for 13 days. When the antibiotic concentration was 100µg/mL the cells kept proliferating rapidly, whereas the cells in the wells with the greatest concentration of antibiotics, which was 1000µg/mL died after 6 days. Therefore, the ideal concentration of G418 was selected as 700µg/mL, which killed the large majority of the cells within that time period **(Figure 4.9)**.

A.

	Day 0	Day 5	Day 9
Control	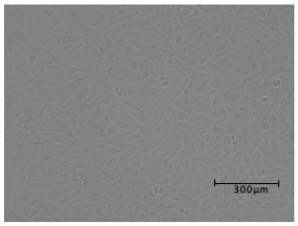	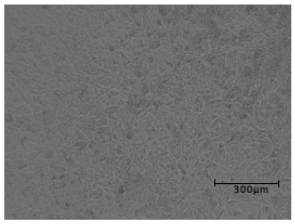	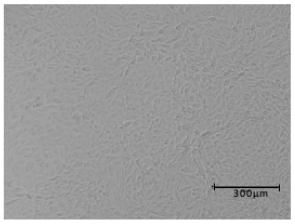
100μg/mL	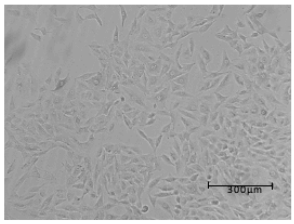	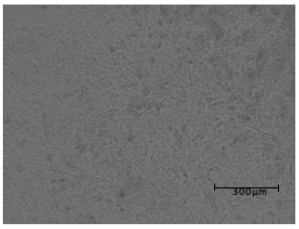	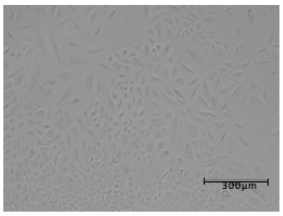
400μg/mL	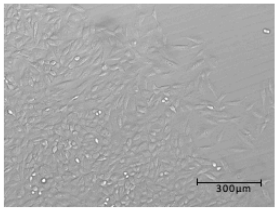	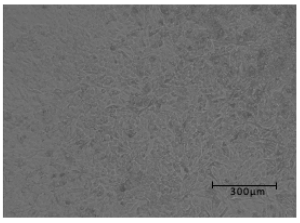	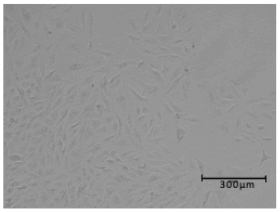
700μg/mL	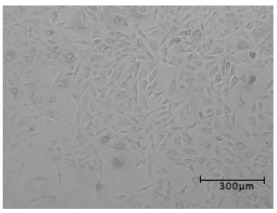	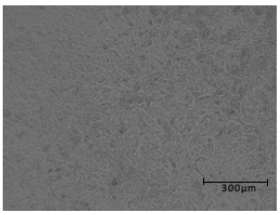	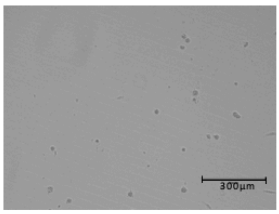
1000μg/mL	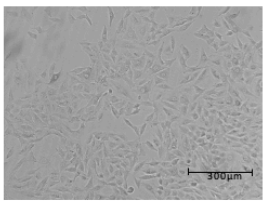	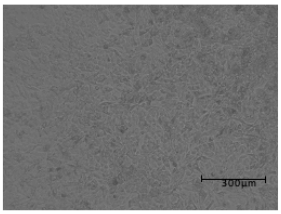	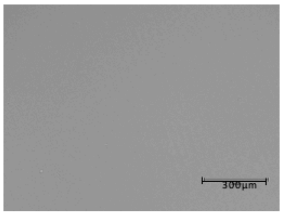

B.

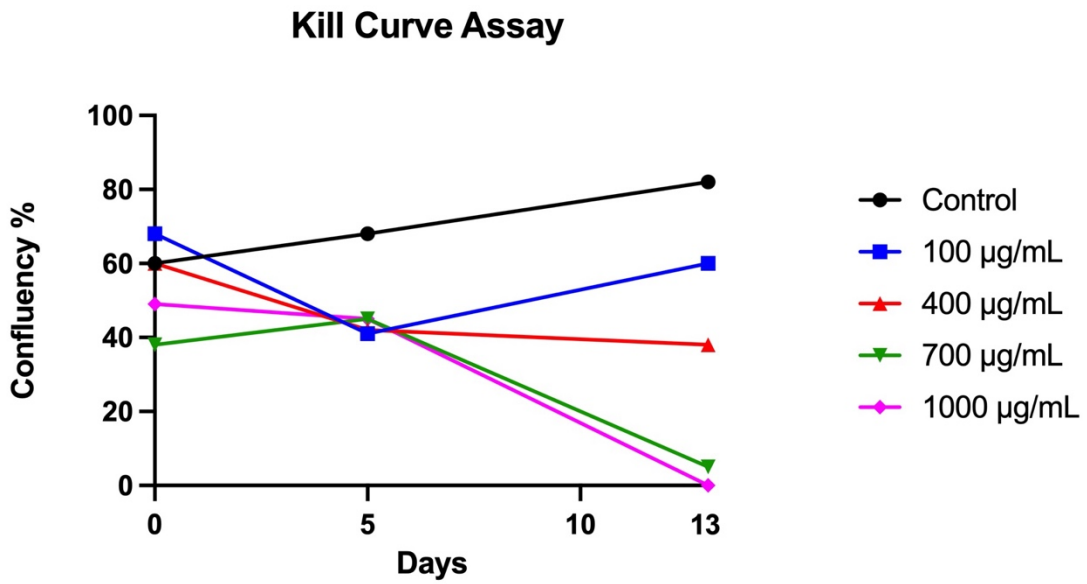

Figure 4.9 Kill curve assay results. A. 10X Microscope images showing the best representative of transfected A549 cells treated with G418. Scale bar 300µm. B. Graph showing the confluency of A549 cells treated with G418.

4.2.2.3 Transfection of *SLPI* cDNA overexpression vector into A549 Cell Line

A549 cells were transfected with the vector containing *SLPI* cDNA and with empty vector with 10ug DNA and 10µL JetOPTIMUS reagent. 3 days post transfection, cells treated with 700µg/mL G418, and medium was changed in every 3 days until all the cells that were not transfected died.

After the selection of all transfected cells, there have been 3 groups:

- SLPI: Cells transfected with *SLPI* overexpression vector,
- Vector only: Cells transfected with empty vector (vector control),
- Untransfected: Cells without any transfection (control).

4.2.3 Confirmation of *SLPI* Overexpression

4.2.3.1 Confirmation of Overexpression via PCR

The RNAs which were isolated from the untransfected, vector only, and *SLPI* transfected cells were converted into cDNA, amplified with PCR, and ran on agarose gel electrophoresis. Two sets of PCRs were performed. In the first set, the vector was detected inside the cell using the FLAG forward primer and the *SLPI* reverse primer, which resulted in a band that was only present in the cells that had been transfected with SLPI. In the second one, each cell type (untransfected, vector only and *SLPI* transfected) showed a band demonstrating the presence of the *SLPI* gene using *SLPI* forward and reverse primers **(Figure 4.10A).** As the level of *SLPI* expression in cells were quite low, second PCR with 20 cycles of extension was performed to demonstrate the *SLPI* overexpression in the transfected cells **(Figure 4.10B).** ImageJ was used to determine the intensity amounts of the bands on the agarose gel. Band intensities were first normalized to *Cyclophilin A*, which is a housekeeping gene used as a positive control, then compared within each cell. One-way ANOVA was performed as a statistical analysis. When the expression levels of *SLPI* were compared among the groups there has been a significant increase in *SLPI* group with a p-value of 0,0159 and 0,0171 between untransfected and vector only groups, respectively **(Figure 4.10C)**.

A.

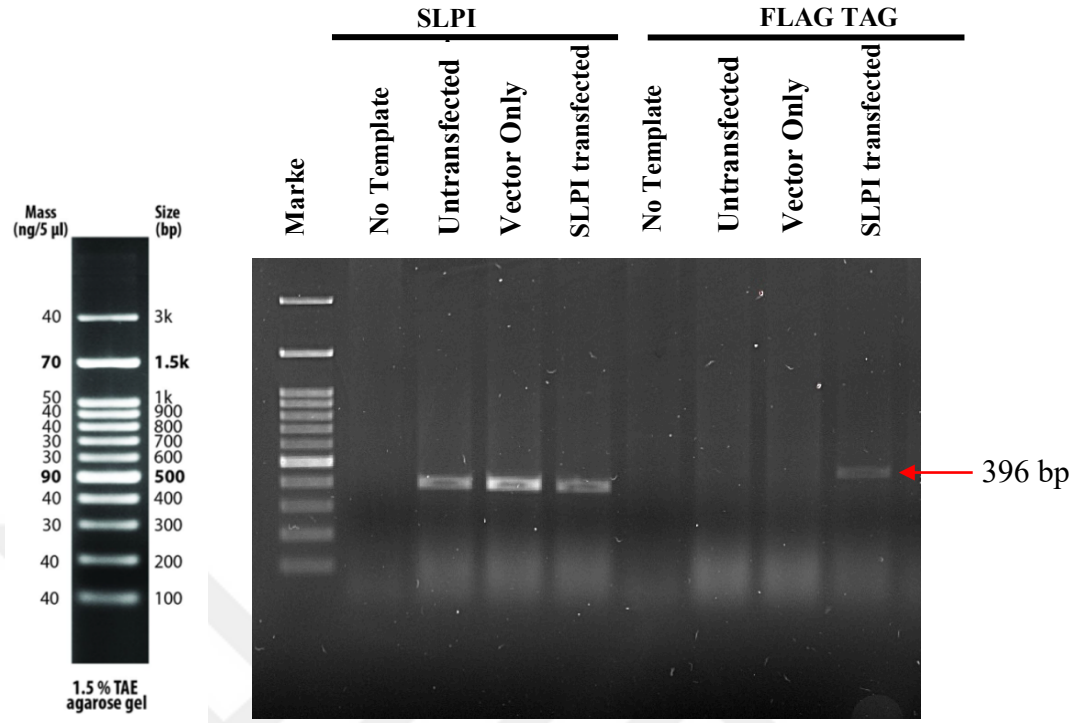
SLPI
FLAG TAG
Marke
No Template
Untransfected
Vector Only
SLPI transfected
No Template
Untransfected
Vector Only
SLPI transfected
Mass (ng/5 µl)
Size (bp)
40 3k
70 1.5k
50 1k
40 900
40 800
30 700
30 600
90 500
40 400
30 300
40 200
40 100
1.5 % TAE agarose gel
396 bp

B.

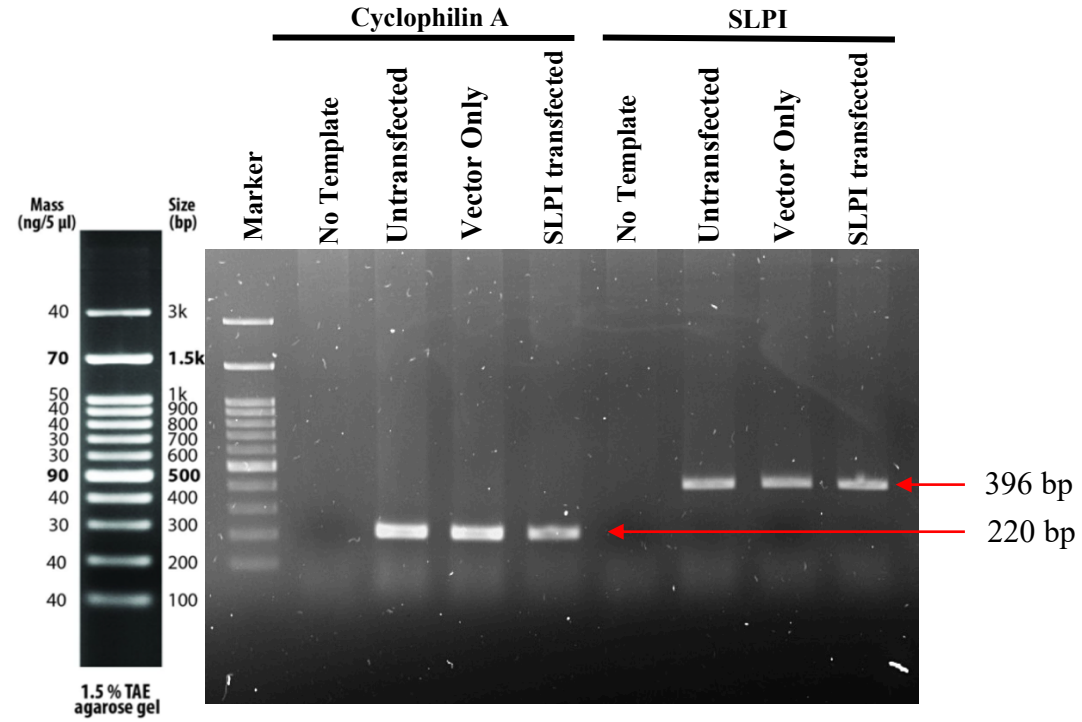
Cyclophilin A
SLPI
Marker
No Template
Untransfected
Vector Only
SLPI transfected
No Template
Untransfected
Vector Only
SLPI transfected
Mass (ng/5 µl)
Size (bp)
40 3k
70 1.5k
50 1k
40 900
40 800
30 700
30 600
90 500
40 400
30 300
40 200
40 100
1.5 % TAE agarose gel
396 bp
220 bp

C.

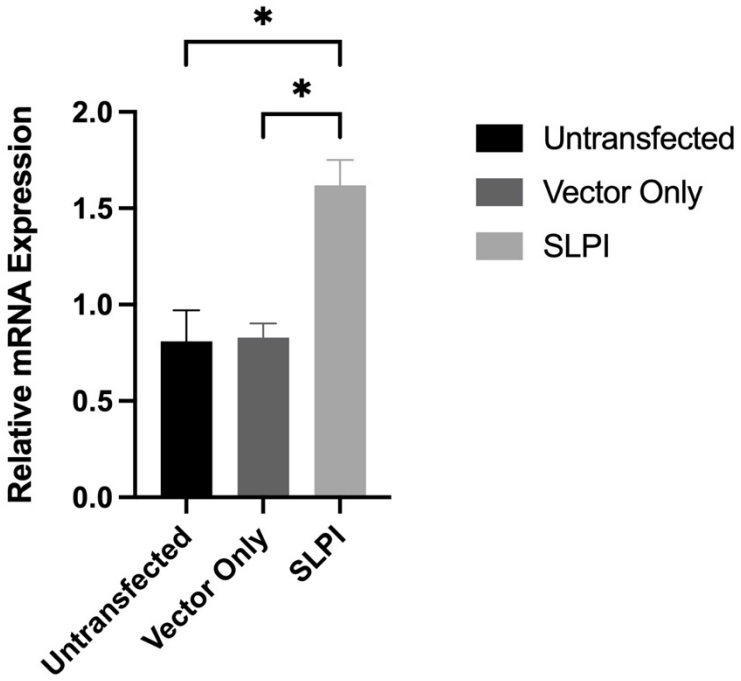

Figure 4.10 Agarose gel image showing the results of PCR demonstrating the presence of the vector and the *SLPI* overexpression. A. First 4 lanes show *SLPI* expression using *SLPI* primers. Last 4 lanes show the expression of the FLAG Tagged *SLPI* cDNA sequence. B. First 4 lanes show Cyclophilin A as positive control. Last 4 lanes show the mRNA levels of *SLPI* gene in each cell type. C. Bar graph showing the relative mRNA expression in each type of cell. DNA Ladder: Eco Tech Biotechnology Clear Band 100 bp DNA marker. (*p value < 0.05)

4.2.3.2 Confirmation of Overexpression via ELISA

ELISA was performed to demonstrate the SLPI protein levels that were secreted into medium. Media of cells were collected at different time points (24h, 48h, and 96h) and incubated at two different conditions for primary antibody binding (37°C, 80min and +4°C, overnight) **(Figure 4.11A and 4.11B)**. However, inconsistent amount of SLPI protein were detected in all media regardless of the medium collecting or the incubation time. SLPI protein levels were also determined by the cell lysates and then their concentrations were normalized to their total protein concentrations.

However, no significant difference found between the cell types (untransfected, vector only, and *SLPI* transfected) **(Figure 4.11C).**

A.

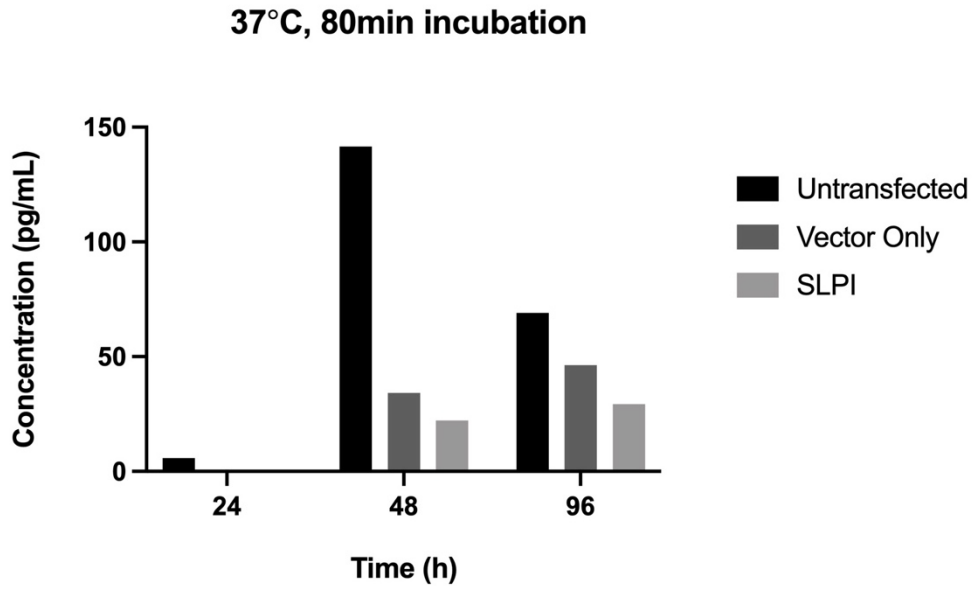

B.

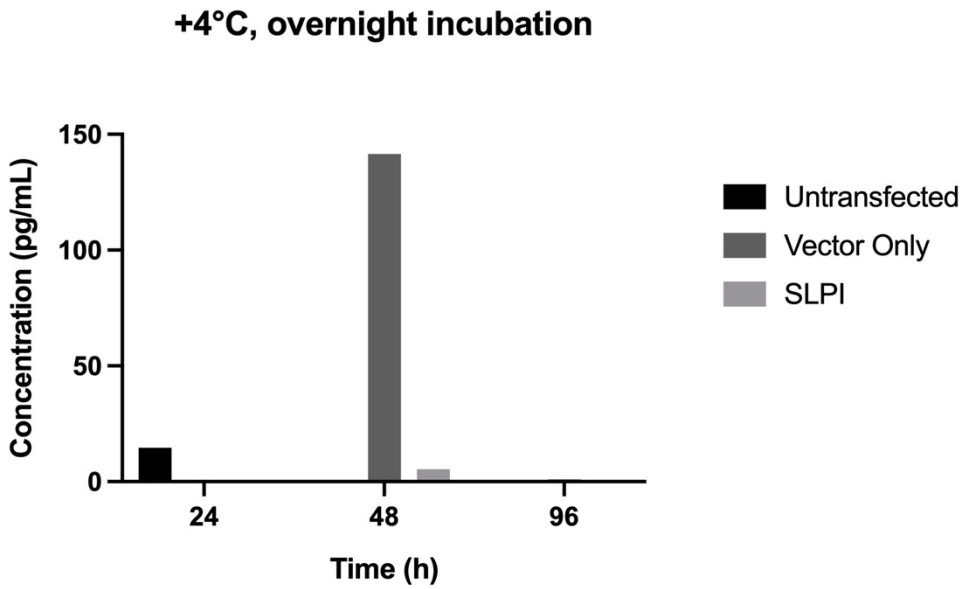

C.

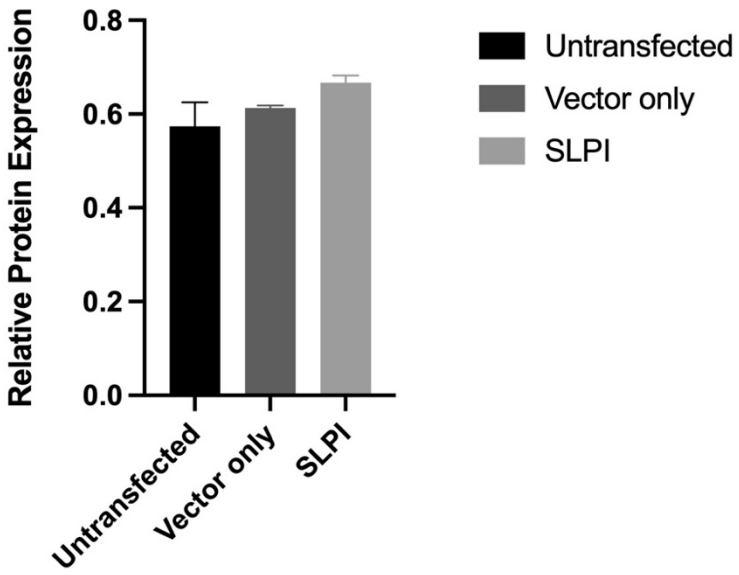

Figure 4.11 Bar graphs showing concentrations of SLPI proteins and relative SLPI protein expression in each type of cell. Medium collected at 24-,48-,96-h and samples incubated at respective wells at A. 37°C, 80min, B. +4°C, overnight. C. Relative SLPI protein expression in each type of cell.

4.2.3.3 Confirmation of Overexpression via Western Blot

Since the overexpressed SLPI protein by ELISA was not detected, Western blots were performed by using both FLAG and SLPI antibodies. GAPDH levels were also detected as a housekeeping protein. Proteins were isolated from the untransfected, vector only, and *SLPI* transfected cells and SDS-PAGE was performed to separate proteins according to their sizes. As SLPI is 11.7kDa, 17% separating gel, and 4% stacking gel were prepared. Semi-dry transfer was performed also due to small size of SLPI. GAPDH (36kDa), which is a housekeeping gene was used as a positive control **(Figure 4.12)**. However, we could neither detect SLPI protein nor FLAG tag and this experiment requires further optimization.

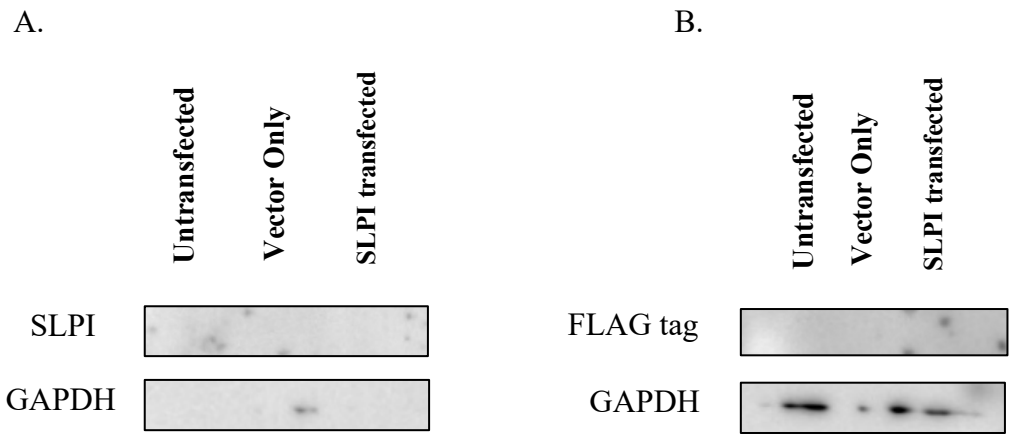

Figure 4.12 Western blot results showing the presence of the vector inside the SLPI transfected cells and the SLPI overexpression. A. SLPI protein levels are shown using SLPI antibody. B. Presence of FLAG tag vector in SLPI transfected cells using FLAG tag antibody. GAPDH is used as positive control.

4.2.4 Wound Healing Assay

Different numbers of cells (200.000, 350.000, and 500.000) were seeded into a 6-well plate containing DMEM with different amounts of FBS (2% and 10%) in order to find the optimum number of cells for the wound healing assay. Wounds were created with 200µL pipette tip and medium was changed with DMEM containing 2% and 10% FBS. 24 and 48 hours post creating the wound, EVOS microscope and ImageJ were used to observe and calculate the percentage of the wounded area, respectively. Wells containing 200.000 cells could not reach enough confluency in both media and time points, whereas 500.000 cells were too confluent in both media, and closed the wound in 24 hours. 350.000 cells in DMEM containing 10% FBS were highly confluent as well. Therefore, the optimal condition for this assay was determined as seeding 350.000 cells in DMEM containing 2% FBS **(Figure 4.13)**. Then the experiment was set with all groups with 5 replicas at 24 h and 48 h. This experiment was repeated twice. The best representative image of the 5 replicas were presented in

the **Figure 4.14A.** 24h after the generation of the scratch, more than 70% of the wound area was closed in *SLPI* transfected cells, whereas around 40-45% of the area was closed in untransfected and vector only cells. Nearly all of the wound area in *SLPI* transfected cells had closed by the end of 48 hours. When the wound area of *SLPI* group were compared among the groups at the end of 48 hours, there has been a significant decrease in *SLPI* group with a p-value less than 0,0001 and a p-value of 0,0037 between untransfected and vector only groups, respectively **(Figure 4.14B).** These results demonstrated that overexpression of *SLPI* in A549 cells increases their ability to migrate.

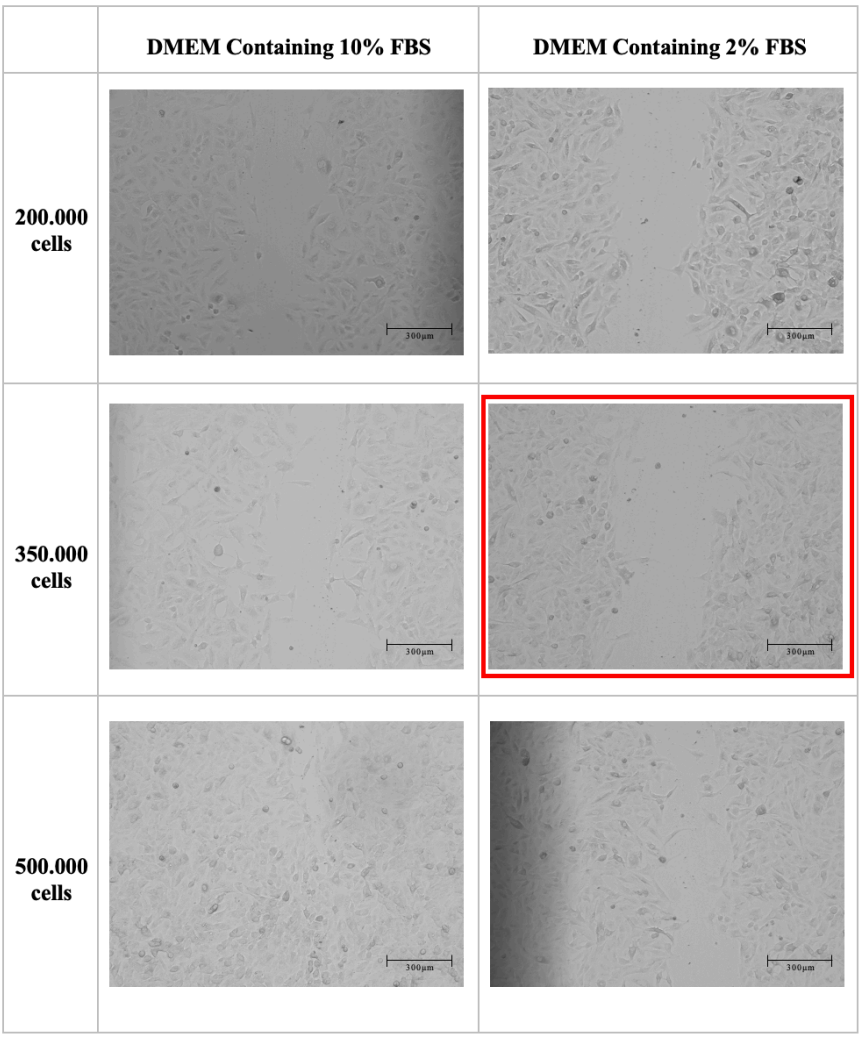

Figure 4.13 Optimization conditions of wound healing assay. 10X microscope images showing the best representative of the wound areas with different seeded cell numbers (200.000, 300.000, 500.000) and FBS% in DMEM. Scale bar 300µm.

A.

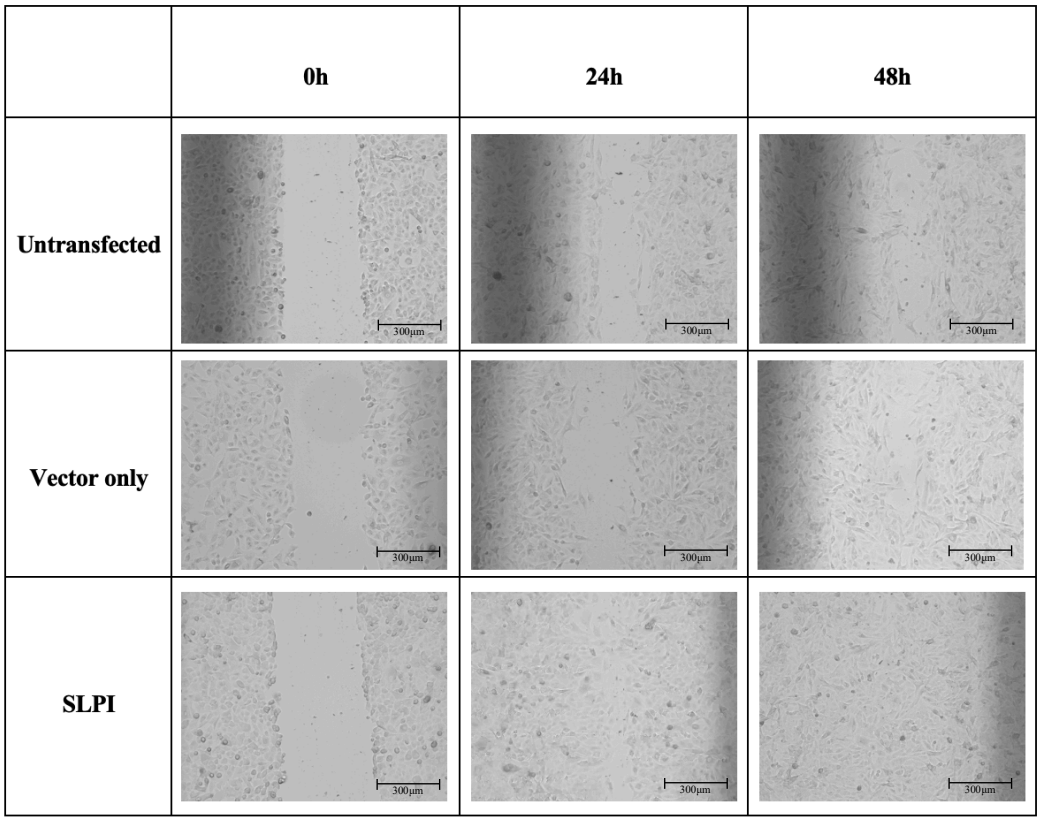

B.

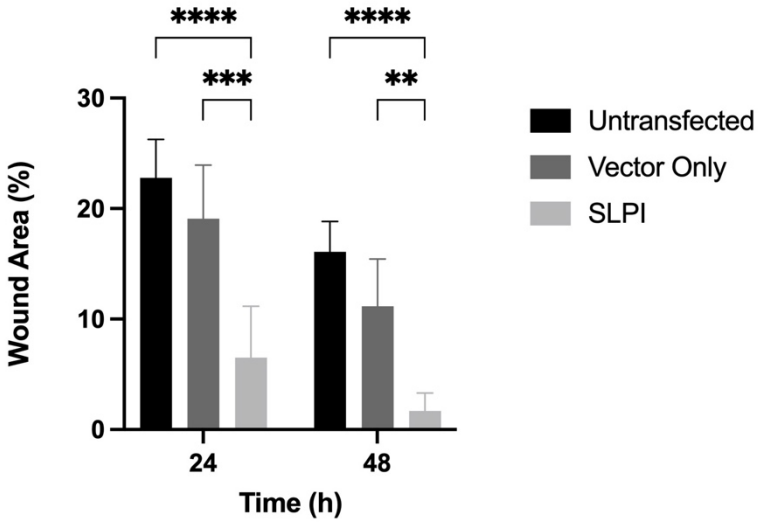

Figure 4.14 Wound healing assay results. A. 10X microscope images showing the best representative of the wound areas. Scale bar 300µm. B. Bar graph showing the wound area % of untransfected, vector only transfected, and *SLPI* transfected cells at three time points (0h, 24h, 48h). (p value<0,05; **0,037, ***0,0001, ****<0,0001)

4.2.5 CCK8 Assay

Different number of cells (1000, 2500, 5000, 7500, 10000) were seeded to find optimal conditions for this assay. OD was measured at 450 nm after 4 hours of incubation post CCK8 treatment. All of these cell numbers yielded an OD above 1 (data not shown). For this purpose, the cell number was decreased to 500 and the experiment was repeated at two different times with 3 replicates and 2 different time points. After seeding 500 cells for all groups (untransfected, vector only, and *SLPI* transfected) they were treated with CCK8 24 and 48 hours later, and their absorbance was measured at 450 nm. There was not any significant difference within the proliferative capacities of untransfected, vector only and *SLPI* transfected cells **(Figure 4.15)**.

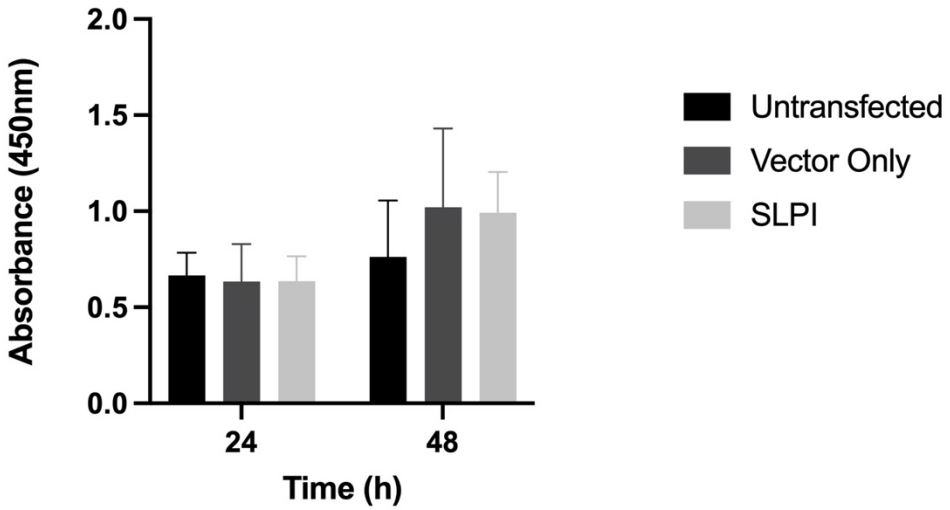

Figure 4.15 CCK8 assay results. Bar graph showing the absorbance at 450nm of cell types (untransfected, vector only transfected, and *SLPI* transfected) at 24h and 48h.

4.2.6 Matrigel Invasion Assay

10000 cells of each cell type (untransfected, vector only, and SLPI transfected) were seeded on Matrigel coated transwell inserts as three replicas. Cells in the transwell inserts were expected to migrate into the bottom chamber of the plate but they may also invade to the bottom of the insert, which demonstrates their metastatic and invasion capabilities, respectively. After 24h and 48h, cells that metastasized into the bottom chamber and invaded into the bottom of the insert were counted as described before. None of the cells were invaded to the bottom of the insert in any cell type after 24h and 48h. 24h post seeding the cells, around 10 untransfected and vector only transfected cells metastasized to the bottom chamber, whereas 17 *SLPI* transfected cells metastasized. This difference was not significant. Due to budget restrictions 24h experiment was not repeated. However, after 48h, repeated twice with 3 replicates, metastasized *SLPI* transfected cell number average increased dramatically, reaching to around 100. Only around 30-40 untransfected and vector only transfected cells metastasized to the bottom chamber. The best representative image of the 3 replicas were presented in the **Figure 4.16A**. These cell numbers metastasized to the bottom chamber were significantly higher at *SLPI* group when compared with the untransfected and vector only groups having p-value of 0,0261 and 0,0340 between untransfected and vector only groups, respectively **(Figure 4.16B)**. These results strongly supported that *SLPI* overexpression increased metastatic capabilities of A549 cells.

A.

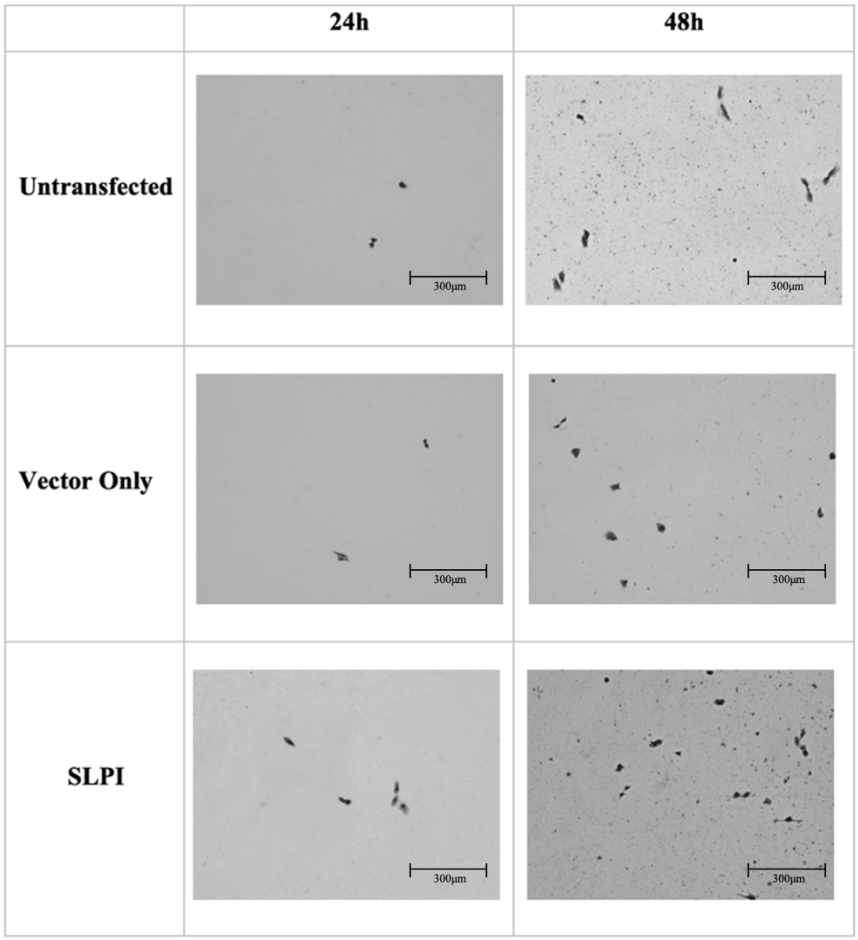

B.

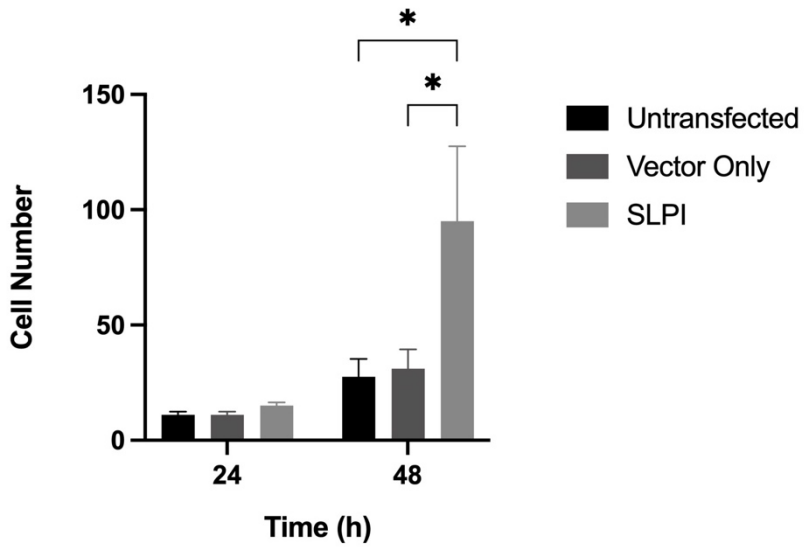

Figure 4.16 Invasion assay results. A. 10X microscope image showing the best representative of metastasized cells. Scale bar 300µm. B. Bar graph showing the metastasized cell number of each group (untransfected, vector only and *SLPI* transfected) ****p-value<0.05.

5. DISCUSSION & CONCLUSION

LMC, which develops when tumor cells are localized to the meninges in the brain, is most frequently seen as a result of metastasis brought on by melanoma, lung, and breast cancer. Regardless of treatment, LMC has a poor prognosis and life-span of patients is less than one year. The prevalence of LMC has risen as a consequence of the development of better diagnostic and monitoring techniques (31). Despite the increase in sequencing applications for LMC patients in recent years, their primary goal is to facilitating disease diagnosis. Because the molecular mechanisms underlying LMC are understood poorly in the literature, molecular research looking into the development of LMC are required.

In the first part of this thesis study, bioinformatic tools were used to analyze genes mutated in NSCLC in order to identify pathways that might be involved in the LMC development. According to our analysis, 87 genes were mutated in NSCLC-LMC patients. The PPI network revealed that 12 proteins did not interact with any other proteins. It was found that some of those proteins were involved in the enriched pathways even though they did not directly interact with other proteins. A pathway enrichment analysis carried out with g:Profiler showed that 856 pathways were associated with the LMC occurrence. According to the MCODE plug-in of Cytoscape, which detects densely connected regions in large PPI networks (39), 25 clusters were created. Six of those clusters were the main focus of this thesis since they might be more important for understanding the mechanism underlying this metastasis and identifying possible therapeutic targets: “response to radiation and environmental stimulus”, “DNA repair and regulation of TP53 activity”, “regulation of cell cycle”, “DNA pairing and transcriptional regulation”, “regulation of protein localization”, and “cell adhesion”. Four of these pathways are connected to each other with the exception of “regulation of protein localization” and “cell adhesion”.

All living organisms are exposed to low amounts of ionizing radiation (IR) that occurs naturally (70). Radiation therapy, one of the treatment methods in cancer, is vital for the local control of illness. Radiation has additional advantages when paired with chemotherapy that help manage the disease and increase the chances of survival for cancer patients. However, the persistence of disease and radioresistance following radiation therapy continue to be serious problems that reduce the effectiveness of the therapy (14). The two primary classes of DNA that are damaged by IR are exogenous and endogenous. Most endogenous DNA damage results from chemically active DNA, which engages in oxidative and hydrolytic reactions with reactive oxygen species (ROS) and water respectively, that are both presents in the cells. On the other side, exogenous DNA damage takes place when the DNA is damaged by environmental, chemical, and physical agents. UV, IR, crosslinking agents, and alkylating agents are some examples (71). Multiple forms of DNA damage such as DNA backbone cleavage and base damage that creates DNA single strand breaks (SSBs) are induced by IR. SSS repair and base excision repair (BER) pathways, respectively, are responsible for detecting and repairing these kinds of DNA damage. When two SSBs take place roughly 10–20 bp apart on opposing DNA strands, double strand breaks (DSBs) are created. Clustered lesions are created by additional types of DNA damage that may be present in the DNA near the DSB. These kinds of lesions may cause cell death if they are not repaired. Misrepaired DSBs can result in genomic instability and chromosomal translocations that can promote progression of cancer (70, 72). In response to IR, several signaling pathways such as apoptosis, activation of cell cycle checkpoints, and the DNA repair pathways are activated immediately to maintain genomic integrity and promote survival of cells (73). These processes work synergistically to shield cancer cells from radiation's damaging effects, ultimately resulting in the radioresistance development (14).

Studies demonstrated that HER receptor family of RTKs are activated by radiation. This receptor family, which consists of HER1 (EGFR), HER2, HER3, and HER4, is localized on the cell membrane (14). *EGFR* is the most well-known molecular biomarker in NSCLC. It is mutated in 10%–15% and 50% of Caucasians' and Asians' tumors respectively. Several human malignancies, as well as NSCLC, are prone to the onset and progression of abnormal ERBB signaling (74). EGFR activation can promote angiogenesis, cell survival, and tumor invasion; hence it has a crucial part in development and progression of NSCLC. Exons 18-21 of EGFR encodes that encodes for its kinase domain are where *EGFR* mutations have mainly been observed to occur (75). In-frame exon 19 deletions and the L858R change are the two most frequent *EGFR* mutations, accounting for approximately 45% of all cases. Point mutations in exon 18 (G719) and exon 21 (L861 and L861Q), and insertions in exons 19 and 20 are the rare mutations of *EGFR*, which account for 10% of all cases (16). Studies indicated that there was a higher prevalence of brain metastasis in NSCLC patients harboring EGFR mutations compared to ones having EGFR wild type tumors (76).

HER receptor activation causes the mitogen activated protein kinases/extracellular signal-regulated kinase (MAPK/ERK) and phosphatidylinositol 3-kinase (PI3K/AKT) signaling pathways to become active (14). The MAPK/ERK pathway is an essential signaling pathway, which controls molecular activities such as cell survival, proliferation, and differentiation, and tumor invasion (15). Rat sarcoma (RAS) and rapidly accelerated fibrosarcoma (RAF) protein families are involved in MAPK/ERK pathway. *KRAS* is one of the most frequently mutated isoforms of RAS and *KRAS* mutations are seen in approximately 33% of NSCLC patients (77). However, unlike *KRAS* in NSCLC, *BRAF* is only mutated in 2% of LUAD patients (78). Feedback regulation of KRAS is affected due to GTPase activity loss as a result of alteration in this gene. Both genes were also mutated in NSCLC-LMC patients in this study. MAPK/ERK and PI3K/AKT pathways are then activated by KRAS to promote cell proliferation continuously (16). Recent studies demonstrated that RAS activity increases cancer cells' radioresistance, whereas inhibiting ERK or MEK

causes cancer cells to become radiosensitive. Research showed that cancer cells become more radiosensitive when HER RTKs are inhibited. Once ERK1/2 is activated upon radiation, it activates more than 160 substrates through phosphorylation. Studies have shown that activation of ERK1/2 signaling is required to activate important regulators of G2/M cell cycle checkpoint, such as BRCA1 and ATR. This signaling pathways also promotes DNA repair by positively regulating ATM-dependent homologous recombination DSB repair (16).

The PI3K/AKT signaling pathway has many important roles including angiogenesis, cell survival, proliferation, growth, metabolism, and migration. It activates many downstream proteins such as AKT by phosphorylation. AKT is a member of a serine-threonine protein kinase family, and it consists of the homologues AKT1, AKT2, and AKT3 (16). Apoptotic signaling cascades are inhibited and pro-survival signals are activated by AKT, which acts as a pro-survival factor. Furthermore, AKT promotes non-homologous end joining (NHEJ) mediated DSB repair, which increases survival of cells. AKT also targets the mammalian target of rapamycin (mTOR) signaling, a master regulator of cell metabolism and growth. mTOR kinase is activated through phosphorylation by AKT (14). Phosphatidylinositol-4,5-bisphosphate 3-kinase catalytic subunit alpha (PIK3CA) is PI3K' the alpha isoform of its catalytic subunit and frequently mutated in NSCLC patients. PTEN, a tumor suppressor, negatively regulates PI3K/AKT pathway. This signaling cascade's aberrant activation has been linked to tumorigenesis and has been seen in a variety of cancers including NSCLC and has higher brain metastasis incidences (14, 79). Many studies have indicated that cancer cells become more radiosensitive both in *vitro* and in *vivo* when PI3K/AKT signaling is inhibited, whether through genetic methods or pharmacological inhibitors (14). Important members of this pathway (*AKT1, AKT2, AKT3, mTOR, PIK3CA,* and *PTEN*) have found to be mutated in NSCLC-LMC patients in this study and they have been also seen in other pathways, such as DNA repairing events and cell cycle regulation.

DSBs cause the DNA repair mechanism to become active. Double strand break repair nuclease MRE11, double strand break repair protein RAD50, and nibrin (NBS1) forms a complex called MRN, which binds to DSBs and activates ATM. Autophosphorylation of ATM at the DNA break site activates itself and variety of substrates in the nearby chromatin. Entire signaling cascade results in the phosphorylation of downstream proteins like CHEK1 and CHEK2, cell division cycle 25 (CDC25), and tumor protein P53 (TP53), which activates checkpoints and causes cell cycle arrest in G1/S or G2/M (64). Several studies who performed NGS or whole exome sequencing (WES) to individuals with brain metastases from NSCLC found that the following genes were altered: *TP53*, *EGFR*, adenomatous polyposis coli (*APC*), *ATM*, cyclin dependent kinase inhibitor 2A (*CDKN2A*), serine/threonine kinase 11 (*STK11*), ataxia telangiectasia and rad3-related protein (*ATR*), and *MYC* proto-oncogene (21). One of the main repair mechanisms, homologous recombinational repair (HRR) functions on DSBs and interstrand crosslink. A mechanism for repairing damaged in the replicated DNA in phases S and G2, without making any errors is provided by HRR. Therefore, it plays a crucial role in eliminating the chromosomal breaks prior to cell division by coordinating with checkpoints S and G2. (80). Through interacting with other DNA repair proteins such as ATM and RAD50, BRCA1 and BRCA2 have a significant role in HRR pathway. Studies in NSCLC demonstrated that *BRCA1* and *BRCA2* had the highest mutation rate among DNA repair genes (81). Most of these genes were also found to be mutated in NSCLC-LMC patients in this meta-analysis **Figure 4.3)**. Moreover, DNA metabolic process is another pathway that many genes mutated in NSCLC-LMC, such as *MYC* and telomerase reverse transcriptase (*TERT*), play role in. Biosynthesis of DNA is upregulated in cells that proliferate as it is crucial for cell division. MYC controls the expression of enzyme-encoding genes involved in the nucleotide biosynthesis (82). Studies showed that telomerase reactivation caused by mutations in the TERT's promoter contributed to the immortality of malignancies (83). A variety of DDR mechanisms are orchestrated by the primary tumor suppressor protein TP53, also referred as the guardian of the genome. In order to give the repair mechanisms enough time to restore genomic integrity, TP53 halts the cell cycle, which plays a significant role in facilitating DNA repair (84). It is the most commonly mutated gene in cancer.

According to studies, TP53 mutations can impair the TP53 protein's normal function, which has been associated to a poor prognosis in NSCLC (85).

Checkpoints in the cell cycle act as DNA surveillance systems to prevent propagation and accumulation of genetic errors in cell division. The checkpoints can delay the progression of cell cycle, or they can cause cell death or exit from the cell cycle in cases of severe DNA damage. Mutations associated to cancer, which affect control of cell cycle enable cell division to be continuous, primarily through impairing cells' ability to exit the cell cycle (86). Cyclins, cyclin dependent kinases (CDKs), retinoblastoma protein (RB) family, and CDK inhibitors tightly regulate the transition between the phases in the cell cycle. Although more than 20 CDKs have been identified, CDK1, 2, 4, and 6 are significant regulators of the progression of cell cycle. Cyclin D activates CDK4 and 6 by interacting with them and promotes the G1 phase progression following transcriptional activation. RB, a tumor suppressor, negatively regulates the progression of the cell cycle. Cyclin E is a key regulator S phase entry and is indirectly regulated by RB. Additionally, CDKN2A, a member of the INK4 family (CDK4 inhibitor), negatively regulates cell cycle (87). Most cancer cells have a defective G1 checkpoint, frequently as a result of mutations or alterations in major G1 checkpoint regulators such as Cyclin D or TP53 (14). Cyclin D1 and E1 (CCND1&CCNE1), CDKN2A, CDK4&6, RB, and TP53 genes are one of the most important regulators of cell cycle that are found to be mutated in NSCLC-LMC patients according to this meta-analysis.

The activity and the content of proteins control cellular processes. There are several ways to control proteins, ranging from post-translational modifications to modulation of gene expression. Cells can rapidly alter the function of local proteins by specifically guiding the localization of an existing protein pool. Various proteins perform specific tasks that are reliant on their localization environment or are required to perform the same tasks in different compartments (88). Genome instability, which promotes hallmark cancer functions via a variety of mechanisms such as protein

mislocalization, is responsible for the transformation of normal cells into cancer cells. Tumor suppressors, oncoproteins, and other proteins associated with cancer can be mislocalized, which can interfere with regular functions of cells and promote formation of tumors and their metastasis. There are few studies that reported aberrant cellular localizations of those proteins. For example, trafficking of EGFR from plasma membrane to the nucleus can cause cancer. In the nucleus, EGFR can induce the expression of genes that promote cell cycle such as Cyclin D. (89).

In healthy tissues, cell to extracellular matrix and cell-to-cell adhesion interactions are crucial for maintaining the homeostasis. The four main categories of the proteins that mediate these various interactions are integrins, cadherins, immunoglobulins, and selectins. These proteins are together referred to as cell adhesion molecules. They serve as a physical anchor for cells and play a crucial role in integrating signals between cells and the extracellular environment. Several disorders, from cancer to developmental intellectual disability, are often linked to mutations and alterations in the expression of cell adhesion proteins, especially integrins and cadherins. Integrins mediate cell-extracellular matrix adhesions, whereases cadherins mediate cell-cell adhesions. Anchorage-independent growth and loss of cell-to-cell adhesion are two hallmarks of cancer that rely on cell adhesion molecules. Genes such as cadherin 18 (CDH18), protein kinase 2 (PTK2), and NOTCH that were mutated in NSCLC-LMC patients play role in cell adhesion. CDH18 is a type 2 classical cadherin that facilitates the homotypic adhesive interactions (90). PTK2 is a focal adhesion kinase and regulates cell invasion, migration, adhesion, and survival (91). Notch signaling depends on cell-to-cell interactions in order to elicit a response to external stimuli. It is one of the signaling pathways that control EMT, which is thought to be primary driver of the metastasis of a tumor (90, 92) Aberrant activity of Notch signaling plays a role in the development of NSCLC (93). To sum up, all these pathways are connected to each other and share common genes. Any mutation of these genes can cause cancer and may have a part in development of leptomeningeal carcinoma. In the future, it may be helpful to investigate mutated genes in all of these pathways to better understand the mechanism

causing tumor cells to metastasize from the lungs to the meninges in the brain. In addition to these, other clusters should also be investigated as they might be important for understanding LMC progression.

There is no established standard LMC treatment due to the disease's rapid progression, low LMC prevalence, and the heterogeneity of the patient population. Currently, radiotherapy, intrathecal and systemic chemotherapy have been used for the treatment of LMC. Due to BBB and blood-CSF barrier, managing the dose levels of therapeutic agents is challenging. Methotrexate, cytarabine, and thiotepa are the most frequently used intrathecal chemotherapeutic agents. In recent years, molecular targeted therapy has been used in the clinic with very promising results (32). In order to identify drugs, which can be used to target mutated genes in NSCLC-LMC, a drug search was performed. Among FDA approved chemotherapy agents used in NSCLC treatment, BBB-crossing ones and the ones that interacting with the mutated genes in NSCLC-LMC were selected. These included EGFR TKI (afatinib, elotinib, gefitinib, and osimertinib), bevacizumab and everolimus (also used to treat brain tumors), capmatinib, and lorlatinib. Methotrexate and cytarabine, drugs used in LMC, were also found to be interacted with few of the mutated genes in NSCLC-LMC.

Methotrexate, an antimetabolite, inhibits the synthesis of thymidylate and purine nucleotide, as well as synthesis of DNA and RNA (94). It was found that, it interacts with GATA3, NOTCH1, NTRK1, RB1, TP53. Methotrexate sodium, which is the sodium salt of methotrexate was also one of the drugs that have been used to treat NSCLC. However, this form did not make any interactions with any genes according to the DGIdb. Cytarabine is an antimetabolite as methotrexate and inhibits DNA synthesis (95). It interacted with *ABCB1, GATA3, KIT, TP53. EGFR* is one of the main molecular biomarkers of NSCLC and hence the main molecular target. Erlotinib and gefitinib are the first-generation EGFR TKIs that can penetrate BBB, although they have a limited concentration in the CSF compared to plasma after their administration (76). They both compete with adenosine triphosphate (ATP) to

reversely bind EGFR's tyrosine kinase domain, inhibit the autophosphorylation of EGFR and inhibit the signal transduction (96,97). Afatinib and Osimertinib are the second- and third-generation EGFR TKIs, respectively. Both can cross BBB effectively and decrease the risk of progression of CNS. Afatinib and Osimertinib inhibits the EGFR signaling by irreversibly binding to several EGFR mutants such as del19, L858R, and T790M (resistant to first-generation EGFR TKIs), which were also seen in NSCLC-LMC patients (76, 98, 99). Four of these drugs also interacted with genes other than EGFR according to DGIdb **(Table 4.3)**. Capmatinib, BBB-crossing therapeutic agent, targets MET. It binds and inhibits the phosphorylation of MET, resulting in a disrupted signaling pathway (100, 101). Everolimus, a chemotherapeutic agent used to treat NSCLC and brain tumors, binds, and inhibits the activation of mTOR, which is the master regulator of cell metabolism and involved in PI3K/AKT pathway (102). It interacts with 18 more genes **(Table 4.3)**. Just like everolimus, bevacizumab also used in the treatment of NSCLC and brain tumors. It is a monoclonal anti- VEGF, which have roles in tumor growth and angiogenesis (103). It blocks VEGF binding to its receptors by binding to VEGF and disrupts its downstream signaling (104). It interacts with *ERBB2, KRAS, MET, PIK3CA, TP53, BRAF, KIT* and *EGFR.* Lorlatinib can cross BBB; it competes with ATP to bind ROS1 and ALK kinases, which disrupts their downstream signaling and inhibits the growth of tumors (105). It is also found to be interacted with TP53.

Studies that seek to create new therapy methods for this kind of cancer are particularly important. Metastatic cancer research can lead to the identification of targeted genes and the discovery of new drugs in that field. By comparing genes that are overexpressed in tumors but normal in healthy controls, these genes can be discovered. Similar procedures were followed in the second part of the thesis by investigating the effects of overexpression of *SLPI* gene, which was found to be overexpressed in NSCLC-LMC patients in one study (2).

SLPI performs a variety of functions, including controlling inflammation and acting as an antibacterial agent as well as preventing tissue destruction. SLPI has a substantial inhibitory effect on serine proteases. Although *SLPI* is increased in several carcinomas, including pancreatic, gastric, and breast cancer, its function in cancer is still not fully known. Previous studies showed that serum SLPI levels were higher in patients with NSCLC compared to healthy controls. This implied a relationship between tumor growth and serum SLPI. However, neither of these studies investigated whether SLPI is secreted by tumor cells or elevated in tumor cells (5). Nevertheless, in the publicly accessible databases UALCAN and GEPIA, it was discovered that the *SLPI* gene expression was reduced relative to normal in patients with LUAD (3, 26). As a result, it is unclear how SLPI affects lung cancer. Therefore, in order to fill the gap in the literature with the correct information, we investigated the expression change of *SLPI* on cancer metastasis and invasion, as well as cells' proliferation on A549 lung cancer cell line in *vitro*. We overexpressed *SLPI* in A549 cell line using p3xFLAG-CMV vector. In the PCR we conducted to confirm the *SLPI* overexpression, *SLPI* mRNA levels were very low. We were able to show the overexpression only after performing a second PCR on these PCR products. This situation may be explained by the fact that levels of *SLPI* was reduced in LUAD in UALCAN and GEPIA, and A549 cells only express a small amount of this gene.

Next, ELISA was performed to detect protein levels in the medium of each cell type, as SLPI is a secreted protein. Cells' medium was collected at 96h after they were seeded, however protein concentrations of each cell type were quite low. We thought that may be half-life of SLPI protein is less than 96h. The half-life of SLPI protein is not fully established in the literature. However, one study demonstrated that levels of SLPI transcripts remained stable in 24h time period in bronchial epithelial cells (106). Therefore, we also collected cells' medium at 24- and 48-hours and repeated ELISA with two different incubation time of antibody-protein binding (37°C, 80min and +4°C, overnight). However, these changes did not affect the results and no significant amount of SLPI proteins were detected. One reason to explain this may be that, as we saw in the PCR results, this gene is expressed in low amounts inside cells and may be

in an amount that cannot be detected when it is secreted by the ELISA kit, which could detect the lowest 62.5pg/mL. Additionally, the half-life of this protein might be less than 24h, which also affect its detection. Another possibility is that due to the fusion of the protein to the cell via a vector from the ATG of the FLAG tag and most probably produced with FLAG tag, its secretion out of the cell may be affected or prevented. We also try to show the SLPI protein overexpression from cell lysates. However, we could not find any significant difference in SLPI protein levels between untrasfected, vector only, and SLPI transfected cells. After we could not demonstrate the protein levels with ELISA, we performed western blot to indicate the protein levels of each type of cell (untransfected, vector only, and SLPI transfected) as well as the ectopic expression of FLAG tag vector. However, this experiment still requires further optimizations and could not yield any results.

Wound healing and transwell invasion assays were performed to evaluate how *SLPI* overexpression impacts the ability of A549 cells to migrate, and invade and metastasize, respectively. Wound healing assay results demonstrated that overexpression of *SLPI* in A549 cells enhanced their migration ability significantly. According to the transwell invasion assay, after 24 hours and 48 hours, results indicated that A549 cells' ability to metastasize was enhanced significantly by *SLPI* overexpression.

Cell migration is an important process wherein cells must be able to adapt and move to the proper position in a specific environment to carry out their function. Moving cells, however, have the potential to become dysregulated and contribute to a variety of clinical conditions, including inflammation and cancer metastasis. Cancer cells can migrate either individually or collectively, using numerous movement mechanisms. Cytoskeletal activity mediates individual cell migration without cell-to-cell contact with their surrounding cells. It has been shown that it plays a crucial role in a variety of in vivo physiological processes, including immune surveillance, early stages of invasion in the metastatic process, and stages of embryonic development.

Cancer cells, for instance, can move independently in a mesenchymal or amoeboid manner. Integrins and matrix-degrading proteases are involved in mesenchymal migration. In contrast, cohesive cell groups that maintain cell-to-cell connections and coordinate cytoskeletal activity with both the surrounding tissue and nearby cells migrate collectively. Cell-cell adhesion and cell-substrate adhesion are two of the mechanisms at action. Using focal adhesion complexes along with associated stress fibers, cells can firmly attach to ECM protein-coated surfaces (107). Sequential events lead to cancer metastasis. Process starts with the detachment of malignant cells from the original tumor mass, which is followed by the digestion of the surrounding ECM and the migration through it. Then, they are transported throughout the body via blood or lymph and transmigrate into the extravascular area upon breaching the vessel wall. Finally, malignant cells adapt to their new site and outgrow. The matrix metalloproteinases (MMPs), which are among the enzymes synthesized and employed by cancerous cells during cancer cell invasion and metastasis, are the key contributors to ECM destruction. Several kinds of human cancer exhibit high MMP levels, which correlate well with the clinical development of such tumors. As a result, MMPs are recognized as either tumor markers or potential targets for cancer treatment. MMP-9, also known as gelatinase B, is one of the MMPs and performs out a variety of functions, the majority of which promote the growth and spread of tumors. Only a small subset of cell types, including macrophages and neutrophils, express MMP-9 constitutively, which is due to its critical function in reactive processes including wound healing and inflammation. MMP-9 is mainly produced by other cells, such as osteoblasts, fibroblasts, endothelial, epithelial, and dendritic cells when they are stimulated by chemokines, growth factors, or cytokines. Expression of MMP-9 and the induction of EMT can be also triggered by PI3K/AKT, MAPK/ERK, and NFκB signaling pathways (108).

There are several studies showing the interaction between SLPI and MMPs in different type of cancers. As a protease inhibitor, SLPI was previously thought to prevent cancer since the ECM must be degraded for tumor development and invasion. Although it seems counterintuitive, as demonstrated by recent research, SLPI promotes tumor growth and metastasis (5). In one study it was found that the secretion of SLPI upregulated the transcription and production of MMP-9 in ovarian cancer cells (109). In another study conducted on gastric cancer cell line, SLPI increased MMP-2 and MMP-9 expression, which in turn accelerated the metastatic process of these cells, including cell migration and invasion (110). Based on these findings, Mikami et al. investigated the effects of SLPI in oral carcinoma cells that express high amounts of *SLPI*. They found that upon inhibition of *SLPI*, migration rate as well as the mRNA levels of *MMP-2* and *MMP-9* of these cells were decreased. These results also indicated that together with MMPs, SLPI is crucial for the invasion of oral cancer cells (111). Although our study does not contain any partnership experiments with SLPI and other proteins, they are in support of the literature by demonstrating the enhanced metastatic ability of A549 cells.

NSCLC was not included in any of the research that examined the relationship between SLPI and MMPs in other malignancies. *MMP* and *SLPI* expression in NSCLC have only been studied independently in just few studies. One study demonstrated that *MMP-9* overexpression in NSCLC caused an aggressiveness in the tumor behavior (112). However, another study showed that activity of MMP-9 was significantly decreased, while activity of MMP-2 was significantly increased in NSCLC tissues compared to normal ones. Their results suggested that MMP-2 implicated in early-stage tumor invasion and metastasis in NSCLC (113). More research is required on this topic as both results are in contradiction of one another. Moreover, one group showed that 3LL-S Lewis Lung Carcinoma cells' tumorigenic and metastatic capacity was enhanced by SLPI (27). Later, the same group discovered a relationship between TNF-α and 3LL-S cells, wherein host TNF-α promoted the expression of *SLPI* in 3LL-S cells, which in turn aided in tumor development and metastasis (114).

We have shown that *SLPI* overexpression increased the migration and metastatic capability of A549 cells in *vitro*. Considering all the research that has been done, we may conclude that SLPI may interact and upregulate MMP-9, which can then facilitate the migration and metastasis of these cells. This might help us to understand the underlying mechanism that drive the metastasis of lung cancer to the meninges in NSCLC-LMC patients. However, if we reach our hypothesis from another perspective, other factors such as TNF-α production may be triggering the overexpression of *SLPI* in NSCLC-LMC patients, which in turn increase the activity of MMP-9 and induce metastasis.

The capacity of cancer cells to maintain persistent proliferation is one of their most essential characteristics. Growth-promoting signals, which guide the initiation and progress of cellular growth and division, are produced and released by normal tissues under strict supervision. By disabling these signals, cancer cells take control of their own fate. In a variety of different methods, cancer cells can develop the ability to maintain proliferative signals. They might produce growth factor ligands on their own or they might transmit signals that activate the normal cells sustaining the tumor-associated stroma. Recent findings have emphasized the significance of negative feedback loops, which typically work to dampen different types of signaling. Proliferative signaling can be increased by defects within these feedback mechanisms (9).

We performed CCK8 assay to investigate the effects of elevated *SLPI* levels on cell proliferation in A549 cells. Although we were unable to demonstrate any difference in the rates of proliferation between the untransfected, vector only, and *SLPI* transfected cells, previous studies conducted on different cell types had shown otherwise. It was shown that knockdown of *SLPI* induced proliferation of pancreatic ductal adenocarcinoma cells (115). Similar results were also obtained in colorectal cancer cells; *SLPI* inhibition also resulted with inhibited proliferation of these cells. Additionally, they indicated an association between the knockdown of *SLPI* and AKT

signaling down regulation (116). Only a few studies investigated how SLPI affected lung cancer cell proliferation. In one study, it was shown that after the treatment with recombinant SLPI, proliferation of A549 cells was increased by 24% in contrast to cells that were not treated (117). In another study conducted on 3LL-S, it was revealed that proliferation of these cells was also enhanced by SLPI. Although, they demonstrated that SLPI contributed to the 3LL-S cells' malignant behavior, it was due to its protease activity, not on its capacity to enhance cell proliferation (27). This circumstance may also support us in explanation of our findings. Although, *SLPI* overexpression did not enhance proliferation of A549 cells, their migration and metastatic capabilities were increased, hence it was not associated to their proliferation.

In conclusion, mutated genes in NSCLC-LMC patients and the effects of overexpression *SLPI* gene on A549 LUAD cell line were investigated. Through the meta-analysis, 87 genes were found to be mutated in these patients. Among the molecular pathways that these genes have role in 6 of them were discussed as they may help us to better understand the mechanism underlying this metastasis and to find potential drug targets: “response to radiation and environmental stimulus”, “DNA repair and regulation of TP53 activity”, “regulation of cell cycle”, “DNA pairing and transcriptional regulation”, “regulation of protein localization”, and “cell adhesion”. We also showed that although *SLPI* overexpression did not have significant effect on A549 cells, it increased their migration and metastatic capabilities, which can provide further insight to the mechanism of this metastasis. Therefore, understanding the mutational landscape and gene expression changes are essential to better understand LMC development.

As there were large number of mutated genes in LMC patients, further research into other molecular pathways that they play role in may be pursued. The exact role of SLPI on migration and metastasis of LUAD cells can be further investigated. It is also possible to investigate how *SLPI* affects these cells' capacity for migration and

metastasis, as well as the proteins with which it interacts and the genes it activates/upregulates in *vitro*/in *vivo*. Larger cohort studies using various omics strategies, as well as the generation of new therapeutic candidates, are also required.

6. REFERENCES

1. Bhambhvani HP, Rodrigues AJ, Umeh-Garcia MC, et al. Leptomeningeal Carcinomatosis. Neurosurgery Clinics of North America 2020; 31: 613–625.
2. Ruan H, Zhou Y, Shen J, et al. Circulating tumor cell characterization of lung cancer brain metastases in the cerebrospinal fluid through single-cell transcriptome analysis. Clinical and Translational Medicine 2020; 10(8):e246
3. Chandrashekar DS, Bashel B, Balasubramanya SAH, et al. UALCAN: A Portal for Facilitating Tumor Subgroup Gene Expression and Survival Analyses. Neoplasia 2017; 19: 649–658.
4. Gene Ontology Consortium. The Gene Ontology (GO) database and informatics resource. Nucleic Acids Research 2004; 32: 258D – 261.
5. Nugteren S, Samsom JN. Secretory Leukocyte Protease Inhibitor (SLPI) in mucosal tissues: Protects against inflammation, but promotes cancer. Cytokine & Growth Factor Reviews 2021; 59: 22–35.
6. Ferlay J, Ervik M, Lam F, Colombet M, Mery L, Piñeros M, Znaor A, Soerjomataram I, Bray F. Global Cancer Observatory: Cancer Today 2020; Available from: https://gco.iarc.fr/today, accessed 09 May 2023.
7. Siegel RL, Miller KD, Wagle NS, et al. Cancer statistics, CA: A Cancer Journal for Clinicians 2023; 73: 17–48.
8. Diori Karidio I, Sanlier SH. Reviewing cancer's biology: an eclectic approach. Journal of the Egyptian National Cancer Institute; 33. Epub ahead of print November 1, 2021.
9. Hanahan D. Hallmarks of Cancer: New Dimensions. Cancer Discovery 2022; 12: 31–46.
10. N Kontomanolis E, Koutras A, Syllaios A, Schizas D, Kalagasidou S, Pagkalos A, Alatzidou D, Kantari P, Ntounis T, Fasoulakis Z. Basic principles of molecular biology of cancer cell-Molecular cancer indicators. J BUON 2021;26(5):1723-1734
11. Jiao Z, Pan Y, Chen F. The Metabolic Landscape of Breast Cancer and Its Therapeutic Implications. Molecular Diagnosis & Therapy 2023; 27: 349–369.
12. Barzaman K, Karami J, Zarei Z, et al. Breast cancer: Biology, biomarkers, and treatments. International Immunopharmacology 2020; 84: 106535.
13. Noh D-Y, Han W, Toi M (eds). Translational Research in Breast Cancer. Advances in Experimental Medicine and Biology. Epub ahead of print 2021.
14. Hein AL, Ouellette MM, Yan Y. Radiation-induced signaling pathways that promote cancer cell survival (Review). International Journal of Oncology 2014; 45: 1813–1819.
15. Sinkala M, Nkhoma P, Mulder N, et al. Integrated molecular characterisation of the MAPK pathways in human cancers reveals pharmacologically vulnerable mutations and gene dependencies. Communications Biology; 4. Epub ahead of print January 4, 2021.
16. Calvayrac O, Pradines A, Pons E, et al. Molecular biomarkers for lung adenocarcinoma. European Respiratory Journal 2017; 49: 1601734.

17. Teixido C, Castillo P, Martinez-Vila C, et al. Molecular Markers and Targets in Melanoma. Cells 2021; 10: 2320.
18. Thai AA, Solomon BJ, Sequist LV, et al. Lung cancer. The Lancet 2021; 398: 535–554.
19. Schabath MB, Cote ML. Cancer Progress and Priorities: Lung Cancer. Cancer Epidemiology, Biomarkers & Prevention 2019; 28: 1563–1579.
20. Wang Y, Zou S, Zhao Z, et al. New insights into small-cell lung cancer development and therapy. Cell Biology International 2020; 44: 1564–1576.
21. Non-Small Cell Lung Cancer Treatment (PDQ®)–Health Professional Version. U. S. National Institutes of Health, National Cancer Institute. https://www.cancer.gov/types/lung/hp/non-small-cell-lung-treatment-pdq (2023) Accessed on 10 April 2023.
22. Fois SS, Paliogiannis P, Zinellu A, et al. Molecular Epidemiology of the Main Druggable Genetic Alterations in Non-Small Cell Lung Cancer. International Journal of Molecular Sciences 2021; 22: 612.
23. Sousa V, Reis D, Silva M, et al. Amplification of FGFR1 gene and expression of FGFR1 protein is found in different histological types of lung carcinoma. Virchows Archiv 2016; 469: 173–182.
24. Miao J-L, Liu R-J, Zhou J-H, et al. Fibroblast Growth Factor Receptor 1 Gene Amplification in Nonsmall Cell Lung Cancer. Chinese Medical Journal 2016; 129: 2868–2872.
25. Pérez-Ramírez C, Cañadas-Garre M, Molina MÁ, et al. PTEN and PI3K/AKT in non-small-cell lung cancer. Pharmacogenomics 2015; 16: 1843–1862.
26. Tang Z, Li C, Kang B, et al. GEPIA: a web server for cancer and normal gene expression profiling and interactive analyses. Nucleic Acids Research 2017; 45: W98–W102.
27. Devoogdt N, Hassanzadeh Ghassabeh G, Zhang J, et al. Secretory leukocyte protease inhibitor promotes the tumorigenic and metastatic potential of cancer cells. Proceedings of the National Academy of Sciences 2003; 100: 5778–5782.
28. Fares J, Fares MY, Khachfe HH, et al. Molecular principles of metastasis: a hallmark of cancer revisited. Signal Transduction and Targeted Therapy; 5. Epub ahead of print March 12, 2020.
29. Yeung KT, Yang J. Epithelial-mesenchymal transition in tumor metastasis. Molecular Oncology 2016; 11: 28–39.
30. Campbell BK, Gao Z, Corcoran NM, et al. Molecular Mechanisms Driving the Formation of Brain Metastases. Cancers 2022; 14: 4963.
31. Pellerino A, Brastianos PK, Rudà R, et al. Leptomeningeal Metastases from Solid Tumors: Recent Advances in Diagnosis and Molecular Approaches. Cancers 2021; 13: 2888.
32. Lee D-W, Lee K-H, Kim J, et al. Molecular Targeted Therapies for the Treatment of Leptomeningeal Carcinomatosis: Current Evidence and Future Directions. International Journal of Molecular Sciences 2016; 17: 1074.
33. Lee YH. An overview of meta-analysis for clinicians. The Korean Journal of Internal Medicine 2018; 33: 277–283.
34. Page MJ, McKenzie JE, Bossuyt PM, et al. The PRISMA 2020 statement: an updated guideline for reporting systematic reviews. BMJ 2021; n71.

35. Szklarczyk D, Kirsch R, Koutrouli M, et al. The STRING database in 2023: protein–protein association networks and functional enrichment analyses for any sequenced genome of interest. Nucleic Acids Research 2022; 51: D638–D646.
36. Raudvere U, Kolberg L, Kuzmin I, et al. g:Profiler: a web server for functional enrichment analysis and conversions of gene lists (2019 update). Nucleic Acids Research 2019; 47: W191–W198.
37. Shannon P, Markiel A, Ozier O, et al. Cytoscape: A Software Environment for Integrated Models of Biomolecular Interaction Networks. Genome Research 2003; 13: 2498–2504.
38. Merico D, Isserlin R, Stueker O, et al. Enrichment Map: A Network-Based Method for Gene-Set Enrichment Visualization and Interpretation. PLoS ONE 2010; 5: e13984.
39. Bader GD, Hogue CW. An automated method for finding molecular complexes in large protein interaction networks. BMC Bioinformatics 2003; 4:2.
40. Freshour SL, Kiwala S, Cotto KC, et al. Integration of the Drug–Gene Interaction Database (DGIdb 4.0) with open crowdsource efforts. Nucleic Acids Research 2020; 49: D1144–D1151.
41. Bright MA. The National Cancer Institute's Cancer Information Service: A premiere cancer information and education resource for the nation. Journal of Cancer Education 2007; 22: S2–S7.
42. Darrow JJ, Avorn J, Kesselheim AS. FDA Approval and Regulation of Pharmaceuticals, 1983-2018. JAMA 2020; 323: 164.
43. Landrum MJ, Lee JM, Benson M, et al. ClinVar: improving access to variant interpretations and supporting evidence. Nucleic Acids Research 2017; 46: D1062–D1067.
44. Sherry ST. dbSNP: the NCBI database of genetic variation. Nucleic Acids Research 2001; 29: 308–311.
45. Tate JG, Bamford S, Jubb HC, et al. COSMIC: the Catalogue Of Somatic Mutations In Cancer. Nucleic Acids Research 2018; 47: D941–D947.
46. Li Y, Liu B, Connolly ID, et al. Recurrently Mutated Genes Differ between Leptomeningeal and Solid Lung Cancer Brain Metastases. Journal of Thoracic Oncology 2018; 13: 1022–1027.
47. Jiang B-Y, Li Y-S, Guo W-B, et al. Detection of Driver and Resistance Mutations in Leptomeningeal Metastases of NSCLC by Next-Generation Sequencing of Cerebrospinal Fluid Circulating Tumor Cells. Clinical Cancer Research 2017; 23: 5480–5488.
48. Li YS, Jiang BY, Yang JJ, et al. Unique genetic profiles from cerebrospinal fluid cell-free DNA in leptomeningeal metastases of EGFR-mutant non-small-cell lung cancer: a new medium of liquid biopsy. Annals of Oncology 2018; 29: 945–952.
49. Ying S, Ke H, Ding Y, et al. Unique genomic profiles obtained from cerebrospinal fluid cell-free DNA of non-small cell lung cancer patients with leptomeningeal metastases. Cancer Biology & Therapy 2018; 20: 562–570.
50. Wang Y, Jiang F, Xia R, et al. Unique Genomic Alterations of Cerebrospinal Fluid Cell-Free DNA Are Critical for Targeted Therapy of Non-Small Cell Lung Cancer With Leptomeningeal Metastasis. Frontiers in Oncology; 11. Epub ahead of print October 4, 2021.

51. Ge M, Zhan Q, Zhang Z, et al. Different next-generation sequencing pipelines based detection of tumor DNA in cerebrospinal fluid of lung adenocarcinoma cancer patients with leptomeningeal metastases. BMC Cancer; 19. Epub ahead of print February 12, 2019.
52. Ma C, Yang X, Xing W, et al. Detection of circulating tumor DNA from non-small cell lung cancer brain metastasis in cerebrospinal fluid samples. Thoracic Cancer 2020; 11: 588–593.
53. Zheng M-M, Li Y-S, Jiang B-Y, et al. Clinical Utility of Cerebrospinal Fluid Cell-Free DNA as Liquid Biopsy for Leptomeningeal Metastases in ALK-Rearranged NSCLC. Journal of Thoracic Oncology 2019; 14: 924–932.
54. Pan W, Gu W, Nagpal S, et al. Brain Tumor Mutations Detected in Cerebral Spinal Fluid. Clinical Chemistry 2015; 61: 514–522.
55. Fan Y, Zhu X, Xu Y, et al. Cell-Cycle and DNA-Damage Response Pathway Is Involved in Leptomeningeal Metastasis of Non–Small Cell Lung Cancer. Clinical Cancer Research 2018; 24: 209–216.
56. Siravegna G, Geuna E, Mussolin B, et al. Genotyping tumour DNA in cerebrospinal fluid and plasma of a HER2-positive breast cancer patient with brain metastases. ESMO Open 2017; 2: e000253.
57. Li X, Zhang Y, Ding J, et al. Clinical significance of detecting CSF-derived tumor cells in breast cancer patients with leptomeningeal metastasis. Oncotarget 2017; 9: 2705–2714.
58. De Mattos-Arruda L, Mayor R, Ng CKY, et al. Cerebrospinal fluid-derived circulating tumour DNA better represents the genomic alterations of brain tumours than plasma. Nature Communications; 6. Epub ahead of print November 10, 2015.
59. Li Y, Pan W, Connolly ID, et al. Tumor DNA in cerebral spinal fluid reflects clinical course in a patient with melanoma leptomeningeal brain metastases. Journal of Neuro-Oncology 2016; 128: 93–100.
60. Ballester LY, Glitza Oliva IC, Douse DY, et al. Evaluating Circulating Tumor DNA From the Cerebrospinal Fluid of Patients With Melanoma and Leptomeningeal Disease. Journal of Neuropathology & Experimental Neurology 2018; 77: 628–635.
61. Szklarczyk D, Gable AL, Lyon D, et al. STRING v11: protein–protein association networks with increased coverage, supporting functional discovery in genome-wide experimental datasets. Nucleic Acids Research 2018; 47: D607–D613.
62. Reimand J, Isserlin R, Voisin V, et al. Pathway enrichment analysis and visualization of omics data using g:Profiler, GSEA, Cytoscape and EnrichmentMap. Nature Protocols 2019; 14: 482–517.
63. Drugs Approved for Different Types of Cancer U. S. National Institutes of Health, National Cancer Institute. https://www.cancer.gov/about-cancer/treatment/drugs/cancer-type (2022). Accessed on 19 October 2022.
64. Cunningham F, Allen JE, Allen J, et al. Ensembl 2022. Nucleic Acids Research 2021; 50: D988–D995.
65. Vincze T. NEBcutter: a program to cleave DNA with restriction enzymes. Nucleic Acids Research 2003; 31: 3688–3691.

66. Kent WJ, Sugnet CW, Furey TS, et al. The Human Genome Browser at UCSC. Genome Research 2002; 12: 996–1006.
67. Ye J, Coulouris G, Zaretskaya I, et al. Primer-BLAST: A tool to design target-specific primers for polymerase chain reaction. BMC Bioinformatics; 13. Epub ahead of print June 18, 2012.
68. Yasuda H, Kobayashi S, Costa DB. EGFR exon 20 insertion mutations in non-small-cell lung cancer: preclinical data and clinical implications. The Lancet Oncology 2012; 13: e23–e31.
69. Duggirala KB, Lee Y, Lee K. Chronicles of EGFR Tyrosine Kinase Inhibitors: Targeting EGFR C797S Containing Triple Mutations. Biomolecules & Therapeutics 2022; 30: 19–27.
70. Mahaney BL, Meek K, Lees-Miller SP. Repair of ionizing radiation-induced DNA double-strand breaks by non-homologous end-joining. Biochemical Journal 2009; 417: 639–650.
71. Chatterjee N, Walker GC. Mechanisms of DNA damage, repair, and mutagenesis. Environmental and Molecular Mutagenesis 2017; 58: 235–263.
72. Vignard J, Mirey G, Salles B. Ionizing-radiation induced DNA double-strand breaks: A direct and indirect lighting up. Radiotherapy and Oncology 2013; 108: 362–369.
73. Li L, Story M, Legerski RJ. Cellular responses to ionizing radiation damage. International Journal of Radiation Oncology*Biology*Physics 2001; 49: 1157–1162.
74. Masood A, Kancha RK, Subramanian J. Epidermal growth factor receptor (EGFR) tyrosine kinase inhibitors in non-small cell lung cancer harboring uncommon EGFR mutations: Focus on afatinib. Seminars in Oncology 2019; 46: 271–283.
75. Bai Y, Liu X, Zheng L, et al. Comprehensive profiling of EGFR mutation subtypes reveals genomic-clinical associations in non-small-cell lung cancer patients on first-generation EGFR inhibitors. Neoplasia 2023; 38: 100888.
76. Hochmair M. Medical Treatment Options for Patients with Epidermal Growth Factor Receptor Mutation-Positive Non-Small Cell Lung Cancer Suffering from Brain Metastases and/or Leptomeningeal Disease. Targeted Oncology 2018; 13: 269–285.
77. Reck M, Carbone DP, Garassino M, et al. Targeting KRAS in non-small-cell lung cancer: recent progress and new approaches. Annals of Oncology 2021; 32: 1101–1110.
78. Yan N, Guo S, Zhang H, et al. BRAF-Mutated Non-Small Cell Lung Cancer: Current Treatment Status and Future Perspective. Frontiers in Oncology; 12. Epub ahead of print March 31, 2022.
79. Tan AC. Targeting the PI3K/Akt/mTOR pathway in non-small cell lung cancer (NSCLC). Thoracic Cancer 2020; 11: 511–518.
80. Thompson LH, Schild D. Homologous recombinational repair of DNA ensures mammalian chromosome stability. Mutation Research/Fundamental and Molecular Mechanisms of Mutagenesis 2001; 477: 131–153.
81. Mekonnen N, Yang H, Shin YK. Homologous Recombination Deficiency in Ovarian, Breast, Colorectal, Pancreatic, Non-Small Cell Lung and Prostate Cancers, and the Mechanisms of Resistance to PARP Inhibitors. Frontiers in Oncology; 12. Epub ahead of print June 17, 2022.
82. Lane AN, Fan TW-M. Regulation of mammalian nucleotide metabolism and biosynthesis. Nucleic Acids Research 2015; 43: 2466–2485.

83. Colebatch AJ, Dobrovic A, Cooper WA. TERT gene: its function and dysregulation in cancer. Journal of Clinical Pathology 2019; 72: 281–284.
84. Williams AB, Schumacher B. p53 in the DNA-Damage-Repair Process. Cold Spring Harbor Perspectives in Medicine 2016; 6: a026070.
85. Chen X, Zhang T, Su W, et al. Mutant p53 in cancer: from molecular mechanism to therapeutic modulation. Cell Death & Disease; 13. Epub ahead of print November 18, 2022.
86. Matthews HK, Bertoli C, de Bruin RAM. Cell cycle control in cancer. Nature Reviews Molecular Cell Biology 2021; 23: 74–88.
87. Leal-Esteban LC, Fajas L. Cell cycle regulators in cancer cell metabolism. Biochimica et Biophysica Acta (BBA) - Molecular Basis of Disease 2020; 1866: 165715.
88. Bauer NC, Doetsch PW, Corbett AH. Mechanisms Regulating Protein Localization. Traffic 2015; 16: 1039–1061.
89. Wang X, Li S. Protein mislocalization: Mechanisms, functions and clinical applications in cancer. Biochimica et Biophysica Acta (BBA) - Reviews on Cancer 2014; 1846: 13–25.
90. Janiszewska M, Primi MC, Izard T. Cell adhesion in cancer: Beyond the migration of single cells. Journal of Biological Chemistry 2020; 295: 2495–2505.
91. Tong X, Tanino R, Sun R, et al. Protein tyrosine kinase 2: a novel therapeutic target to overcome acquired EGFR-TKI resistance in non-small cell lung cancer. Respiratory Research; 20. Epub ahead of print December 2019.
92. Aster JC, Pear WS, Blacklow SC. The Varied Roles of Notch in Cancer. Annual Review of Pathology: Mechanisms of Disease 2017; 12: 245–275.
93. Sharif A, Shaji A, Chammaa M, et al. Notch Transduction in Non-Small Cell Lung Cancer. International Journal of Molecular Sciences 2020; 21: 5691.
94. National Center for Biotechnology Information (2023). PubChem Compound Summary for CID 126941, Methotrexate. Retrieved March 28, 2023 from https://pubchem.ncbi.nlm.nih.gov/compound/Methotrexate.
95. National Center for Biotechnology Information (2023). PubChem Compound Summary for CID 6253, Cytarabine. Retrieved March 28, 2023 from https://pubchem.ncbi.nlm.nih.gov/compound/Cytarabine.
96. National Center for Biotechnology Information (2023). PubChem Compound Summary for CID 176870, Erlotinib. Retrieved March 28, 2023 from https://pubchem.ncbi.nlm.nih.gov/compound/Erlotinib.
97. National Center for Biotechnology Information (2023). PubChem Compound Summary for CID 123631, Gefitinib. Retrieved March 28, 2023 from https://pubchem.ncbi.nlm.nih.gov/compound/Gefitinib.
98. National Center for Biotechnology Information (2023). PubChem Compound Summary for CID 10184653, Afatinib. Retrieved March 28, 2023 from https://pubchem.ncbi.nlm.nih.gov/compound/Afatinib.

99. National Center for Biotechnology Information (2023). PubChem Compound Summary for CID 71496458, Osimertinib. Retrieved March 28, 2023 from https://pubchem.ncbi.nlm.nih.gov/compound/Osimertinib.
100. Heist RS, Seto T, Han J-Y, et al. CMET-22. CAPMATINIB (INC280) IN METΔEX14-MUTATED ADVANCED NON-SMALL CELL LUNG CANCER (NSCLC): EFFICACY DATA FROM THE PHASE 2 GEOMETRY MONO-1 STUDY. Neuro-Oncology 2019; 21: vi56–vi56.
101. National Center for Biotechnology Information (2023). PubChem Compound Summary for CID 25145656, Capmatinib. Retrieved March 28, 2023 from https://pubchem.ncbi.nlm.nih.gov/compound/Capmatinib.
102. National Center for Biotechnology Information (2023). PubChem Compound Summary for CID 6442177, Everolimus. Retrieved March 28, 2023 from https://pubchem.ncbi.nlm.nih.gov/compound/Everolimus.
103. Stacker SA, Achen MG. Where to now with the VEGF signalling pathway in cancer? Chinese Journal of Cancer. Epub ahead of print February 19, 2013.
104. Brandes AA, Bartolotti M, Tosoni A, et al. Practical Management of Bevacizumab-Related Toxicities in Glioblastoma. The Oncologist 2015; 20: 166–175.
105. National Center for Biotechnology Information (2023). PubChem Compound Summary for CID 71731823, Lorlatinib. Retrieved March 28, 2023 from https://pubchem.ncbi.nlm.nih.gov/compound/Lorlatinib.
106. Abe T, Kobayashi N, Yoshimura K, et al. Expression of the secretory leukoprotease Inhibitor gene in epithelial cells. Journal of Clinical Investigation 1991; 87: 2207–2215.
107. Pijuan J, Barceló C, Moreno DF, et al. In vitro Cell Migration, Invasion, and Adhesion Assays: From Cell Imaging to Data Analysis. Frontiers in Cell and Developmental Biology; 7. Epub ahead of print June 14, 2019.
108. Barillari G. The Impact of Matrix Metalloproteinase-9 on the Sequential Steps of the Metastatic Process. International Journal of Molecular Sciences 2020; 21: 4526.
109. Hoskins E, Rodriguez-Canales J, Hewitt SM, et al. Paracrine SLPI secretion upregulates MMP-9 transcription and secretion in ovarian cancer cells. Gynecologic Oncology 2011; 122: 656–662.
110. Jeong M-J. Secretory leukocyte protease inhibitor is associated with MMP-2 and MMP-9 to promote migration and invasion in SNU638 gastric cancer cells. International Journal of Molecular Medicine. Epub ahead of print June 17, 2011.
111. Mikami Y, Fukushima A, Komiyama Y, et al. Human uterus myoma and gene expression profiling: A novel in vitro model for studying secretory leukocyte protease inhibitor-mediated tumor invasion. Cancer Letters 2016; 379: 84–93.
112. Leinonen T, Pirinen R, Böhm J, et al. Expression of matrix metalloproteinases 7 and 9 in non-small cell lung cancer. Lung Cancer 2006; 51: 313–321.
113. Weng Y, Cai M, Zhu J, et al. Matrix Metalloproteinase Activity in Early-Stage Lung Cancer. Oncology Research and Treatment 2013; 36: 256–259.

114. Devoogdt N, Revets H, Kindt A, et al. The Tumor-Promoting Effect of TNF-α Involves the Induction of Secretory Leukocyte Protease Inhibitor. The Journal of Immunology 2006; 177: 8046–8052.
115. Zhang W, Yao J-L, Dong S-C, et al. SLPI knockdown induced pancreatic ductal adenocarcinoma cells proliferation and invasion. Cancer Cell International; 15. Epub ahead of print April 1, 2015. DOI: 10.1186/s12935-015-0182-4.
116. Wei Z, Liu G, Jia R, et al. Targeting secretory leukocyte protease inhibitor (SLPI) inhibits colorectal cancer cell growth, migration and invasion via downregulation of AKT. PeerJ 2020; 8: e9400.
117. Jan Treda C, Fukuhara T, Suzuki T, et al. Secretory leukocyte protease inhibitor modulates urethane-induced lung carcinogenesis. Carcinogenesis 2013; 35: 896–904.

7. CURRICULUM VITAE

Personal Information

Name	İrem	**Surname**	Çongur
Birth of place	İstanbul	**Date of birth**	17.03.1998
Nationality	T.C.	**Telephone number**	
E-mail			

Educational Level

	Institution Name	**Graduate Year**
Master	Mehmet Ali Aydınlar Acibadem University	2023
Undergraduate	Mehmet Ali Aydınlar Acibadem University	2020
High-School	Arnavutkoy Korkmaz Yigit Anatolian High School	2016

Work Experience

	Position	**Enterprise**	**Duration**
1	Undergraduate Teaching Assistant	Acıbadem Mehmet Ali Aydınlar University Faculty of Arts and Sciences, Molecular Biology and Genetics Department	09.2019 - 01.2020
2	Internship	Istanbul University, Istanbul Faculty of Medicine, Medical Genetics Department, Molecular Genetics Laboratory	06.2019
3	Internship	Liv Hospital, in Vitro Fertilization Laboratory	06.2018

Foreign Languages	**Reading***	**Speaking***	**Writing***
English	Very good	Very Good	Very Good

Foreign Languages Exams•

YÖK-DİL	**UDS**	**IELTS**	**TOEFL IBT**	**TOEFL PBT**	**TOEFL CBT**	**FCE**	**CAE**	**CPE**
83/100		7/9						

	Quantitative	**Equally Weighted**	**Verbal**
ALES Exam	72,15	67,93	61,38

Projects				
	Granted Program	**Active Years**	**Position**	**Project Name**
1	TÜSEB 2022-ACİL-01 (11899)	2022-2023	Scholar	Investigation of the effects of increased SLPI and CXCL17 gene expression on A549 cell line in leptomeningeal carcinoma

Presentations & Awards			
	Organization	**Presentation Type**	**Title of the Presentation**
1	PeerJ	Publication	Meta-analysis of commonly mutated genes in leptomeningeal carcinomatosis
2	8th International Congress of the Molecular Biology Association of Turkey	Poster	Bioinformatic analysis of mutated genes in leptomeningeal carcinoma caused by non-small cell lung cancer
3	ISCB SC RSG Turkey, Open Student Webinars	Webinar	Bioinformatic analysis of mutated genes in leptomeningeal carcinoma caused by non-small cell lung cancer

ELSEVIER LICENSE
TERMS AND CONDITIONS

Jul 03, 2023

This Agreement between Ms. Irem Congur ("You") and Elsevier ("Elsevier") consists of your license details and the terms and conditions provided by Elsevier and Copyright Clearance Center.

License Number	5581231291068
License date	Jul 03, 2023
Licensed Content Publisher	Elsevier
Licensed Content Publication	Cell
Licensed Content Title	Hallmarks of Cancer: The Next Generation
Licensed Content Author	Douglas Hanahan,Robert A. Weinberg
Licensed Content Date	Mar 4, 2011
Licensed Content Volume	144
Licensed Content Issue	5
Licensed Content Pages	29
Start Page	646
End Page	674
Type of Use	reuse in a thesis/dissertation
Portion	figures/tables/illustrations

Number of figures/tables/illustrations	1
Format	both print and electronic
Are you the author of this Elsevier article?	No
Will you be translating?	No
Title	MUTATED GENES IN LEPTOMENINGEAL CARCINOMA CAUSED BY NON-SMALL CELL LUNG CANCER AND THE EFFECTS OF INCREASED SLPI GENE IN THE A549 CELL LINE
Institution name	Acibadem Mehmet Ali Aydinlar University
Expected presentation date	Jul 2023
Portions	Figure 1
Requestor Location	Ms. Irem Congur Dikilitas Mah. Emirhan Cad. No:24 Hatira Apt. Kat:5 D:41 - Besiktas Istanbul, 34349 Turkey Attn: Ms. Irem Congur
Publisher Tax ID	GB 494 6272 12
Total	0.00 USD

Terms and Conditions

INTRODUCTION

1. The publisher for this copyrighted material is Elsevier. By clicking "accept" in connection with completing this licensing transaction, you agree that the following terms and conditions apply to this transaction (along with the Billing and Payment terms and conditions established by Copyright Clearance Center, Inc. ("CCC"), at the time that you opened your RightsLink account and that are available at any time at https://myaccount.copyright.com).

GENERAL TERMS

2. Elsevier hereby grants you permission to reproduce the aforementioned material subject to the terms and conditions indicated.

3. Acknowledgement: If any part of the material to be used (for example, figures) has appeared in our publication with credit or acknowledgement to another source, permission must also be sought from that source. If such permission is not obtained then that material may not be included in your publication/copies. Suitable acknowledgement to the source must be made, either as a footnote or in a reference list at the end of your publication, as follows:

"Reprinted from Publication title, Vol /edition number, Author(s), Title of article / title of chapter, Pages No., Copyright (Year), with permission from Elsevier [OR APPLICABLE SOCIETY COPYRIGHT OWNER]." Also Lancet special credit - "Reprinted from The Lancet, Vol. number, Author(s), Title of article, Pages No., Copyright (Year), with permission from Elsevier."

4. Reproduction of this material is confined to the purpose and/or media for which permission is hereby given. The material may not be reproduced or used in any other way, including use in combination with an artificial intelligence tool (including to train an algorithm, test, process, analyse, generate output and/or develop any form of artificial intelligence tool), or to create any derivative work and/or service (including resulting from the use of artificial intelligence tools).

5. Altering/Modifying Material: Not Permitted. However figures and illustrations may be altered/adapted minimally to serve your work. Any other abbreviations, additions, deletions and/or any other alterations shall be made only with prior written authorization of Elsevier Ltd. (Please contact Elsevier's permissions helpdesk here). No modifications can be made to any Lancet figures/tables and they must be reproduced in full.

6. If the permission fee for the requested use of our material is waived in this instance, please be advised that your future requests for Elsevier materials may attract a fee.

7. Reservation of Rights: Publisher reserves all rights not specifically granted in the combination of (i) the license details provided by you and accepted in the course of this licensing transaction, (ii) these terms and conditions and (iii) CCC's Billing and Payment terms and conditions.

8. License Contingent Upon Payment: While you may exercise the rights licensed immediately upon issuance of the license at the end of the licensing process for the transaction, provided that you have disclosed complete and accurate details of your proposed use, no license is finally effective unless and until full payment is received from you (either by publisher or by CCC) as provided in CCC's Billing and Payment terms and conditions. If full payment is not received on a timely basis, then any license preliminarily granted shall be deemed automatically revoked and shall be void as if never granted. Further, in the event that you breach any of these terms and conditions or any of CCC's Billing and Payment terms and conditions, the license is automatically revoked and shall be void as if never granted. Use of materials as described in a revoked license, as well as any use of the materials beyond the scope of an unrevoked license, may constitute copyright infringement and publisher reserves the right to take any and all action to protect its copyright in the materials.

9. Warranties: Publisher makes no representations or warranties with respect to the licensed material.

10. Indemnity: You hereby indemnify and agree to hold harmless publisher and CCC, and their respective officers, directors, employees and agents, from and against any and all claims arising out of your use of the licensed material other than as specifically authorized pursuant to this license.

11. No Transfer of License: This license is personal to you and may not be sublicensed, assigned, or transferred by you to any other person without publisher's written permission.

12. No Amendment Except in Writing: This license may not be amended except in a writing signed by both parties (or, in the case of publisher, by CCC on publisher's behalf).

13. Objection to Contrary Terms: Publisher hereby objects to any terms contained in any purchase order, acknowledgment, check endorsement or other writing prepared by you, which terms are inconsistent with these terms and conditions or CCC's Billing and Payment terms and conditions. These terms and conditions, together with CCC's Billing and Payment terms and conditions (which are incorporated herein), comprise the entire agreement between you and publisher (and CCC) concerning this licensing transaction. In the event of any conflict between your obligations established by these terms and conditions and those established by CCC's Billing and Payment terms and conditions, these terms and conditions shall control.

14. Revocation: Elsevier or Copyright Clearance Center may deny the permissions described in this License at their sole discretion, for any reason or no reason, with a full refund payable to you. Notice of such denial will be made using the contact information provided by you. Failure to receive such notice will not alter or invalidate the denial. In no event will Elsevier or Copyright Clearance Center be responsible or liable for any costs, expenses or damage incurred by you as a result of a denial of your permission request, other than a refund of the amount(s) paid by you to Elsevier and/or Copyright Clearance Center for denied permissions.

LIMITED LICENSE

The following terms and conditions apply only to specific license types:

15. **Translation**: This permission is granted for non-exclusive world **English** rights only unless your license was granted for translation rights. If you licensed translation rights you may only translate this content into the languages you requested. A professional translator must perform all translations and reproduce the content word for word preserving the integrity of the article.

16. **Posting licensed content on any Website**: The following terms and conditions apply as follows: Licensing material from an Elsevier journal: All content posted to the web site must maintain the copyright information line on the bottom of each image; A hyper-text must be included to the Homepage of the journal from which you are licensing at http://www.sciencedirect.com/science/journal/xxxxx or the Elsevier homepage for books at http://www.elsevier.com; Central Storage: This license does not include permission for a scanned version of the material to be stored in a central repository such as that provided by Heron/XanEdu.

Licensing material from an Elsevier book: A hyper-text link must be included to the Elsevier homepage at http://www.elsevier.com . All content posted to the web site must maintain the copyright information line on the bottom of each image.

Posting licensed content on Electronic reserve: In addition to the above the following clauses are applicable: The web site must be password-protected and made available only to bona fide students registered on a relevant course. This permission is granted for 1 year only. You may obtain a new license for future website posting.

17. **For journal authors:** the following clauses are applicable in addition to the above:

Preprints:

A preprint is an author's own write-up of research results and analysis, it has not been peer-reviewed, nor has it had any other value added to it by a publisher (such as formatting, copyright, technical enhancement etc.).

Authors can share their preprints anywhere at any time. Preprints should not be added to or enhanced in any way in order to appear more like, or to substitute for, the final versions of articles however authors can update their preprints on arXiv or RePEc with their Accepted Author Manuscript (see below).

If accepted for publication, we encourage authors to link from the preprint to their formal publication via its DOI. Millions of researchers have access to the formal publications on ScienceDirect, and so links will help users to find, access, cite and use the best available version. Please note that Cell Press, The Lancet and some society-owned have different preprint policies. Information on these policies is available on the journal homepage.

Accepted Author Manuscripts: An accepted author manuscript is the manuscript of an article that has been accepted for publication and which typically includes author-incorporated changes suggested during submission, peer review and editor-author communications.

Authors can share their accepted author manuscript:

- immediately
    - via their non-commercial person homepage or blog
    - by updating a preprint in arXiv or RePEc with the accepted manuscript
    - via their research institute or institutional repository for internal institutional uses or as part of an invitation-only research collaboration work-group
    - directly by providing copies to their students or to research collaborators for their personal use
    - for private scholarly sharing as part of an invitation-only work group on commercial sites with which Elsevier has an agreement
- After the embargo period
    - via non-commercial hosting platforms such as their institutional repository
    - via commercial sites with which Elsevier has an agreement

In all cases accepted manuscripts should:

- link to the formal publication via its DOI
- bear a CC-BY-NC-ND license - this is easy to do
- if aggregated with other manuscripts, for example in a repository or other site, be shared in alignment with our hosting policy not be added to or enhanced in any way to appear more like, or to substitute for, the published journal article.

Published journal article (JPA): A published journal article (PJA) is the definitive final record of published research that appears or will appear in the journal and embodies all value-adding publishing activities including peer review co-ordination, copy-editing, formatting, (if relevant) pagination and online enrichment.

Policies for sharing publishing journal articles differ for subscription and gold open access articles:

Subscription Articles: If you are an author, please share a link to your article rather than the full-text. Millions of researchers have access to the formal publications on ScienceDirect, and so links will help your users to find, access, cite, and use the best available version.

Theses and dissertations which contain embedded PJAs as part of the formal submission can be posted publicly by the awarding institution with DOI links back to the formal publications on ScienceDirect.

If you are affiliated with a library that subscribes to ScienceDirect you have additional private sharing rights for others' research accessed under that agreement. This includes use for classroom teaching and internal training at the institution (including use in course packs and courseware programs), and inclusion of the article for grant funding purposes.

Gold Open Access Articles: May be shared according to the author-selected end-user license and should contain a CrossMark logo, the end user license, and a DOI link to the formal publication on ScienceDirect.

Please refer to Elsevier's posting policy for further information.

18. **For book authors** the following clauses are applicable in addition to the above: Authors are permitted to place a brief summary of their work online only. You are not allowed to download and post the published electronic version of your chapter, nor may you scan the printed edition to create an electronic version. **Posting to a repository:** Authors are permitted to post a summary of their chapter only in their institution's repository.

19. **Thesis/Dissertation**: If your license is for use in a thesis/dissertation your thesis may be submitted to your institution in either print or electronic form. Should your thesis be published commercially, please reapply for permission. These requirements include permission for the Library and Archives of Canada to supply single copies, on demand, of the complete thesis and include permission for Proquest/UMI to supply single copies, on demand, of the complete thesis. Should your thesis be published commercially, please reapply for permission. Theses and dissertations which contain embedded PJAs as part of the formal submission can be posted publicly by the awarding institution with DOI links back to the formal publications on ScienceDirect.

Elsevier Open Access Terms and Conditions

You can publish open access with Elsevier in hundreds of open access journals or in nearly 2000 established subscription journals that support open access publishing. Permitted third party re-use of these open access articles is defined by the author's choice of Creative Commons user license. See our open access license policy for more information.

Terms & Conditions applicable to all Open Access articles published with Elsevier:

Any reuse of the article must not represent the author as endorsing the adaptation of the article nor should the article be modified in such a way as to damage the author's honour or reputation. If any changes have been made, such changes must be clearly indicated.

The author(s) must be appropriately credited and we ask that you include the end user license and a DOI link to the formal publication on ScienceDirect.

If any part of the material to be used (for example, figures) has appeared in our publication with credit or acknowledgement to another source it is the responsibility of the user to ensure their reuse complies with the terms and conditions determined by the rights holder.

Additional Terms & Conditions applicable to each Creative Commons user license:

CC BY: The CC-BY license allows users to copy, to create extracts, abstracts and new works from the Article, to alter and revise the Article and to make commercial use of the Article (including reuse and/or resale of the Article by commercial entities), provided the user gives appropriate credit (with a link to the formal publication through the relevant DOI), provides a link to the license, indicates if changes were made and the licensor is not represented as endorsing the use made of the work. The full details of the license are available at http://creativecommons.org/licenses/by/4.0.

CC BY NC SA: The CC BY-NC-SA license allows users to copy, to create extracts, abstracts and new works from the Article, to alter and revise the Article, provided this is not done for commercial purposes, and that the user gives appropriate credit (with a link to the formal publication through the relevant DOI), provides a link to the license, indicates if changes were made and the licensor is not represented as endorsing the use made of the work. Further, any new works must be made available on the same conditions. The full details of the license are available at http://creativecommons.org/licenses/by-nc-sa/4.0.

CC BY NC ND: The CC BY-NC-ND license allows users to copy and distribute the Article, provided this is not done for commercial purposes and further does not permit distribution of the Article if it is changed or edited in any way, and provided the user gives appropriate credit (with a link to the formal publication through the relevant DOI), provides a link to the license, and that the licensor is not represented as endorsing the use made of the work. The full details of the license are available at http://creativecommons.org/licenses/by-nc-nd/4.0. Any commercial reuse of Open Access articles published with a CC BY NC SA or CC BY NC ND license requires permission from Elsevier and will be subject to a fee.

Commercial reuse includes:

- Associating advertising with the full text of the Article
- Charging fees for document delivery or access
- Article aggregation
- Systematic distribution via e-mail lists or share buttons

Posting or linking by commercial companies for use by customers of those companies.

20. **Other Conditions**:

v1.10

Questions? customercare@copyright.com.

ELSEVIER LICENSE
TERMS AND CONDITIONS

Jul 03, 2023

This Agreement between Ms. Irem Congur ("You") and Elsevier ("Elsevier") consists of your license details and the terms and conditions provided by Elsevier and Copyright Clearance Center.

License Number	5581240084425
License date	Jul 03, 2023
Licensed Content Publisher	Elsevier
Licensed Content Publication	Neurosurgery Clinics of North America
Licensed Content Title	Leptomeningeal Carcinomatosis Molecular Landscape, Current Management, and Emerging Therapies
Licensed Content Author	Hriday P. Bhambhvani,Adrian J. Rodrigues,Maxine C. Umeh-Garcia,Melanie Hayden Gephart
Licensed Content Date	Oct 1, 2020
Licensed Content Volume	31
Licensed Content Issue	4
Licensed Content Pages	13
Start Page	613
End Page	625
Type of Use	reuse in a thesis/dissertation
Portion	figures/tables/illustrations

Number of figures/tables/illustrations	1
Format	both print and electronic
Are you the author of this Elsevier article?	No
Will you be translating?	No
Title	MUTATED GENES IN LEPTOMENINGEAL CARCINOMA CAUSED BY NON-SMALL CELL LUNG CANCER AND THE EFFECTS OF INCREASED SLPI GENE IN THE A549 CELL LINE
Institution name	Acibadem Mehmet Ali Aydinlar University
Expected presentation date	Jul 2023
Portions	Figure 1
Requestor Location	Ms. Irem Congur Dikilitas Mah. Emirhan Cad. No:24 Hatira Apt. Kat:5 D:41 - Besiktas Istanbul, 34349 Turkey Attn: Ms. Irem Congur
Publisher Tax ID	GB 494 6272 12
Total	0.00 USD
Terms and Conditions	

INTRODUCTION

1. The publisher for this copyrighted material is Elsevier. By clicking "accept" in connection with completing this licensing transaction, you agree that the following terms and conditions apply to this transaction (along with the Billing and Payment terms and conditions established by Copyright Clearance Center, Inc. ("CCC"), at the time that you opened your RightsLink account and that are available at any time at https://myaccount.copyright.com).

GENERAL TERMS

2. Elsevier hereby grants you permission to reproduce the aforementioned material subject to the terms and conditions indicated.

3. Acknowledgement: If any part of the material to be used (for example, figures) has appeared in our publication with credit or acknowledgement to another source, permission must also be sought from that source. If such permission is not obtained then that material may not be included in your publication/copies. Suitable acknowledgement to the source must be made, either as a footnote or in a reference list at the end of your publication, as follows:

"Reprinted from Publication title, Vol /edition number, Author(s), Title of article / title of chapter, Pages No., Copyright (Year), with permission from Elsevier [OR APPLICABLE SOCIETY COPYRIGHT OWNER]." Also Lancet special credit - "Reprinted from The Lancet, Vol. number, Author(s), Title of article, Pages No., Copyright (Year), with permission from Elsevier."

4. Reproduction of this material is confined to the purpose and/or media for which permission is hereby given. The material may not be reproduced or used in any other way, including use in combination with an artificial intelligence tool (including to train an algorithm, test, process, analyse, generate output and/or develop any form of artificial intelligence tool), or to create any derivative work and/or service (including resulting from the use of artificial intelligence tools).

5. Altering/Modifying Material: Not Permitted. However figures and illustrations may be altered/adapted minimally to serve your work. Any other abbreviations, additions, deletions and/or any other alterations shall be made only with prior written authorization of Elsevier Ltd. (Please contact Elsevier's permissions helpdesk here). No modifications can be made to any Lancet figures/tables and they must be reproduced in full.

6. If the permission fee for the requested use of our material is waived in this instance, please be advised that your future requests for Elsevier materials may attract a fee.

7. Reservation of Rights: Publisher reserves all rights not specifically granted in the combination of (i) the license details provided by you and accepted in the course of this licensing transaction, (ii) these terms and conditions and (iii) CCC's Billing and Payment terms and conditions.

8. License Contingent Upon Payment: While you may exercise the rights licensed immediately upon issuance of the license at the end of the licensing process for the transaction, provided that you have disclosed complete and accurate details of your proposed use, no license is finally effective unless and until full payment is received from you (either by publisher or by CCC) as provided in CCC's Billing and Payment terms and conditions. If full payment is not received on a timely basis, then any license preliminarily granted shall be deemed automatically revoked and shall be void as if never granted. Further, in the event that you breach any of these terms and conditions or any of CCC's Billing and Payment terms and conditions, the license is automatically revoked and shall be void as if never granted. Use of materials as described in a revoked license, as well as any use of the materials beyond the scope of an unrevoked license, may constitute copyright infringement and publisher reserves the right to take any and all action to protect its copyright in the materials.

9. Warranties: Publisher makes no representations or warranties with respect to the licensed material.

10. Indemnity: You hereby indemnify and agree to hold harmless publisher and CCC, and their respective officers, directors, employees and agents, from and against any and all claims arising out of your use of the licensed material other than as specifically authorized pursuant to this license.

11. No Transfer of License: This license is personal to you and may not be sublicensed, assigned, or transferred by you to any other person without publisher's written permission.

12. No Amendment Except in Writing: This license may not be amended except in a writing signed by both parties (or, in the case of publisher, by CCC on publisher's behalf).

13. Objection to Contrary Terms: Publisher hereby objects to any terms contained in any purchase order, acknowledgment, check endorsement or other writing prepared by you, which terms are inconsistent with these terms and conditions or CCC's Billing and Payment terms and conditions. These terms and conditions, together with CCC's Billing and Payment terms and conditions (which are incorporated herein), comprise the entire agreement between you and publisher (and CCC) concerning this licensing transaction. In the event of any conflict between your obligations established by these terms and conditions and those established by CCC's Billing and Payment terms and conditions, these terms and conditions shall control.

14. Revocation: Elsevier or Copyright Clearance Center may deny the permissions described in this License at their sole discretion, for any reason or no reason, with a full refund payable to you. Notice of such denial will be made using the contact information provided by you. Failure to receive such notice will not alter or invalidate the denial. In no event will Elsevier or Copyright Clearance Center be responsible or liable for any costs, expenses or damage incurred by you as a result of a denial of your permission request, other than a refund of the amount(s) paid by you to Elsevier and/or Copyright Clearance Center for denied permissions.

LIMITED LICENSE

The following terms and conditions apply only to specific license types:

15. **Translation**: This permission is granted for non-exclusive world **English** rights only unless your license was granted for translation rights. If you licensed translation rights you may only translate this content into the languages you requested. A professional translator must perform all translations and reproduce the content word for word preserving the integrity of the article.

16. **Posting licensed content on any Website**: The following terms and conditions apply as follows: Licensing material from an Elsevier journal: All content posted to the web site must maintain the copyright information line on the bottom of each image; A hyper-text must be included to the Homepage of the journal from which you are licensing at http://www.sciencedirect.com/science/journal/xxxxx or the Elsevier homepage for books at http://www.elsevier.com; Central Storage: This license does not include permission for a scanned version of the material to be stored in a central repository such as that provided by Heron/XanEdu.

Licensing material from an Elsevier book: A hyper-text link must be included to the Elsevier homepage at http://www.elsevier.com . All content posted to the web site must maintain the copyright information line on the bottom of each image.

Posting licensed content on Electronic reserve: In addition to the above the following clauses are applicable: The web site must be password-protected and made available only to bona fide students registered on a relevant course. This permission is granted for 1 year only. You may obtain a new license for future website posting.

17. **For journal authors:** the following clauses are applicable in addition to the above:

Preprints:

A preprint is an author's own write-up of research results and analysis, it has not been peer-reviewed, nor has it had any other value added to it by a publisher (such as formatting, copyright, technical enhancement etc.).

Authors can share their preprints anywhere at any time. Preprints should not be added to or enhanced in any way in order to appear more like, or to substitute for, the final versions of articles however authors can update their preprints on arXiv or RePEc with their Accepted Author Manuscript (see below).

If accepted for publication, we encourage authors to link from the preprint to their formal publication via its DOI. Millions of researchers have access to the formal publications on ScienceDirect, and so links will help users to find, access, cite and use the best available version. Please note that Cell Press, The Lancet and some society-owned have different preprint policies. Information on these policies is available on the journal homepage.

Accepted Author Manuscripts: An accepted author manuscript is the manuscript of an article that has been accepted for publication and which typically includes author-incorporated changes suggested during submission, peer review and editor-author communications.

Authors can share their accepted author manuscript:

- immediately
    - via their non-commercial person homepage or blog
    - by updating a preprint in arXiv or RePEc with the accepted manuscript
    - via their research institute or institutional repository for internal institutional uses or as part of an invitation-only research collaboration work-group
    - directly by providing copies to their students or to research collaborators for their personal use
    - for private scholarly sharing as part of an invitation-only work group on commercial sites with which Elsevier has an agreement
- After the embargo period
    - via non-commercial hosting platforms such as their institutional repository
    - via commercial sites with which Elsevier has an agreement

In all cases accepted manuscripts should:

- link to the formal publication via its DOI
- bear a CC-BY-NC-ND license - this is easy to do
- if aggregated with other manuscripts, for example in a repository or other site, be shared in alignment with our hosting policy not be added to or enhanced in any way to appear more like, or to substitute for, the published journal article.

Published journal article (JPA): A published journal article (PJA) is the definitive final record of published research that appears or will appear in the journal and embodies all value-adding publishing activities including peer review co-ordination, copy-editing, formatting, (if relevant) pagination and online enrichment.

Policies for sharing publishing journal articles differ for subscription and gold open access articles:

Subscription Articles: If you are an author, please share a link to your article rather than the full-text. Millions of researchers have access to the formal publications on ScienceDirect, and so links will help your users to find, access, cite, and use the best available version.

Theses and dissertations which contain embedded PJAs as part of the formal submission can be posted publicly by the awarding institution with DOI links back to the formal publications on ScienceDirect.

If you are affiliated with a library that subscribes to ScienceDirect you have additional private sharing rights for others' research accessed under that agreement. This includes use for classroom teaching and internal training at the institution (including use in course packs and courseware programs), and inclusion of the article for grant funding purposes.

Gold Open Access Articles: May be shared according to the author-selected end-user license and should contain a CrossMark logo, the end user license, and a DOI link to the formal publication on ScienceDirect.

Please refer to Elsevier's posting policy for further information.

18. **For book authors** the following clauses are applicable in addition to the above: Authors are permitted to place a brief summary of their work online only. You are not allowed to download and post the published electronic version of your chapter, nor may you scan the printed edition to create an electronic version. **Posting to a repository:** Authors are permitted to post a summary of their chapter only in their institution's repository.

19. **Thesis/Dissertation**: If your license is for use in a thesis/dissertation your thesis may be submitted to your institution in either print or electronic form. Should your thesis be published commercially, please reapply for permission. These requirements include permission for the Library and Archives of Canada to supply single copies, on demand, of the complete thesis and include permission for Proquest/UMI to supply single copies, on demand, of the complete thesis. Should your thesis be published commercially, please reapply for permission. Theses and dissertations which contain embedded PJAs as part of the formal submission can be posted publicly by the awarding institution with DOI links back to the formal publications on ScienceDirect.

Elsevier Open Access Terms and Conditions

You can publish open access with Elsevier in hundreds of open access journals or in nearly 2000 established subscription journals that support open access publishing. Permitted third party re-use of these open access articles is defined by the author's choice of Creative Commons user license. See our open access license policy for more information.

Terms & Conditions applicable to all Open Access articles published with Elsevier:

Any reuse of the article must not represent the author as endorsing the adaptation of the article nor should the article be modified in such a way as to damage the author's honour or reputation. If any changes have been made, such changes must be clearly indicated.

The author(s) must be appropriately credited and we ask that you include the end user license and a DOI link to the formal publication on ScienceDirect.

If any part of the material to be used (for example, figures) has appeared in our publication with credit or acknowledgement to another source it is the responsibility of the user to ensure their reuse complies with the terms and conditions determined by the rights holder.

Additional Terms & Conditions applicable to each Creative Commons user license:

CC BY: The CC-BY license allows users to copy, to create extracts, abstracts and new works from the Article, to alter and revise the Article and to make commercial use of the Article (including reuse and/or resale of the Article by commercial entities), provided the user gives appropriate credit (with a link to the formal publication through the relevant DOI), provides a link to the license, indicates if changes were made and the licensor is not represented as endorsing the use made of the work. The full details of the license are available at http://creativecommons.org/licenses/by/4.0.

CC BY NC SA: The CC BY-NC-SA license allows users to copy, to create extracts, abstracts and new works from the Article, to alter and revise the Article, provided this is not done for commercial purposes, and that the user gives appropriate credit (with a link to the formal publication through the relevant DOI), provides a link to the license, indicates if changes were made and the licensor is not represented as endorsing the use made of the work. Further, any new works must be made available on the same conditions. The full details of the license are available at http://creativecommons.org/licenses/by-nc-sa/4.0.

CC BY NC ND: The CC BY-NC-ND license allows users to copy and distribute the Article, provided this is not done for commercial purposes and further does not permit distribution of the Article if it is changed or edited in any way, and provided the user gives appropriate credit (with a link to the formal publication through the relevant DOI), provides a link to the license, and that the licensor is not represented as endorsing the use made of the work. The full details of the license are available at http://creativecommons.org/licenses/by-nc-nd/4.0. Any commercial reuse of Open Access articles published with a CC BY NC SA or CC BY NC ND license requires permission from Elsevier and will be subject to a fee.

Commercial reuse includes:

- Associating advertising with the full text of the Article
- Charging fees for document delivery or access
- Article aggregation
- Systematic distribution via e-mail lists or share buttons

Posting or linking by commercial companies for use by customers of those companies.

20. **Other Conditions**:

v1.10

Questions? customercare@copyright.com.